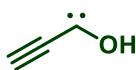
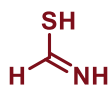


# Matrix Isolation of Novel Reactive Intermediates

– Quantum Mechanical Tunneling in Atmospherically and Astrochemically Relevant Compounds –

---

Inauguraldissertation zur Erlangung des Doktorgrades der naturwissenschaftlichen Fachbereiche  
im Fachgebiet Organische Chemie (Fachbereich 08)  
der Justus-Liebig-Universität Gießen



vorgelegt von

**Bastian Bernhardt**

aus Langen

angefertigt im Zeitraum von Oktober 2018 bis September 2021

am Institut für Organische Chemie  
der Justus-Liebig-Universität Gießen

**Betreuer: Prof. Dr. Peter R. Schreiner, PhD**



## **Eidesstattliche Erklärung**

Hiermit versichere ich, die vorgelegte Dissertation selbständig und ohne unerlaubte fremde Hilfe und nur mit den Hilfen angefertigt zu haben, die ich in der Dissertation angegeben habe. Alle Textstellen, die wörtlich oder sinngemäß aus veröffentlichten Schriften entnommen sind, und alle Angaben, die auf mündlichen Auskünften beruhen, sind als solche kenntlich gemacht.

Bei den von mir durchgeführten und in der Dissertation erwähnten Untersuchungen habe ich die Grundsätze guter wissenschaftlicher Praxis, wie sie in der „Satzung der Justus-Liebig-Universität zur Sicherung guter wissenschaftlicher Praxis“ niedergelegt sind, eingehalten.

---

Ort, Datum

---

Unterschrift

Dekan: Prof. Dr. Thomas Wilke

Prodekan: Prof. Dr. Klaus Müller-Buschbaum

Studiendekan: Prof. Dr. Richard Göttlich

Erstgutachter: Prof. Dr. Peter R. Schreiner, PhD

Zweitgutachter: Prof. Dr. Bernd Smarsly



## Zusammenfassung

Kleine, reaktive Moleküle werden als Intermediate in atmosphärischen und astronomischen Prozessen postuliert, sind jedoch häufig kaum oder überhaupt nicht untersucht. Mithilfe der Matrixisolationstechnik gelingt es, die Lebensdauer solcher Spezies unter kryogenen Bedingungen zu verlängern und somit ihre Charakterisierung mit spektroskopischen Methoden zu ermöglichen. Der quantenmechanische Tunneleffekt führt dazu, dass selbst manche matrixisolierte Moleküle nicht persistent sind. Untersuchungen dieses Effekts führten schließlich zu einem neuen Prinzip in der Chemie, nämlich dem der Tunnelkontrolle.

Im Rahmen dieser Arbeit wurden, unter anderem, zwei neue Hydroxycarbene dargestellt und bezüglich ihrer Tunnelreaktivität analysiert. Von besonderem Interesse ist der Einfluss des Substituenten auf die Tunnelkinetik. So soll dazu beigetragen werden, ein besseres und intuitives Verständnis chemischer Tunnelprozesse zu erlangen, damit der Effekt beispielsweise in synthetischen Aufgabenstellungen gezielt eingesetzt werden kann. Die in dieser Arbeit erstmals dargestellten Spezies wurden außerdem in der Literatur bezüglich ihrer Rolle in atmosphärischen oder astronomischen Vorgängen diskutiert. Ihre direkte spektroskopische Charakterisierung stellt die chemische Grundlage postulierter Mechanismen und Modelle solcher Prozesse dar.

In der ersten Veröffentlichung wurde das bisher unbekannte Thiolimintautomer  $\text{HC}(\text{NH})\text{SH}$  des Thioformamids ( $\text{HC}(\text{S})\text{NH}_2$ ) in kryogenen Argon- und Stickstoffmatrices photochemisch generiert. Eines der beobachteten vier Konformere dieser neuen Verbindung geht eine durch Tunneln ermöglichte Torsion um die C–S Bindung ein.

Die erstmalige Darstellung und spektroskopische Charakterisierung des Aminohydroxymethylens ( $\text{H}_2\text{N}-\ddot{\text{C}}-\text{OH}$ ) ist Gegenstand der zweiten Publikation. Aminohydroxymethylen ist in einer Argonmatrix bei 3 K persistent und zerfällt unter Bestrahlung mit UV-Licht zu  $\text{NH}_3 + \text{CO}$  sowie  $\text{HNCO} + \text{H}_2$ .

Über ein weiteres neues Hydroxycarben, nämlich Ethynylhydroxycarben ( $\text{HC}\equiv\text{C}-\ddot{\text{C}}-\text{OH}$ ), wird in der dritten Veröffentlichung berichtet. Dieses reagiert in einem konformerspezifischen und für Hydroxycarbene typischen Tunnelprozess zu Propinal.

In der vierten Publikation wurde das bisher unbekannte *cis-cis*-Konformer des Dihydroxycarbens ( $\text{HO}-\ddot{\text{C}}-\text{OH}$ ) durch Bestrahlung mit nahem Infrarotlicht aus energetisch niedrigeren Konformeren in einer Stickstoffmatrix erzeugt. Neben Konformerentunneln deuten die gemessenen Kinetiken des Abbaus dieser Verbindung auf eine Nebenreaktion, nämlich den Zerfall zu  $\text{CO}_2$  und  $\text{H}_2$ , hin.



## Abstract

Small, reactive molecules are intermediates postulated in atmospheric and astrochemical processes. However, little to nothing is known about many such species. With the help of the matrix isolation technique the lifetime of reactive molecules can be increased allowing for their direct spectroscopic investigation. Quantum mechanical tunneling leads to the depletion of some matrix-isolated species. Investigating this effect eventually led to a novel chemical principle, namely tunneling control.

During this work, two novel hydroxycarbenes, among others, were generated and their tunneling behaviors were studied. The focus lies on the effect of substitution on tunneling half-lives, aiming to create a better and more intuitive understanding of quantum mechanical tunneling in chemistry. This might eventually enable exploiting this effect, *e.g.*, in chemical synthesis. The species generated herein were discussed regarding their role in atmospheric and astrochemical processes in the literature and their direct spectroscopic characterization provides the chemical basis for models used in these fields.

In the first publication, the hitherto unknown thiolimine tautomer HC(NH)SH of thioformamide (HC(S)NH<sub>2</sub>) was generated photochemically in cryogenic argon and dinitrogen matrices. One of the four observed conformers of this species reacts in a tunneling-enabled C–S rotamerization.

The second publication reports the first generation and spectroscopic characterization of aminohydroxymethylene (H<sub>2</sub>N– $\ddot{C}$ –OH). Aminohydroxymethylene is persistent in solid argon at 3 K and decomposes to NH<sub>3</sub> + CO as well as HNCO + H<sub>2</sub> upon UV excitation.

Another novel hydroxycarbene, namely ethynylhydroxycarbene (HC≡C– $\ddot{C}$ –OH), is the subject of the third publication. The compound reacts in a conformer-specific quantum mechanical tunneling process, which is typical for hydroxycarbenes, to propynal.

The fourth publication describes the formation of the hitherto unknown *cis-cis*-conformer of dihydroxycarbene (HO– $\ddot{C}$ –OH) from energetically lower-lying conformers by irradiation with near-infrared light in solid dinitrogen. Besides conformational tunneling, the measured kinetic profiles of the decay of this new compound hint towards a side reaction, namely its decomposition to CO<sub>2</sub> and H<sub>2</sub>.



## **Preface**

This thesis comprises the work conducted during my doctoral studies in the group of Prof. Dr. P. R. Schreiner. Its first chapter contains an overview of the advances in tunneling studies applied in Organic Chemistry. These mainly highlight matrix isolation experiments, but also include some references to chemistry conducted in standard wet laboratories. Starting from the physical foundation of tunneling and its first observations in chemical reactions we proceed to examples that led to what is nowadays called *tunneling control*. We report that tunneling is able of qualitatively influencing a reaction's outcome, which is in contrast to the mainstream chemist's viewpoint of only some years ago.

As most examples, including our own work, are related to chemistry discussed in the context of atmospheric and astrochemical processes, we provide some background information about these issues in the beginning of Chapter 1. However, we take a rather chemical perspective and do not go into details of the more general implications of the (chemical) findings presented herein.

At the end of Chapter 1, we briefly discuss our preliminary results in projects that have not been published yet. They further stress the possibilities one can realize when exploiting tunneling effects.

While our own work is mentioned in the Introduction, detailed information can be obtained from the respective peer-reviewed publications, which are reproduced with permission from the publishers in Chapter 2. For experimental details we refer to the corresponding Supporting Information, which is publicly available on the publishers' websites.

This work would not have been possible if it were not for the help of many. I thank all my mentors, colleagues, and friends, who supported me during the past years. I hope that the findings presented herein will be helpful for other researchers or even inspire completely new projects.

*Bastian Bernhardt*

*Gießen, 11<sup>th</sup> October 2021*



## Table of Contents

Eidesstattliche Erklärung .....	3
Zusammenfassung .....	5
Abstract .....	7
Preface .....	9
<b>1. Introduction.....</b>	<b>13</b>
1.1 Motivation and Goals.....	13
1.2 Sulfur-Containing Compounds in Atmospheric and Prebiotic Chemistry .....	14
1.3 Quantum Mechanical Tunneling in Chemistry.....	17
1.3.1 The Physical Background of Quantum Mechanical Tunneling .....	18
1.3.2 Matrix Isolation Studies on Quantum Mechanical Tunneling .....	19
1.3.3 Quantum Mechanical Tunneling in Reactions Conducted under Ambient Conditions .....	27
1.3.4 Computational Predictions on Quantum Mechanical Tunneling .....	28
1.4 Outlook .....	29
1.4.1 CO <sub>2</sub> Activation with Aminomercaptocarbene .....	29
1.4.2 Isotope-Controlled Selectivity by QMT .....	31
1.5 Concluding Remarks.....	33
1.6 Bibliography .....	33
<b>2. Publications .....</b>	<b>41</b>
2.1 Characterization of the Simplest Thiolimine: The Higher Energy Tautomer of Thioformamide .....	41
2.2 Ethynylhydroxycarbene (H–C≡C– $\ddot{C}$ –OH) .....	51
2.3 Aminohydroxymethylene (H <sub>2</sub> N– $\ddot{C}$ –OH), the Simplest Aminooxycarbene.....	59
2.4 Identification and Reactivity of <i>s-cis,s-cis</i> -Dihydroxycarbene, a New [CH <sub>2</sub> O <sub>2</sub> ] Intermediate .....	67
2.5 Further co-Authored Publications.....	73
<b>3. Acknowledgment – Danksagung .....</b>	<b>75</b>



## 1. Introduction

### 1.1 Motivation and Goals

Advances in synthetic organic chemistry during the last decades tremendously increased the pool of accessible molecules benefitting vital areas like medicinal drug design and materials research. In stark contrast, an estimate from 2012 shows that >99.9% of small molecules have never been synthesized.<sup>[1]</sup> These data refer to stable compounds, typically meaning such molecules that are persistent under ambient conditions. Taking fleeting (*i.e.*, reactive) species such as radicals or carbenes into account, even molecules consisting of only a handful of atoms are only scarcely studied. Many of these compounds potentially play a role in astrochemistry and atmospheric chemistry. About 200 different compounds have been found in space until today;<sup>[2]</sup> some examples are depicted in Figure 1. While insights in astrochemistry provoke profound questions about the origin of life, chemical reactions in Earth's atmosphere directly impact our climate. The latter issue is of special interest in current times of climate crisis.

The conditions in outer space allow for the existence of seemingly exotic species (*e.g.*, tricarbon monoxide<sup>[3,4]</sup> in Figure 1). Low temperatures and extremely high dilution prevent the occurrence of most intermolecular chemical reactions that would lead to their depletion. However, in denser parts of space, like molecular clouds, a manifold of reactions has been observed or proposed.<sup>[5]</sup> These often seem unfamiliar considering reactivity we know from ambient laboratory conditions. However, from a universal point of view, space is governed by the reactivity of such small molecules and our planet represents only a small – and in many regards even very special – subsystem. The assumption that a lot of knowledge in (organic) chemistry exists crumbles when thinking outside typical wet-laboratory conditions.

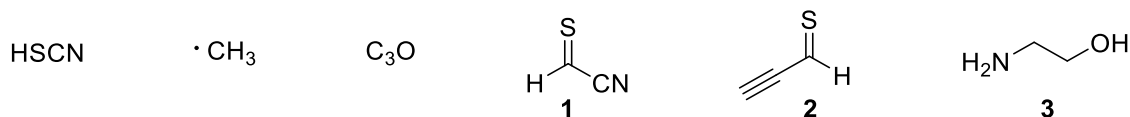


**Figure 1:** Examples of molecules detected in space<sup>[3,4,6-10]</sup> showing that a variety of functional groups are present (**1-3**). These relate to the compounds characterized herein. More than 200 species have hitherto been identified in space.<sup>[2]</sup>

During my doctoral studies, we isolated and characterized such hitherto elusive species using the matrix isolation technique in conjunction with infrared (IR) and ultraviolet/visible (UV/Vis) spectroscopy. We were especially interested in the study of quantum mechanical tunneling and photochemical reactions of such molecules. In a typical experiment, a volatile sample is evaporated together with an excess of a host gas (here argon (Ar) or dinitrogen (N<sub>2</sub>); the matrix material) onto a cold CsI (for IR) or BaF<sub>2</sub> (for UV/Vis measurements) window (Figure 2). Reactive species can be generated *in situ* either by pyrolysis of the substrate prior to deposition or *via* photolysis directly on the cold window. The technique allows probing intramolecular reactivity of species trapped in an inert matrix, a situation resembling conditions found in interstellar ice grains.

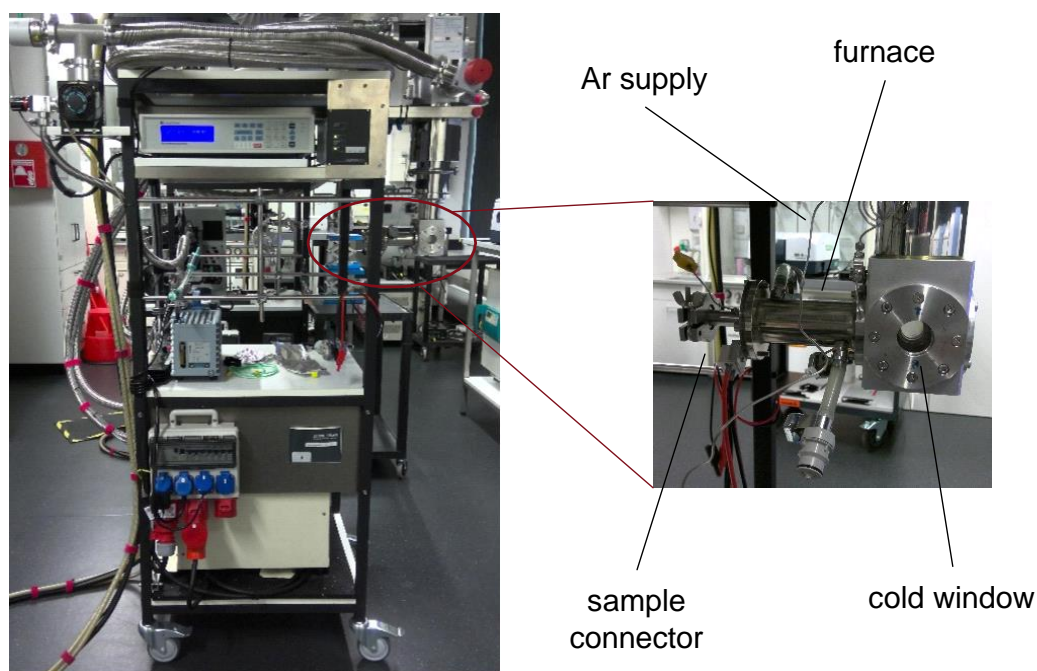


**Figure 2:** *Top:* Matrix apparatus. *Bottom:* Schematic representation.

This thesis aims probing the tunneling reactivity of the parent thiolimine and hitherto unknown hydroxycarbenes, all of which resemble candidates of atmospherically or astronomically relevant compounds. Another goal is exploring the conformational reactivity in dihydroxycarbene. The last project raises the question of the feasibility to activate  $\text{CO}_2$  in a tunneling process. Generally, deciphering tunneling mechanisms and disentangling the various influences on this quantum effect is a key step in transferring quantum mechanical tunneling from a curiosity to a tool that can be used to control chemical reactions.

## 1.2 Sulfur-Containing Compounds in Atmospheric and Prebiotic Chemistry

Sulfur-containing compounds affect cloud formation in Earth's atmosphere as they form grain-like structures, which induce water condensation.<sup>[11]</sup> The main channel for the formation of such structures is the oxidation of dimethyl sulfide (**4**), which is released in

huge amounts by phytoplankton from the oceans into the marine boundary layer.<sup>[12,13]</sup> Among the most abundant oxidizing agents in the atmosphere are OH and NO<sub>3</sub> radicals.<sup>[14,15]</sup> Other conceivable oxidizers, which have been widely discussed in recent years, are carbonyl oxides, also known as Criegee intermediates (**12**, Figure 3).<sup>[16]</sup> The simplest Criegee intermediate (R = R' = H) was characterized in the last decade,<sup>[17,18]</sup> while its structure had already been correctly predicted in 1949.<sup>[19,20]</sup> We report a new isomer (*cis-cis*-dihydroxycarbene) of this intriguing species further below. A simplified overview of the mechanism of the oxidation of **4** is depicted in Figure 3.<sup>[15]</sup>

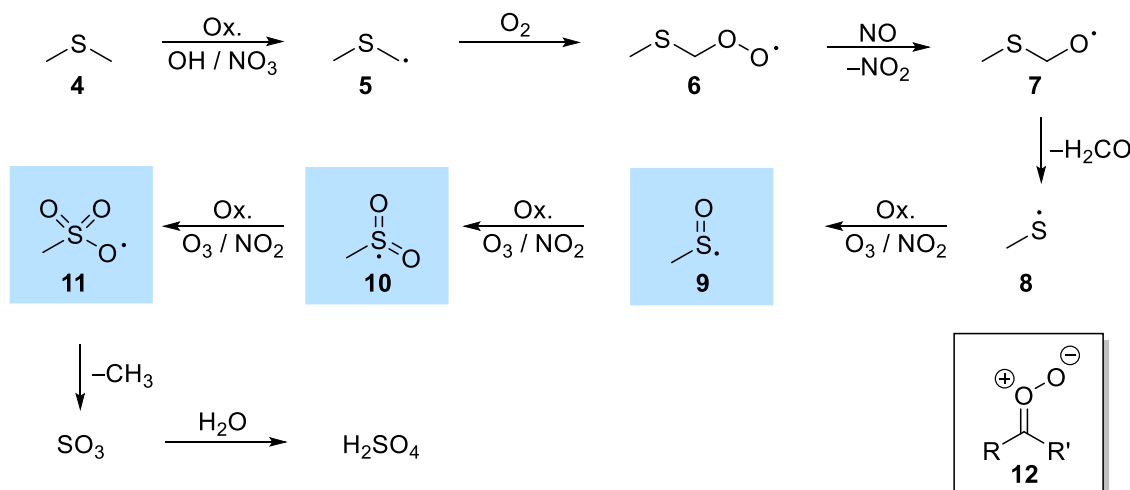


**Figure 3:** Overview of the oxidation of **4** in the earth's atmosphere adapted from Barnes *et al.*<sup>[15]</sup> Spectroscopically characterized intermediates (*vide infra*) are highlighted in blue. *Bottom-right edge:* General structure of Criegee intermediates, which may act as oxidizing agents besides OH and NO<sub>3</sub> radicals in atmospheric processes.

While the methyl sulfinyl (**9**),<sup>[21,22]</sup> methyl sulfonyl (**10**),<sup>[23]</sup> and methyl sulfonyloxyl (**11**)<sup>[24]</sup> radicals have been characterized by matrix isolation spectroscopy, the very first intermediate (methyl thiomethyl, **5**) in Figure 3, a carbon-centered radical bearing a sulfur atom in  $\alpha$ -position, remains elusive.<sup>[25]</sup> In our recent investigation, we could isolate a derivative of such a species (**15**) and subsequently investigated its intramolecular and intermolecular reactivity by doping the matrix with triplet dioxygen <sup>3</sup>O<sub>2</sub> (Figure 4).<sup>[26]</sup>

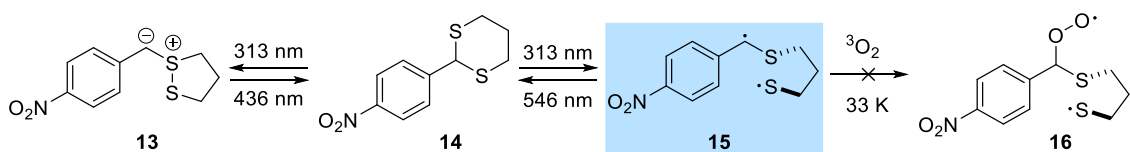


**Figure 4:** Generation of an  $\alpha$ -sulfenyl radical (**15**) via photochemical C–S bond cleavage in *para*-nitrobenzaldehyde dithiane (**14**).<sup>[26]</sup> Biradical **15** does not react with <sup>3</sup>O<sub>2</sub>.

Many more sulfur-containing compounds have been matrix-isolated and discussed regarding their role in atmospheric reactions (Figure 5) like, *inter alia*, the vinylsulfinyl radical (**17**),<sup>[27]</sup> alkynyl thiocyanate and isomers (**18**),<sup>[28]</sup> the phenylsulfinyl radical (**19**),<sup>[29]</sup> disulfur dioxide (**20**),<sup>[30]</sup> the methoxysulfinyl radical (**21**),<sup>[31]</sup> the sulfinyl radical **22**,<sup>[32]</sup> and the hypothiocyanite radical (**23**).<sup>[33]</sup> While climate scientists build models to predict Earth's climate or evaluate data for accurate weather forecasts, the underlying chemical reactions are still poorly understood and many postulated intermediates

unknown. Chemical studies as the ones listed are needed to build the chemical foundation of such models.

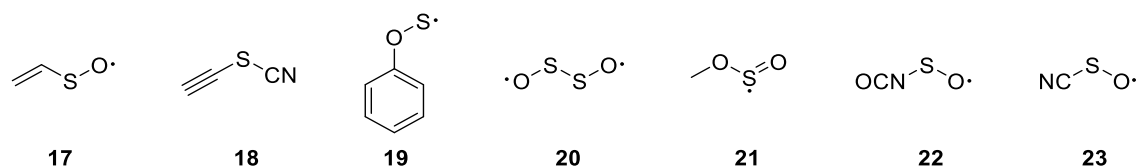


**Figure 5:** Examples of matrix-isolated sulfur-containing compounds with potential relevance in atmospheric processes.<sup>[27–33]</sup>

With the same motivation, we studied the photochemistry of *N*-sulfonylamine (**24**, Figure 6) in cooperation with Xiaoqing Zeng’s research group.<sup>[34]</sup> The reactivity of **24** represents another example of the rich and somewhat unfamiliar monomolecular chemistry of small molecules similar to those depicted in Figure 5.

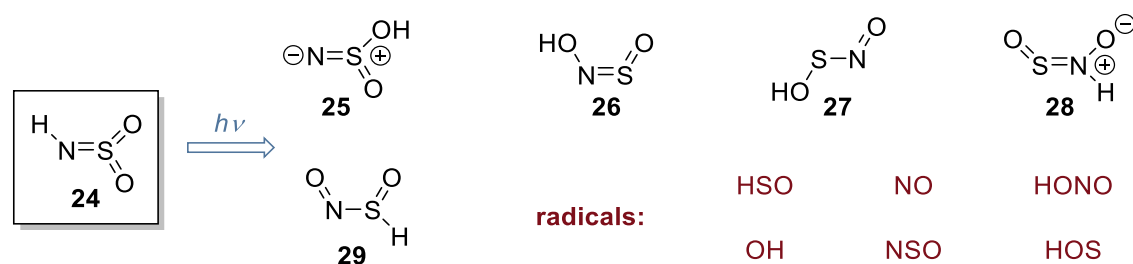


**Figure 6:** Species observed upon photolysis at different wavelengths of matrix-isolated **24**.<sup>[34]</sup>

Thioamides represent a widely abundant class of sulfur-containing compounds. They have, *e.g.*, been used synthetically to generate biorelevant thiazoles *via* the reaction with aldehydes.<sup>[35]</sup> In the prebiotic context, their intermediacy in the formation of various amino acids has been implied experimentally.<sup>[36]</sup> While plenty of data exist on thioamides (**30**), surprisingly little is known about parent thioformamide (**30a**).<sup>[37]</sup> Thioformamide is a likely candidate for detection in space as it can be generated from HCN and H<sub>2</sub>S,<sup>[38]</sup> both of which have been detected in interstellar media.<sup>[39,40]</sup> During my doctoral studies, we isolated **30a** (prepared from formamide and phosphorus pentasulfide)<sup>[41]</sup> in solid Ar and N<sub>2</sub> matrices and photochemically generated four conformers of the tautomeric thiolimine (**31a**), a compound which had remained elusive up to now.<sup>[42]</sup> In the course of this project, we also recorded the first X-ray diffraction data of **30a**.

Some thioamides and their thioamide → thiolimine tautomerizations have been investigated under matrix isolation conditions – both photochemically and in terms of quantum mechanical tunneling (QMT) by keeping the matrix in the dark for a certain period of time (Figure 7).<sup>[43–53]</sup> Only for thiourea (**30c**)<sup>[49,50]</sup> and dithiooxamide (**30d**)<sup>[45]</sup> a thiolimine → thioamide QMT reaction has been reported. The absence of such reactivity in parent **30a** clearly shows that thiolimine → thioamide QMT is not the intrinsic reactivity of thioamides, but only (remote) substitution enhances this process. We discuss the effect of substitution on QMT in more detail in the next section.

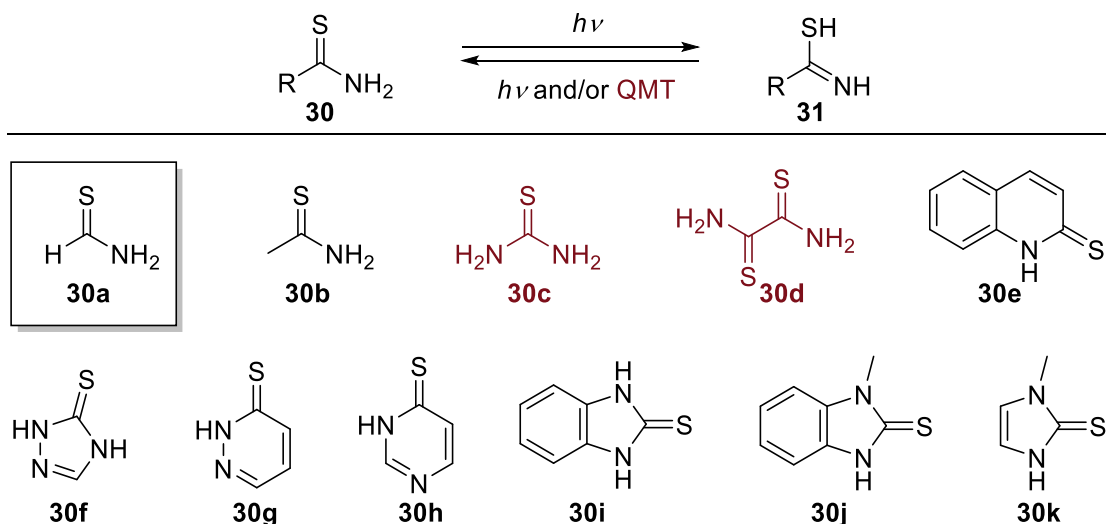


**Figure 7:** Matrix-isolated thioamides which have been tautomerized to their corresponding thiolimine isomer.<sup>[43–53]</sup> The cases for which thiolimine  $\rightarrow$  thioamide tautomerization occurs *via* QMT are highlighted in red.

In our study, we observed a different QMT reaction, namely *trans-trans*-thiolimine (**31a-tt**)  $\rightarrow$  *cis-trans*-thiolimine (**31a-ct**) with a half-life of ca. 30 min in both matrix materials (Figure 8).<sup>[42]</sup> This result is analogous to that of two studies on the methyl derivative (**31b**), which have been conducted simultaneously in Coimbra.<sup>[52,53]</sup> The reactions depicted in Figure 8 represent the first examples of QMT in C–SH rotations. QMT induced rotations around C–OH bonds, which are much more common, are discussed in the next section. We also showed that the analogous rotamerization is absent in the perdeuterated isotopologue, which is a clear indication for QMT.



**Figure 8:** Conformational QMT of thiolimine tautomers of thioformamide<sup>[42]</sup> (**31a-tt**, *left*) and thioacetamide<sup>[52]</sup> (**31b-tt**, *right*).

### 1.3 Quantum Mechanical Tunneling in Chemistry

The previous section concludes with an example illustrating the importance of quantum mechanical tunneling (QMT) in chemical reactions under cryogenic conditions. Note that these resemble the conditions encountered in space rather closely. In this section, we will briefly explain the background and physical foundations of QMT before illustrating its emergence in (organic) chemistry by discussing key examples from literature. We will mention our contributions where fit.

### 1.3.1 The Physical Background of Quantum Mechanical Tunneling

Classically, the kinetics of chemical reactions can be described by transition state theory (TST) as developed independently by Eyring<sup>[54]</sup> as well as Evans and Polanyi<sup>[55,56]</sup> in 1935. The rate constant  $k$  of any reaction is given by equation (1) where  $k_B$  is Boltzmann's constant,  $T$  the absolute temperature, and  $h$  Planck's constant.

$$k = \frac{k_B \cdot T}{h} \cdot K^\ddagger \quad (1)$$

The equilibrium constant  $K^\ddagger$  between the transition state and the reactants is given by equation (2), with the Gibbs free energy of activation  $\Delta G^\ddagger$  and the gas constant  $R$ . Typically,  $\Delta G^\ddagger$  is obtained from quantum chemical computations *via* partition functions.

$$K^\ddagger = \exp\left(-\frac{\Delta G^\ddagger}{R \cdot T}\right) \quad (2)$$

QMT is a direct consequence of the laws of quantum mechanics. While, classically, particles trapped in a potential energy well can only escape if their energy exceeds the activation barrier  $\Delta G^\ddagger$ , quantum mechanics dictates that there is a probability for escape even if this criterion is not met. This can be illustrated by representing the particle with its wavefunction  $\Psi$  as in Figure 9.

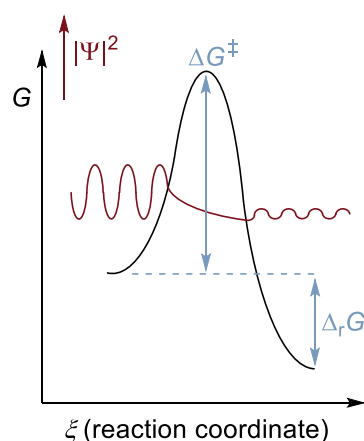


**Figure 9:** The probability for the detection of a particle on the right side of the barrier is not zero even if its energy does not exceed  $\Delta G^\ddagger$ . The particle (red) is represented by the square of the absolute value of its wavefunction  $|\Psi|^2$ , *i.e.*, the probability of localizing the particle at a specific position in space. For an observer, the particle appears to tunnel through the barrier.

Applying this concept on chemical reactions implies that there is a chance to observe reactivity even though there is not enough energy available for the starting material to overcome the transition state. This can be accounted for in TST by multiplying a correcting factor  $\kappa$ .

$$k = \kappa \cdot \frac{k_B \cdot T}{h} \cdot K^\ddagger \quad (3)$$

Jeffreys,<sup>[57]</sup> Wentzel,<sup>[58]</sup> Kramers,<sup>[59]</sup> and Brillouin<sup>[60]</sup> (JWKB) developed an approximate solution to the eigenproblem originating from Schrödinger's equation<sup>[61]</sup> to calculate the probability of a random particle to tunnel through an arbitrary energy barrier. The resulting barrier penetration integral  $\theta$  is given by equation (4).

$$\theta = \int_{s_1}^{s_2} \sqrt{2(V(x) - \varepsilon)} dx \quad (4)$$

In equation (4),  $V(x)$  is the energy potential,  $\varepsilon$  the collision energy (sometimes called attempt energy related to the attempt frequency  $\omega_0$ ), and  $s_1$  and  $s_2$  two points (known as turning points) on  $V(x)$  on either side of the barrier at the energy level  $\varepsilon$ . In terms of  $\theta$ , the JWKB transmission probability  $\kappa_{\text{JWKB}}$  is given by equation (5).

$$\kappa_{\text{JWKB}} = \frac{1}{1 + \exp(2\theta)} \quad (5)$$

The JWKB tunneling half-life  $\tau_{\text{JWKB}}$  can be calculated from equation (6) by using the speed of light  $c$  as a conversion factor.

$$\tau_{\text{JWKB}} = \frac{\log(2)}{\omega_0 \cdot c \cdot \kappa_{\text{JWKB}}} \quad (6)$$

A somewhat more instructive way to quantify QMT within the JWKB approximation for a parabolic barrier is given by equation (7). A particle's energy-dependent JWKB tunneling probability  $P(E)$  depends linearly on the activation barrier's width  $w$  and on the square root of its height  $V_0$  as well as the effective mass  $m$ . Hence, the impact on  $P(E)$  upon changing the barrier width is larger compared to a change in barrier height or particle mass. We will encounter this aspect in the case studies considered in the following section.

$$P(E) = \exp\left(\frac{-\pi^2 \cdot w \cdot \sqrt{2 \cdot m \cdot (V_0 - E)}}{h}\right) \quad (7)$$

### 1.3.2 Matrix Isolation Studies on Quantum Mechanical Tunneling

As under matrix isolation conditions most reactions cannot be realized classically (meaning the situation is similar as in Figure 9), it is not surprising that this technique proved to be of utmost importance to directly observe QMT reactions experimentally. The second requirement to elucidate the effect of QMT is the availability of reliable computational methods to predict  $\Delta G^\ddagger$ . While temperature-independent reaction rates (constant Arrhenius plots) or anomalously large kinetic isotope effects (KIE) are experimental indications for QMT, for many systems QMT rates can readily be computed.<sup>[62–64]</sup> Different software packages designed for this purpose are available.<sup>[62,65,66]</sup>

Before the emergence of the studies discussed in the following, QMT has been considered, if any, only as a means of indecisive rate acceleration by most organic chemists.<sup>[67]</sup> Note that the first experimental observation of QMT in 1928 was based on the emission of  $\text{He}^{2+}$ , a chemically relevant mass.<sup>[68]</sup> The perception of QMT as a merely quantitative (and in many cases negligible) effect on reaction rates (*e.g.*, derived from activation barriers obtained from Arrhenius plots) only changed in the last decades, when more and more examples were reported in which QMT changes the experimental outcome in a qualitative fashion.

In 2011, our group introduced the novel concept of *tunneling control*, expanding the notion of thermodynamic *versus* kinetic control.<sup>[69–71]</sup> Matrix-isolated methylhydroxycarbene (**33a**) reacts to the thermodynamic product acetaldehyde (**34a**) instead of the kinetic product vinyl alcohol (**32**) at 11 K and in the absence of external stimuli (Figure 10). Only QMT explains that any reaction occurs at all, but, what is more, only tunneling control can explain the qualitative reaction outcome. Note that a similar example has already been reported in 1994 on the C–H insertion in *tert*-butylchlorocarbene,<sup>[72]</sup> but the concept of tunneling control had not been noticed back then. Again, the availability of high-level computational tools was key to decipher the underlying reaction mechanism: for example, in the 2011 study the focal point analysis (FPA) technique<sup>[73–77]</sup> was employed on coupled-cluster<sup>[78–82]</sup>-optimized geometries.

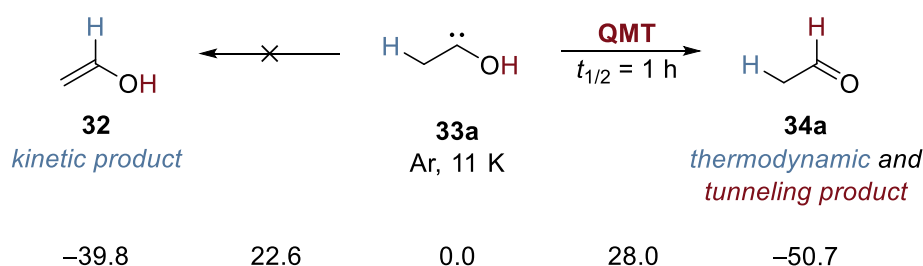


**Figure 10:** QMT control in methylhydroxycarbene (**33a**). Relative energies in kcal mol<sup>-1</sup> were computed at the FPA//AE-CCSD(T)/cc-pCVQZ<sup>[83,84]</sup> level of theory.<sup>[69]</sup>

The notion of tunneling control as the third reactivity paradigm<sup>[70]</sup> opens the door for exploiting QMT in order to achieve a desired reaction outcome that is qualitatively different from classical expectations. In 2017, Gerbig and Schreiner showed that it is even possible to obtain a tunneling product (Figure 11),<sup>[85]</sup> which could neither have formed under thermodynamic nor kinetic control.

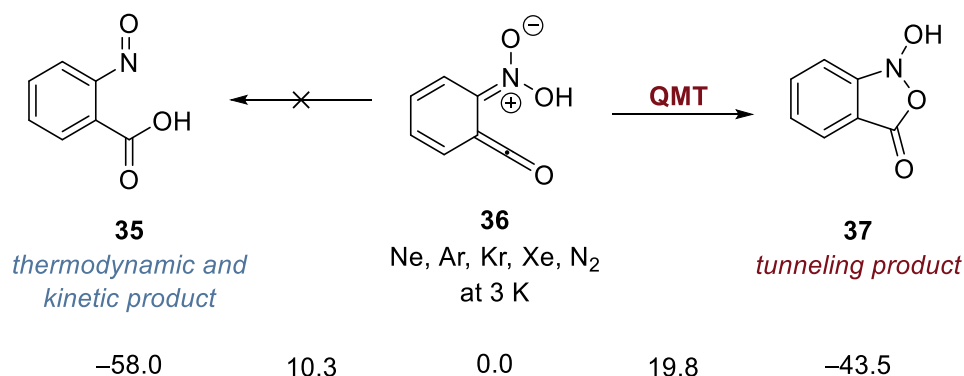


**Figure 11:** Formation of a tunneling product (**37**) from ketene **36** generated photochemically from *ortho*-nitrobenzaldehyde in various matrix hosts. Relative energies in kcal mol<sup>-1</sup> were computed at the CCSD(T)/cc-pVTZ//MP2<sup>[86]</sup>/aug-cc-pVDZ level of theory.<sup>[85]</sup>

Some systems display multiple QMT-reaction channels, *e.g.*, benzazirine **39** (Figure 12) reacts to nitrene **38** *via* nitrogen tunneling as well as to the cyclic ketenimine **40** *via* carbon tunneling.<sup>[87]</sup> A possibility of influencing the selectivity in related cases by incorporating isotope labeling of the starting material is discussed in the outlook section.

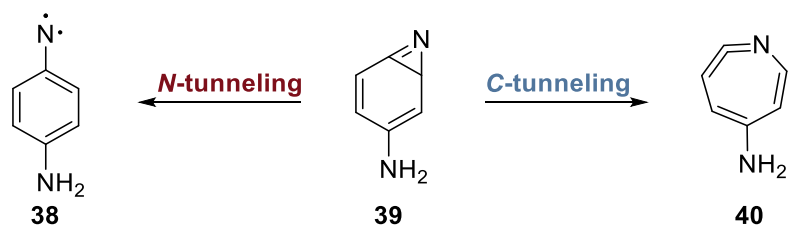


**Figure 12:** Competitive nitrogen and carbon tunneling in benzazirine **39**.<sup>[87]</sup>

The example in Figure 12 illustrates the possibility for atoms other than hydrogen to undergo QMT processes. Such reactions are summarized under the term *heavy-atom tunneling*.<sup>[88]</sup> It becomes feasible if the reaction barrier is very narrow, which is often the case in pericyclic reactions when trajectories are short.<sup>[89]</sup> Experimental examples of carbon tunneling include the unsubstituted benzazirine  $\rightarrow$  ketene rearrangement in Figure 12<sup>[90]</sup> and Cope rearrangements in substituted semibullvalenes.<sup>[91,92]</sup> The first observed of such reactions is the automerization of cyclobutadiene (**41**), which was studied using deuterium isotopologues in 1983.<sup>[93,94]</sup> The first QMT reaction of a nitrene, the nitrogen analogs of carbenes,<sup>[95]</sup> has been reported in the reaction of 2-formyl phenylnitrene to the corresponding imino ketene.<sup>[96]</sup> Some pericyclic reactions displaying QMT are depicted in Figure 13, also including cases for which QMT has been predicted computationally.

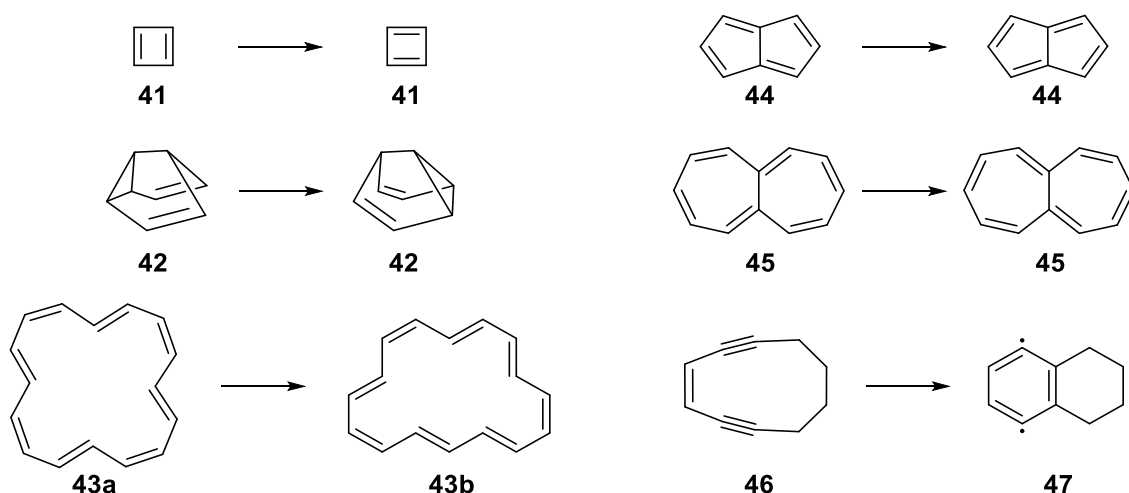


**Figure 13:** Examples of heavy-atom QMT in pericyclic reactions. The automerization in cyclobutadiene (**41**) was studied on deuterium isotopologues.<sup>[94]</sup> The Cope rearrangement in semibullvalene (**42**) was investigated using methyl derivatives.<sup>[92]</sup> The QMT reactions of [16]annulene (**43**),<sup>[97]</sup> pentalene (**44**), heptalene (**45**),<sup>[98]</sup> and the Bergman cyclization in **46** were predicted computationally.<sup>[99]</sup>

Another feature of QMT is its conformer-specificity and, in some cases, the inapplicability of the Curtin-Hammett principle.<sup>[100–102]</sup> This has been demonstrated for the hydroxycarbenes in Figure 14, for which both conceivable conformers were matrix isolated and only the *trans*-conformers (**33-t**) undergo QMT to the corresponding aldehyde (**34**).<sup>[103–105]</sup> This finding implies that QMT can be selectively switched off when generating the higher-energy *cis*-conformer (**33-c**) photochemically. Only very recently, a study reported a case where QMT can be switched on by generating a higher-energy conformer (Figure 14, *right*).<sup>[106]</sup> Again, these findings provide tools to control QMT reactivity in a desired fashion with the potential to use QMT in reaction design. The effect

is not limited to H-tunneling, but has also been observed in heavy-atom tunneling reactions of benzazirines.<sup>[107]</sup>

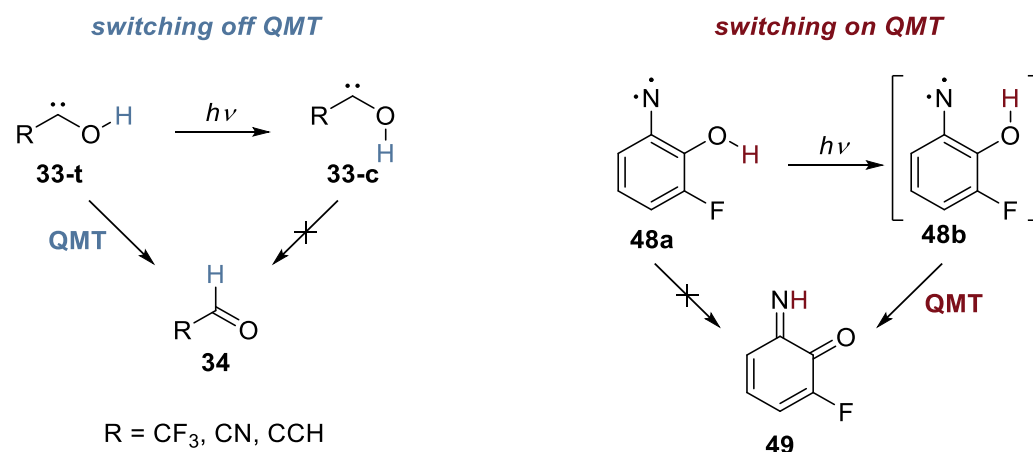


**Figure 14:** Left: Only the *trans*-conformers (**33-t**) of F<sub>3</sub>C- $\ddot{C}$ -OH,<sup>[103]</sup> NC- $\ddot{C}$ -OH,<sup>[104]</sup> and HC $\equiv$ C- $\ddot{C}$ -OH<sup>[105]</sup> undergo QMT to the corresponding carbonyl compound **34**. Right: Switching on QMT in **48**  $\rightarrow$  **49**.<sup>[106]</sup> Note that **48b** only exists as an intermediate and was not detected spectroscopically due to its short QMT half-life.

During the last years, some other hydroxycarbenes (**33**) have been isolated; the general strategy is depicted in Figure 15. Most hydroxycarbenes undergo [1,2]H-tunneling to the corresponding aldehyde (**34**). Deuteration of the OH moiety leads to the persistence of these hydroxycarbenes. The resulting huge KIEs and high-level computed activation barriers ranging from 20 to 30 kcal mol<sup>-1</sup>, which are insurmountable at cryogenic conditions, provide compelling evidence that QMT indeed enables the observed reactions. Note that the trajectory of the [1,2]H-shift (and, therefore, the barrier width) does play a decisive role as well: a computational study on mercapto- and selenomethylene excludes QMT in these compounds as the barrier widths are increased due to the longer bond lengths in H- $\ddot{C}$ -S-H and H- $\ddot{C}$ -Se-H compared to those in H- $\ddot{C}$ -O-H.<sup>[108]</sup>

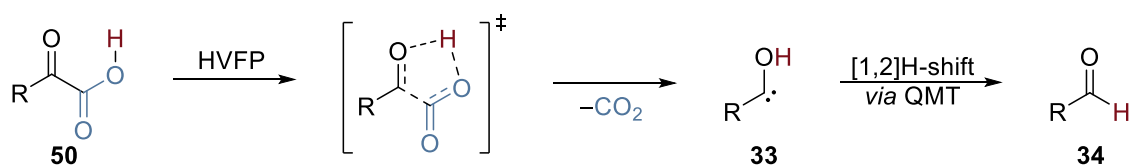


**Figure 15:** Strategy to matrix isolate hydroxycarbenes (**33**). Hydroxycarbenes with R = H,<sup>[109]</sup> Me,<sup>[69]</sup> Ph,<sup>[110]</sup> <sup>t</sup>Bu,<sup>[111]</sup> cyclopropyl,<sup>[112]</sup> CF<sub>3</sub>,<sup>[103]</sup> CN,<sup>[104]</sup> CCH,<sup>[105]</sup> OH,<sup>[113]</sup> OMe,<sup>[113]</sup> and NH<sub>2</sub><sup>[114]</sup> are known. Only the latter three do not undergo [1,2]H-shifts to the corresponding carbonyl compound **34**. Note that NC- $\ddot{C}$ -OH and HC $\equiv$ C- $\ddot{C}$ -OH were generated from the corresponding ethyl ester yielding the free  $\alpha$ -keto carboxylic acid (**50**) as intermediate *in situ*.

Hydroxycarbenes possess a singlet ground state. This is in contrast to the prototypical triplet electron configuration of carbenes according to Hund's rule.<sup>[115]</sup> However, electron donation from the oxygen lone-pairs adjacent to the carbene center stabilizes the singlet state. As this results in a double-occupied *sp*<sup>2</sup>-type ( $\sigma_{\text{out}}$ -type) orbital at carbon, such carbenes are nucleophilic in nature. Furthermore, the partial double bond character of the C-O bond leads to relatively high rotamerization barriers. Note that in some

bimagnetically stable carbenes like diphenylcarbene<sup>[116–118]</sup> and bis(*para*-methoxyphenyl)carbene<sup>[119]</sup> the singlet-triplet energy gap is so low that the spin state can be photochemically switched under matrix isolation conditions.

The simplest hydroxycarbene (R = H, **33b**) is a high-energy isomer of astrochemically relevant formaldehyde.<sup>[120]</sup> As we showed prior to my doctoral studies, hydroxymethylene can be envisaged as a building block in extraterrestrial sugar formation (*cf.* formose/Butlerow reaction<sup>[121,122]</sup>), which occurs without the need for solvent or base and is essentially barrierless.<sup>[123]</sup> The gas-phase carbonyl-ene-type reaction depicted in Figure 16 provides a rationale for the dimerization of two formaldehyde molecules: formaldehyde (**34b**, an electrophile) reacts with a nucleophilic carbene counterpart (**33b**), which can effectively be regarded as a case of Umpolung.<sup>[124]</sup> In our study, we detected C<sub>2</sub> (**51**) and C<sub>3</sub> sugars, the latter forming in a stepwise process.

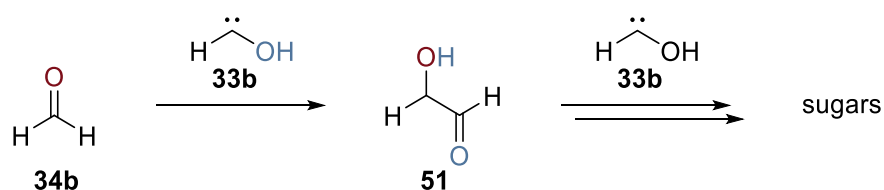


**Figure 16:** Carbonyl-ene reaction between formaldehyde (**34b**) and its high-energy isomer hydroxymethylene (**33b**).<sup>[123]</sup> This iterative gas-phase reaction might well represent an entrance channel for the formation of sugar molecules in space.

Aminohydroxymethylene (**33c**) is an H<sub>2</sub>N–C̈–OH species which might form from HCN and H<sub>2</sub>O in space. During my doctoral studies, we isolated **33c** in an Ar matrix and investigated its photoreactivity.<sup>[114]</sup> In contrast to hydroxymethylene (**33b**)<sup>[109]</sup> and aminomethylene (**53**),<sup>[125]</sup> **33c** decomposes (Figure 17) and does not undergo [1,2]H-shifts to the corresponding carbonyl (**55**, formamide) or imine (**54**, formimidic acid). However, upon pyrolysis of the precursor (oxalic acid monoamide) both **54** and **55** form among several other side products. Similar to other diheteroatom-stabilized hydroxycarbenes, **33c** does not undergo intramolecular QMT (Figure 18).

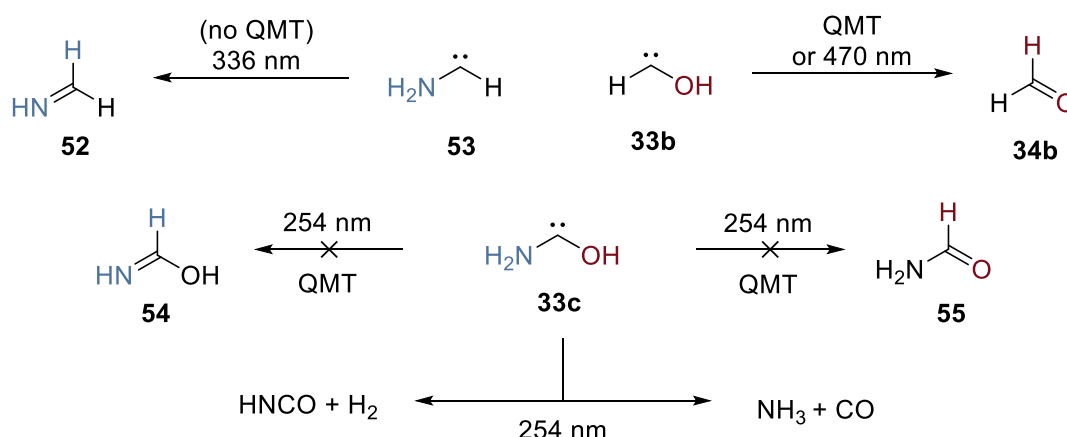


**Figure 17:** Photochemistry of aminohydroxymethylene (**33c**)<sup>[114]</sup> compared to hydroxymethylene (**33b**)<sup>[109]</sup> and aminomethylene (**53**).<sup>[125]</sup>

Another hydroxycarbene of potential astrochemical relevance is ethynylhydroxycarbene (**33d**). This compound has been suggested as an intermediate in the formation of small



acid,<sup>[145]</sup> oxalic acid monoamide (our precursor of aminohydroxymethylene, *vide supra*),<sup>[146]</sup> and a domino QMT process in oxalic acid.<sup>[147]</sup> The smaller QMT half-life of the rotamerization in acetic acid compared to formic acid was explained by the facilitated energy dissipation after formation of the lower-lying rotamer due to the presence of an alkyl rotor.<sup>[137]</sup>

In 2018, we performed an analogous investigation on the rotamerization in carbonic acid<sup>[148,149]</sup> and its monomethyl ester.<sup>[150]</sup> Somewhat counterintuitively, the QMT half-life in this system increases with the mass of the remote substituent. This is in contrast to the trend in formic, acetic, and propionic acid (Figure 19). Until now, there is no satisfactory rationale for this behavior as all barrier shapes are similar according to computed data. As intrinsic effects are to be ruled out, the effect of the surroundings, *i.e.*, the matrix material's interaction with the substrate, is likely to account for the different trends.

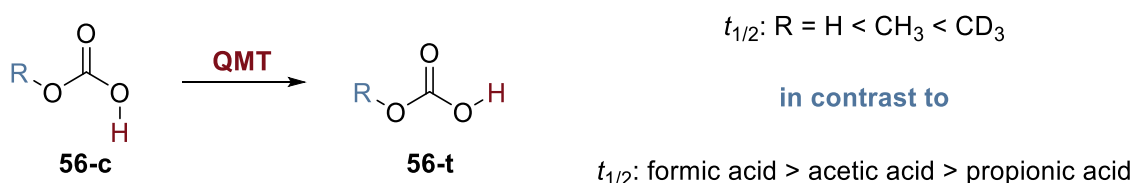


**Figure 19:** Intricate conformational QMT in carbonic acid and its (trideuterated) methyl ester.<sup>[149,150]</sup>

All case studies of conformational QMT discussed so far involve the generation of the higher-energy rotamer by irradiation at energies above the corresponding activation barrier. In 2003, however, for formic acid, C–O rotamerization could even be observed when irradiating at lower energies.<sup>[151]</sup> Such light-induced or “pumped” tunneling has been controversially debated ever since and could only be shown in another system in 2019 when the methyl-substituted Criegee intermediate was photochemically decomposed to OH radicals and various side products.<sup>[152,153]</sup> It is assumed that the lifetime of the excited species and the time spent by a tunneling atom within the barrier region must be comparable in order to observe pumped QMT. The latter was only measured in 2020 for Rb atoms and lies in the millisecond range.<sup>[154]</sup> Before this study, it was not even clear if a single QMT process can be associated with a time at all or happens instantaneously.<sup>[155]</sup>

When studying high-energy conformers, it becomes obvious that the matrix host material has a severe impact on their persistence. For example, the high-energy conformer of the hydrocarboxyl radical (HOCO) was only detected in N<sub>2</sub> but not in Ar matrices.<sup>[156]</sup> Its QMT reaction to the low-energy conformer in Ar is too fast to be measurable. The same is true for *cis-cis*-dihydroxycarbene (HO–C̈–OH, *vide infra*). The stabilizing effect of N<sub>2</sub> is attributed to its higher polarizability compared to Ar. A similar trend can be observed when comparing Ar with Kr matrices. As external parameters influence QMT, these provide another tool to control this effect, especially when thinking about standard wet-laboratory conditions and the variety of accessible solvents. One might also think about enhancing QMT in a catalytic manner. Just recently, the first Lewis acid catalyzed QMT reaction under matrix isolation conditions was reported.<sup>[157]</sup>

Conformational equilibria can be well studied by using near-infrared (NIR) light to interconvert specific conformers into each other. This is usually achieved by excitation

of overtones or combinational bands of O–H or N–H stretching vibrations with the help of lasers. While such irradiation typically leads to rotamerizations in the proximity of the excited bond, other examples are known where the above mentioned groups serve as antennae to induce remote reactions. These include 6-methoxyindole,<sup>[158]</sup> kojic acid,<sup>[159]</sup> NH<sub>2</sub>- and OH-substituted 2-formyl-2*H*-azirine,<sup>[160]</sup> and 2,6-difluoro-4-hydroxy-2*H*-benzazirine.<sup>[161]</sup> Generally, the reactions induced by this method are very clean, *i.e.*, the resulting IR difference spectra are relatively easy to interpret as ideally only one reaction occurs at a time. This is in contrast to UV excitation, which often leads to various side reactions due to the higher energy input into the system and the generation of electronically excited states. The main drawback is that overtones or combinational bands in the NIR region are usually small in intensity and, hence, difficult to detect. There are, however, exceptions, *e.g.*, the first overtone of the N–H stretching vibration in the thiolimine tautomer of thioacetamide is slightly more intense than its fundamental band.<sup>[53]</sup> In some carboxylic acids rotamerization could even be induced by excitation of the second O–H overtone.<sup>[162]</sup>

We applied the strategy of NIR excitation to generate the hitherto unreported *cis-cis*-conformer of dihydroxycarbene (**33j-cc**, Figure 20),<sup>[163]</sup> an underappreciated isomer of the simplest Criegee intermediate (*vide supra*) although it is *lower* in energy.

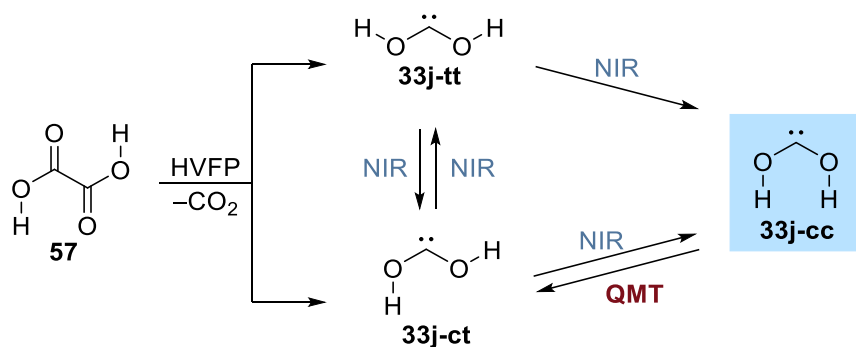


**Figure 20:** Generation and reactivity of *cis-cis*-dihydroxycarbene (**33j-cc**).<sup>[163]</sup>

Once generated, **33j-cc** spontaneously interconverts to *cis-trans*-dihydroxycarbene (**33j-ct**) *via* QMT within a half-life of ca. 22 min in an N<sub>2</sub> matrix. When evaluating the decay of **33j-cc** and the increase of **33j-ct**, both rates cannot be satisfactorily fit when using the identical mathematical model. Only when allowing for a competitive reaction, good agreement can be achieved (Figure 21). Note that the **33j-cc** depletion in Ar is too fast to record its kinetics.

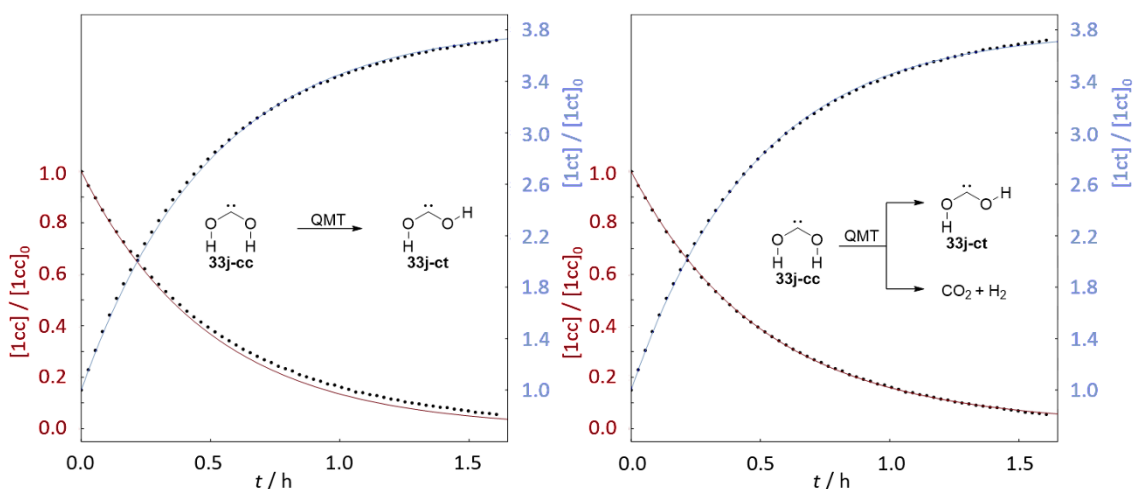


**Figure 21:** Kinetics of the IR band profile of **33j-cc** and **33j-ct** using models that do not (*left*) and do (*right*) account for a side reaction forming  $\text{CO}_2 + \text{H}_2$ .<sup>[163]</sup> Experimental values are shown in black and fit curves in red and blue, respectively.

Computations suggest that the side reaction taking place is the decomposition of **33j-cc** to  $\text{CO}_2$  and  $\text{H}_2$ , both of which are, unfortunately, not detectable spectroscopically: the high amounts of  $\text{CO}_2$  after pyrolysis prohibit the observability of small changes in the  $\text{CO}_2$  concentration. Attempts to indirectly prove the occurrence of this reaction using the mono- and dideuterated isotopologues of **33j** failed due to very low concentrations of the carbene after pyrolysis or the inability to overcome the rotamerization barrier when exciting O–D overtones. Nevertheless, our study indicates that  $\text{CO}_2$  might take part in QMT reactions. The outlook section presents ongoing work to activate  $\text{CO}_2$  in a heavy-atom QMT process using a carbene.

### 1.3.3 Quantum Mechanical Tunneling in Reactions Conducted under Ambient Conditions

Before briefly discussing our ongoing work, it is worthwhile to have a look at QMT reactions that have been observed under ambient conditions.<sup>[164]</sup> In the following case studies, QMT usually is more concealed than under cryogenic conditions, as many activation barriers can be overcome. Hence, measuring temperature effects as well as KIEs and comparing them to computed data is crucial to determine the contribution of QMT to a reaction rate. Nowadays, sufficient studies exist to conclude that QMT is an effect that does not play a role under matrix isolation conditions exclusively. While the focus of the work conducted herein is on matrix isolation studies, it will be interesting to see which effects discussed in Section 1.3.2 reappear in future ambient-condition experiments.

The [1,2]H-shift in phenylhydroxycarbene (**33h**, Figures 15 and 18) has been studied at temperatures between 320 and 350 K.<sup>[165]</sup> The measured  $k(\text{OH})/k(\text{OD})$  KIE of ca. 20 suggests that QMT still has a large contribution in this reaction even at elevated temperatures and not only under matrix isolation conditions, as discussed above.

An example of a typical laboratory reaction in which measured  $^{13}\text{C}$  KIEs are higher than conventional TST values (neglecting QMT) is provided by the Roush allylboration of *para*-anisaldehyde.<sup>[166]</sup> Only when incorporating QMT into the computations the measured rates can be fit satisfactorily. The acceleration due to QMT is a factor of 1.36 at the reaction temperature of  $-78\text{ }^\circ\text{C}$ . The authors conclude that “heavy-atom tunneling plays a role in simple everyday organic reactions”.<sup>[166]</sup>

In 2016, a study showed that a nonheme manganese(III)-peroxo complex reacts with aldehydes through hydrogen atom abstraction instead of nucleophilic addition.<sup>[167,168]</sup> Later, temperature-dependent kinetic measurements performed on the reaction of a nonheme iron(III)-hydroperoxo complex (**59**) with **58** concluded that QMT can dominate such hydrogen abstractions (Figure 22, *left*).<sup>[169]</sup> The reaction mechanism of this reaction changes from nucleophilic addition to hydrogen atom abstraction when going from higher to lower temperatures; the latter mechanism is associated with a KIE of 93 at 203 K. Note that classic  $k(\text{H})/k(\text{D})$  KIEs have maximum values between 6 and 8. In a related system, deuteration changes the regioselectivity of the hydrogen abstraction leading to the deformylation product **61** or carboxylic acid **62**, respectively (Figure 22, *right*).<sup>[170]</sup> Although QMT was not discussed in the latter study, it opens the door to control reactivity in new ways by exploiting large KIEs.

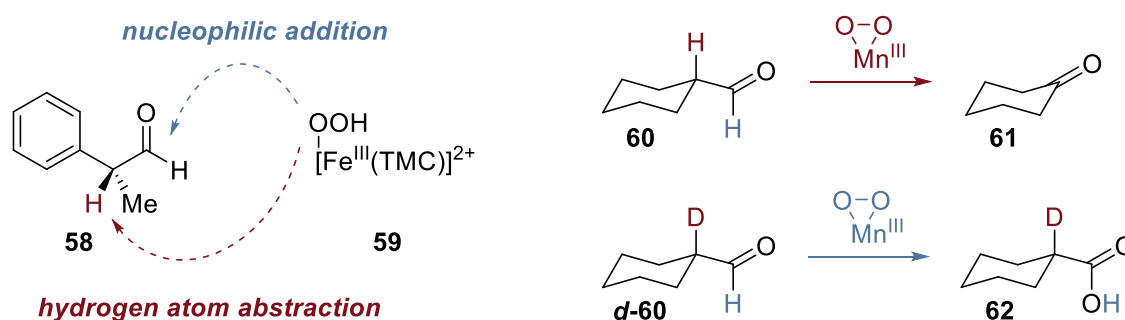


**Figure 22:** *Left:* The reaction mechanism depends on the temperature with the hydrogen atom abstraction being dominated by QMT at lower temperatures (TMC = 1,4,8,11-tetramethyl-1,4,8,11-tetraazacyclotetradecane).<sup>[169]</sup> *Right:* Deuteration changes the reaction outcome due to an immense KIE.<sup>[170]</sup> The ligands of the manganese(III)-peroxo complex are omitted for clarity.

With such intriguing results at hand, we are confident that QMT will be exploited in ambient-condition reactions in the future and are looking forward to new possibilities to manage reaction control.

### 1.3.4 Computational Predictions on Quantum Mechanical Tunneling

As mentioned in the previous sections, the role of quantum chemical computations to detect QMT cannot be overestimated. In this section, we briefly summarize a few examples, which elucidate aspects of QMT not discussed in earlier sections. However, other studies predicting QMT have already been mentioned above.

A somewhat exotic example of the possibility of fluoride tunneling in **63**<sup>[171]</sup> was reported by Kozuch *et al.* in 2018 (Figure 23, *left*).<sup>[172]</sup> The effect of the linker (Y) on QMT half-lives was studied computationally. Such “ping-pong QMT” has later also been suggested for boron and carbon in similar compounds.<sup>[173]</sup> The same group also proposed carbon

QMT automerizations in specially designed fulvalenes.<sup>[174]</sup> Similarly, results were published on the automerization of the cyclopropenyl anion.<sup>[175]</sup> However, if the ring is substituted with groups other than hydrogen, QMT is inhibited due to the non-planarity of the system and the resulting long trajectories of the attached groups.<sup>[175]</sup> These studies test the limits of QMT (*i.e.*, heavy atoms or long trajectories) and aim to establish rules of thumb for when to expect QMT.

In a different vein, QMT deemed the computationally predicted record of the shortest C–C bond in a bridged tetrahedryl-tetrahedrane (**64**)<sup>[176]</sup> impossible to observe, because the molecule would rearrange very quickly even under cryogenic conditions *via* QMT (Figure 23, *right*).<sup>[177]</sup> The reaction is highly exergonic even though the resulting product is a carbene (**65**). Hence, when discussing the viability of computed minimum structures,<sup>[178]</sup> QMT has to be taken into account apart from activation barriers' heights.

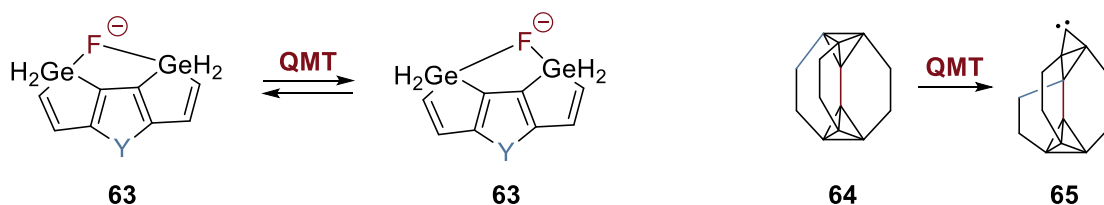


**Figure 23:** Computationally predicted QMT reactions. *Left:* Ping-pong tunneling of fluoride (Y = S, SO<sub>2</sub>, Se, SeO<sub>2</sub>, SiH<sub>2</sub>, CH<sub>2</sub>, O).<sup>[172]</sup> *Right:* **64** is not persistent even at 0 K, because it quickly rearranges to **65** *via* QMT.<sup>[177]</sup>

## 1.4 Outlook

During my doctoral studies, we worked on two more projects, which have not been published yet. Preliminary results are presented briefly in the following.

### 1.4.1 CO<sub>2</sub> Activation with Aminomercaptocarbene

In a hitherto unpublished cooperation with Markus Schauermann, we investigated the possibility of activating CO<sub>2</sub> in a QMT reaction using a carbene, namely aminomercaptocarbene (**67**). Mercaptocarbenes are hitherto rather elusive species as only parent thiohydroxymethylene could be detected.<sup>[179]</sup> Initial attempts to generate **67** *via* pyrolysis of 2-amino-2-thioxoacetic acid (**68**) employing the standard procedure discussed in Figure 15 failed, because the reaction profiles of the decarboxylation of oxalic acid monoamide (**66**) and **68** are highly temperature dependent (Figure 24). While aminohydroxymethylene (**33c**) lies in a rather deep potential well, **67** readily undergoes a consecutive reaction to thioformamide (**30a**) at 1000 °C. This temperature resembles the pyrolysis conditions and we observed **30a** as the main pyrolysis product in agreement with our computed data.

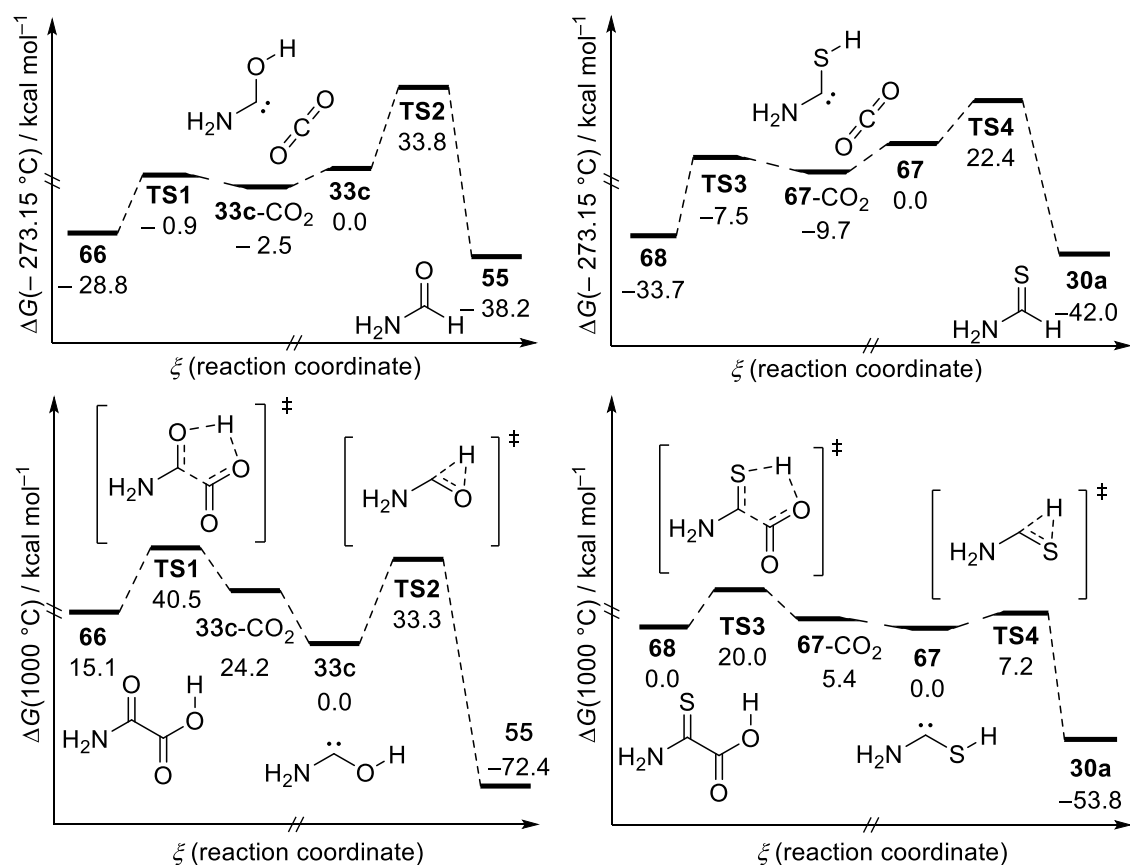


**Figure 24:** Potential energy surfaces of the decarboxylation of **66** (left) and **68** (right) at 0 K (top) and 1000 °C (bottom), respectively, computed at the B3LYP/6-311+G(3df,3pd) level of theory.<sup>[114]</sup>

Therefore, we decided to perform the decarboxylation of **68** photochemically and indeed were able to generate **67** complexed with CO<sub>2</sub> (**67-CO<sub>2</sub>**). Once generated, **67-CO<sub>2</sub>** reacts back to the starting material **68** at 3 K. This reaction occurs spontaneously *via* heavy-atom QMT when keeping the matrix in the dark as deduced from measured and computed Arrhenius plots (Figure 25). The possibility to activate CO<sub>2</sub> and form a neutral product (and not a zwitterion) using a carbene is unprecedented. Note that the underlying mechanism is analogous to the carbonyl-ene reaction presented above (Figure 16), but uses CO<sub>2</sub> as the carbonyl species.

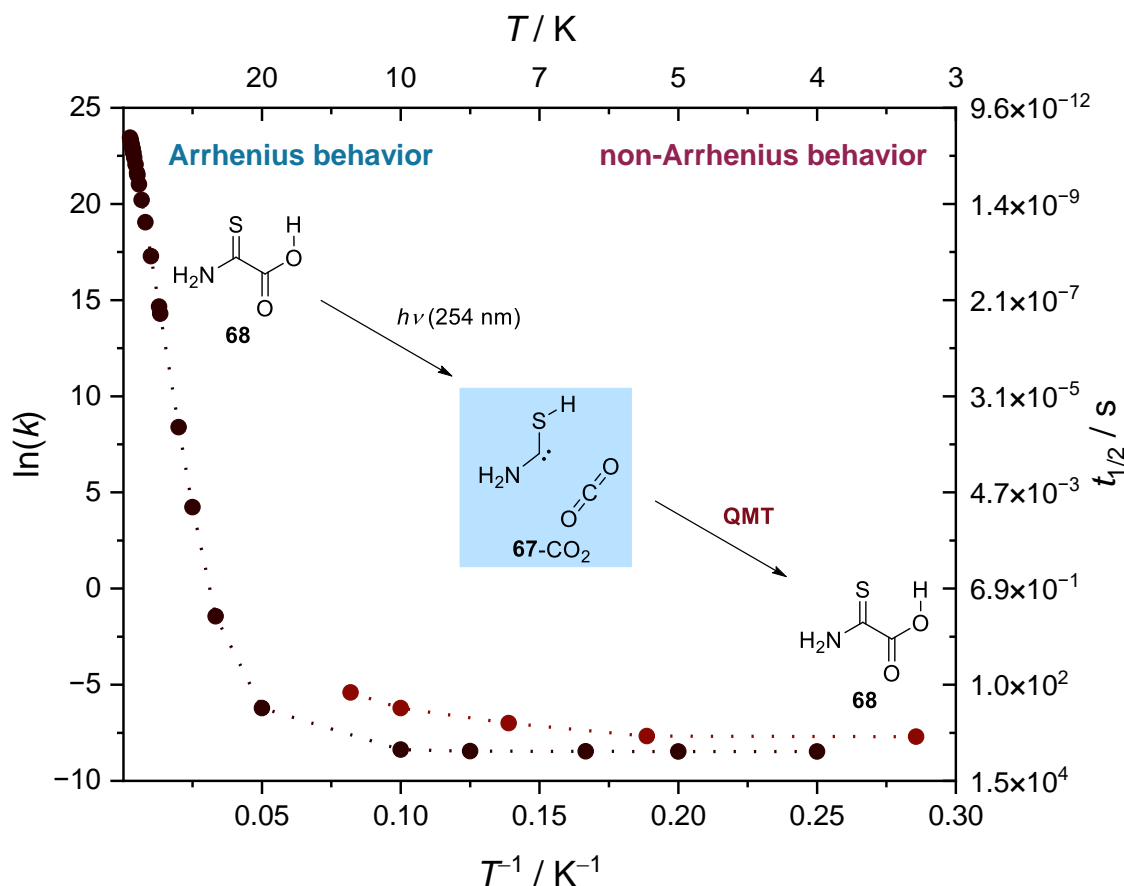


**Figure 25:** Arrhenius plot of the  $67\text{-CO}_2 \rightarrow 68$  reaction. *Red points:* Experimental data. *Black points:* Values computed at the CVT/SCT//B3LYP/6-311+G(d,p) level of theory. The left-hand trend of the computed values agrees with classical Arrhenius behavior while the constant right-hand trend represents the QMT limit of the reaction.

### 1.4.2 Isotope-Controlled Selectivity by QMT

As QMT is highly dependent on the mass of the atoms moving throughout the reaction, isotope-controlled selectivity by QMT seems feasible. In a computational study such cases were predicted (Figure 26).<sup>[180]</sup> However, an experimental study on this effect remains yet to be conducted.

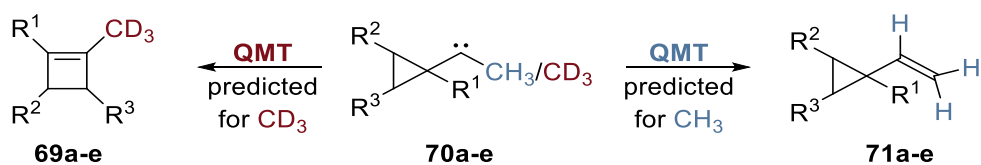


**Figure 26:** Isotope-controlled selectivity by QMT. The isotopologue determines whether **70** reacts to **69** or **71** as shown by computations.<sup>[180]</sup> **a:**  $R_1 = \text{OMe}$ ,  $R_2 = \text{H}$ ,  $R_3 = \text{H}$ ; **b:**  $R_1 = \text{F}$ ,  $R_2 = \text{H}$ ,  $R_3 = \text{CH}_3$ ; **c:**  $R_1 = \text{F}$ ,  $R_2 = \text{CH}_3$ ,  $R_3 = \text{CH}_3$ ; **d:**  $R_1 = \text{F}$ ,  $R_2 = \text{F}$ ,  $R_3 = \text{H}$ ; **e:**  $R_1 = \text{F}$ ,  $R_2 = \text{F}$ ,  $R_3 = \text{F}$ .

During my research visit at the Institut Ruđer Bošković (Zagreb, Croatia), we synthesized various diazirines (**74**, **78**, and **82**) depicted in Figure 27 according to established literature procedures.<sup>[181–183]</sup>

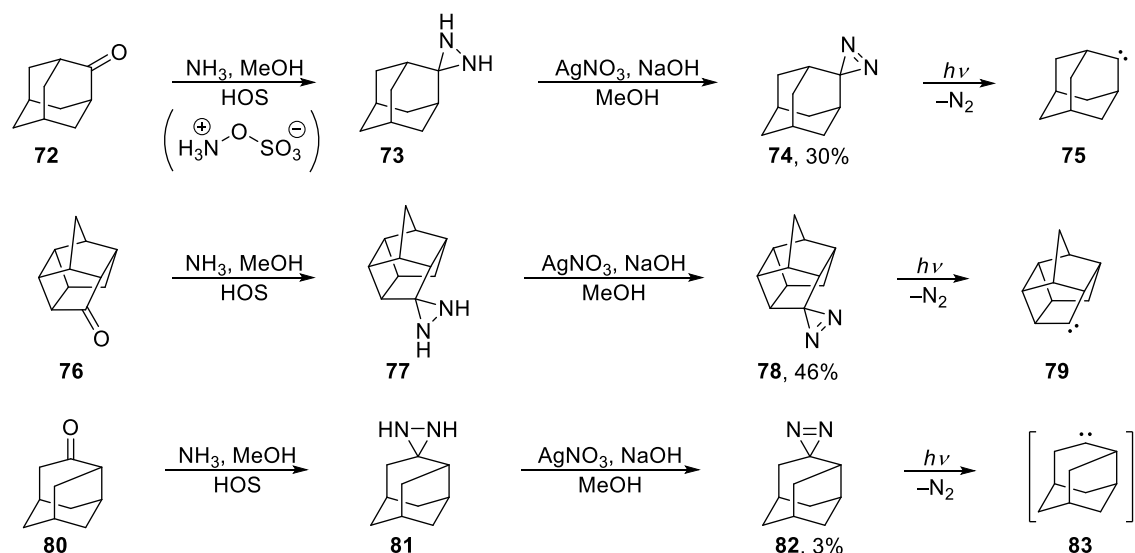


**Figure 27:** Syntheses of diazirines **74**, **78**, and **82**. Yields of the isolated diazirines are given with respect to both steps. Carbenes **75**, **79**, and **83** were photochemically generated under matrix isolation conditions.

In a hitherto unpublished matrix isolation study, we photochemically generated the polycyclic singlet carbenes **75** and **79** from **74** and **78**, respectively. While **79** is persistent in an Ar matrix at 3 K, adamantylidene (**75**) tunnels to 2,4-dehydroadamantane (**84**) within a half-life of ca. 10 h (Figure 28). This confirms a computational prediction by Kozuch from 2014<sup>[184]</sup> and adds to an experimental study by Bally *et al.* from 1994.<sup>[185]</sup> Irradiating **79** at 627 nm leads to its interconversion, presumably to homopentaprismane (churchane, **85**). The latter finding still needs to be verified with reference experiments.

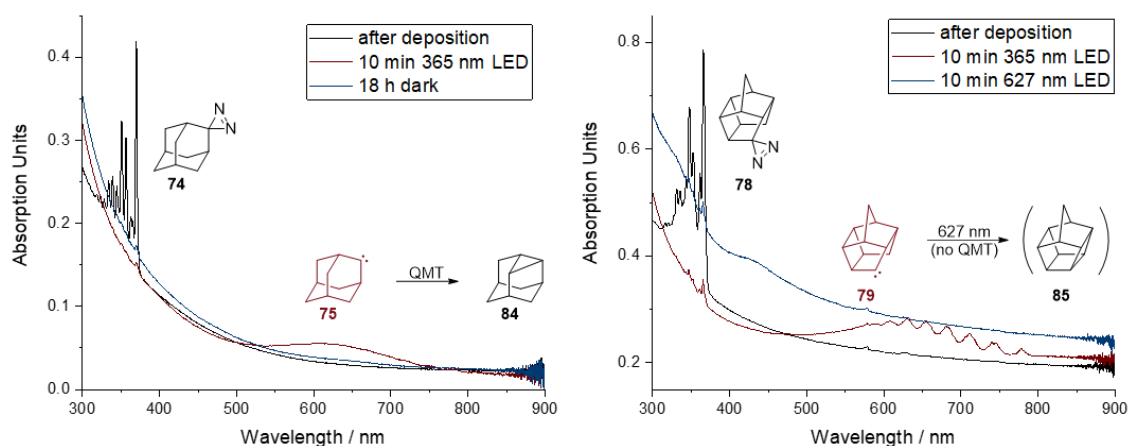


**Figure 28:** Experimental matrix UV/Vis spectra displaying the reactivity of **75** (left) and **79** (right). Note that the presence of **85** needs further experimental verification.

Performing the analogous experiment with protoadamantane diazirine (**82**) does not yield the corresponding carbene **83**, but rather its [1,2]H-shift product **86** (Figure 29). This is in accord with our computed half-life of only 33 ms of protoadamantylidene (**83**) making it unobservable even at cryogenic temperatures. We also synthesized the  $\alpha,\alpha$ -dideuterated isotopologue of **82**. We expect a different reaction outcome for the corresponding carbene isotopologue ( $d_2$ -**83**) as depicted in Figure 29. If this holds true, this would provide the first experimental example of isotope-controlled selectivity by QMT.

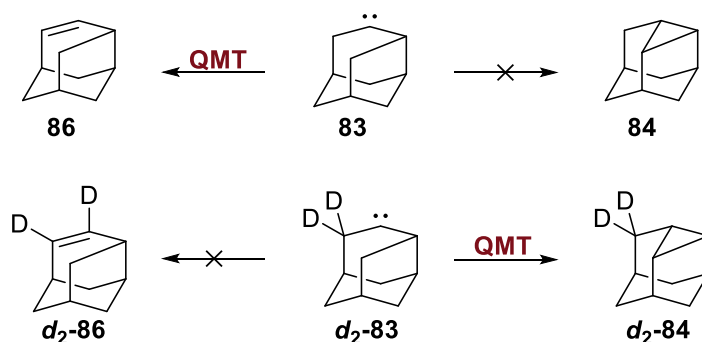


**Figure 29:** Isotope-controlled selectivity by QMT in protoadamantylidene (**83**) and its dideuterated isotopologue (**d<sub>2</sub>-83**).

## 1.5 Concluding Remarks

We isolated two novel hydroxycarbenes, **33d** and **33c**, whose reactivity is in line with the other members of this compound class. While QMT half-lives of hydroxycarbenes can be rationalized on the basis of the electronic properties of the substituent, this is not as easily conceived for other reactions like thiolimine  $\rightarrow$  thioamide tunneling or rotamerizations in carboxylic acids. In the latter case, external effects, like the matrix material, presumably play a decisive role, which we just begin to comprehend. Future work should focus on disentangling intrinsic and external influences on QMT. This might enable controlling QMT *via* external parameters and, eventually, introducing a new technique to manage reaction control even under standard laboratory conditions.



**Figure 30:** Overview of novel compounds generated in this work.

The four species displayed in Figure 30 potentially play a role in astrochemical or atmospheric processes. For instance, thioformamide and its thiolimine tautomer **31a** are viable interstellar compounds and *cis-cis*-dihydroxycarbene (**33j-cc**), an isomer of the simplest Criegee intermediate, is a likely active species in the reaction of CO<sub>2</sub> with H<sub>2</sub> towards formic acid. The latter example hints towards the possibility of CO<sub>2</sub> to participate in QMT processes. Activating CO<sub>2</sub> in a heavy-atom QMT reaction as presented in Section 1.4.1. provides a new means for this high-interest endeavor. Generally, QMT is an abundant phenomenon in chemical reactions and we are looking forward to future studies proceeding from observing to controlling and using this intriguing quantum effect.

## 1.6 Bibliography

- [1] Reymond, J. L.; Awale, M. Exploring chemical space for drug discovery using the chemical universe database. *ACS Chem. Neurosci.* **2012**, *3*, 649–657.
- [2] Woon, D. E. Interstellar and circumstellar molecules. **2021**, [http://www.astrochymist.org/astrochymist\\_ism.html](http://www.astrochymist.org/astrochymist_ism.html)
- [3] Matthews, H. E.; Irvine, W. M.; Friberg, P.; Brown, R. D.; Godfrey, P. D. A new interstellar molecule:

- tricarbon monoxide. *Nature* **1984**, *310*, 125–126.
- [4] Brown, R. D.; Godfrey, P. D.; Cragg, D. M.; Rice, E. H. N.; Irvine, W. M.; Friberg, P.; Suzuki, H.; Ohishi, M.; Kaifu, N.; Morimoto, M. Tricarbon monoxide in TMC-1. *Astrophys. J.* **1985**, *297*, 302–308.
- [5] Herbst, E. Chemistry in the interstellar medium. *Annu. Rev. Phys. Chem.* **1995**, *46*, 27–53.
- [6] Feuchtgruber, H.; Helmich, F. P.; van Dishoeck, E. F.; Wright, C. M. Detection of interstellar CH<sub>3</sub>. *Astrophys. J.* **2000**, *535*, 111–114.
- [7] Irvine, W. M.; Brown, R. D.; Cragg, D. M.; Friberg, P.; Godfrey, P. D.; Kaifu, N.; Matthews, H. E.; Ohishi, M.; Suzuki, H.; Takeo, H. A new interstellar polyatomic molecule: detection of propynal in the cold cloud TMC-1. *Astrophys. J.* **1988**, *335*, 89–93.
- [8] Halfen, D. T.; Ziurys, L. M.; Brünken, S.; Gottlieb, C. A.; McCarthy, M. C.; Thaddeus, P. Detection of a new interstellar molecule: thiocyanic acid HSCN. *Astrophys. J.* **2009**, *702*, 124–127.
- [9] Cernicharo, J.; Cabezas, C.; Endo, Y.; Agúndez, M.; Tercero, B.; Pardo, J. R.; Marcelino, N.; de Vicente, P. The sulphur saga in TMC-1: discovery of HCSCN and HCSCCH. *Astron. Astrophys.* **2021**, *650*, 10–17.
- [10] Rivilla, V. M.; Jiménez-Serra, I.; Martín-Pintado, J.; Briones, C.; Rodríguez-Almeida, L. F.; Rico-Villas, F.; Tercero, B.; Zeng, S.; Colzi, L.; de Vicente, P.; Martín, S.; Requena-Torres, M. A. Discovery in space of ethanolamine, the simplest phospholipid head group. *Proc. Natl. Acad. Sci. USA* **2021**, *118*, 1–8.
- [11] Wang, S.; Maltrud, M.; Elliott, S.; Cameron-Smith, P.; Jonko, A. Influence of dimethyl sulfide on the carbon cycle and biological production. *Biogeochemistry* **2018**, *138*, 49–68.
- [12] Bates, T. S.; Lamb, B. K.; Guenther, A.; Dignon, J.; Stoiber, R. E. Sulfur emissions to the atmosphere from natural sources. *J. Atmos. Chem.* **1992**, *14*, 315–337.
- [13] Tyndall, G. S.; Ravishankara, A. R. Atmospheric oxidation of reduced sulfur species. *Int. J. Chem. Kinet.* **1991**, *23*, 483–527.
- [14] Stephens, E. R. Chemistry of atmospheric oxidants. *J. Air Pollut. Control Assoc.* **1969**, *19*, 181–185.
- [15] Barnes, I.; Hjorth, J.; Mihalopoulos, N. Dimethyl sulfide and dimethyl sulfoxide and their oxidation in the atmosphere. *Chem. Rev.* **2006**, *106*, 940–975.
- [16] Heard, D. The X factor. *Nature* **2012**, *488*, 164–165.
- [17] Su, Y.-T.; Lin, H. Y.; Putikam, R.; Matsui, H.; Lin, M. C.; Lee, Y. P. Extremely rapid self-reaction of the simplest Criegee intermediate CH<sub>2</sub>OO and its implications in atmospheric chemistry. *Nat. Chem.* **2014**, *6*, 477–483.
- [18] Lee, Y. P. Perspective: Spectroscopy and kinetics of small gaseous Criegee intermediates. *J. Chem. Phys.* **2015**, *143*, 1–16.
- [19] Criegee, R.; Wenner, G. Die Ozonisierung des 9,10-Oktalins. *Liebigs Ann. Chem.* **1949**, *564*, 9–15.
- [20] Criegee, R. Mechanismus der Ozonolyse. *Angew. Chem.* **1975**, *87*, 765–771.
- [21] Reisenauer, H. P.; Romański, J.; Młostoń, G.; Schreiner, P. R. Matrix isolation and spectroscopic properties of the methylsulfinyl radical CH<sub>3</sub>(O)S'. *Chem. Commun.* **2013**, *49*, 9467–9469.
- [22] Reisenauer, H. P.; Romański, J.; Młostoń, G.; Schreiner, P. R. Reactions of the methylsulfinyl radical [CH<sub>3</sub>(O)S'] with oxygen (<sup>3</sup>O<sub>2</sub>) in solid argon. *Chem. Commun.* **2015**, *51*, 10022–10025.
- [23] Reisenauer, H. P.; Schreiner, P. R.; Romański, J.; Młostoń, G. Gas-phase generation and matrix isolation of the methylsulfonyl radical CH<sub>3</sub>SO<sub>2</sub>' from allylmethylsulfone. *J. Phys. Chem. A* **2015**, *119*, 2211–2216.
- [24] Zhu, B.; Zeng, X.; Beckers, H.; Francisco, J. S.; Willner, H. The methylsulfonyloxyl radical, CH<sub>3</sub>SO<sub>3</sub>. *Angew. Chem. Int. Ed.* **2015**, *54*, 11404–11408.
- [25] Mardyukov, A.; Schreiner, P. R. Atmospherically relevant radicals derived from the oxidation of dimethyl sulfide. *Acc. Chem. Res.* **2018**, *51*, 475–483.
- [26] Gerbig, D.; Bernhardt, B.; Wende, R. C.; Schreiner, P. R. Capture and reactivity of an elusive carbon–sulfur centered biradical. *J. Phys. Chem. A* **2020**, *124*, 2014–2018.
- [27] Wu, Z.; Wang, L.; Lu, B.; Eckhardt, A. K.; Schreiner, P. R.; Zeng, X. Spectroscopic characterization and photochemistry of the vinylsulfinyl radical. *Phys. Chem. Chem. Phys.* **2021**, *23*, 16307–16315.
- [28] Lu, B.; Wu, Z.; Wang, L.; Zhu, B.; Rauhut, G.; Zeng, X. The simplest alkynyl thiocyanate HCCSCN and its isomers. *Chem. Commun.* **2021**, *57*, 3343–3346.
- [29] Xu, J.; Wu, Z.; Wan, H.; Deng, G.; Lu, B.; Eckhardt, A. K.; Schreiner, P. R.; Trabelsi, T.; Francisco, J. S.; Zeng, X. Phenylsulfinyl radical: gas-phase generation, photoisomerization, and oxidation. *J. Am. Chem. Soc.* **2018**, *140*, 9972–9978.
- [30] Wu, Z.; Wan, H.; Xu, J.; Lu, B.; Lu, Y.; Eckhardt, A. K.; Schreiner, P. R.; Xie, C.; Guo, H.; Zeng, X. The near-UV absorber OSSO and its isomers. *Chem. Commun.* **2018**, *54*, 4517–4520.
- [31] Liu, Q.; Wu, Z.; Xu, J.; Lu, Y.; Li, H.; Zeng, X. Methoxysulfinyl radical CH<sub>3</sub>OSO: gas-phase generation, photochemistry, and oxidation. *J. Phys. Chem. A* **2017**, *121*, 3818–3825.
- [32] Wu, Z.; Liu, Q.; Xu, J.; Sun, H.; Li, D.; Song, C.; Andrada, D. M.; Frenking, G.; Trabelsi, T.; Francisco, J. S.; Zeng, X. Heterocumulene sulfinyl radical OCNSO. *Angew. Chem. Int. Ed.* **2017**, *56*, 2140–2144.
- [33] Wu, Z.; Xu, J.; Liu, Q.; Dong, X.; Li, D.; Holzmann, N.; Frenking, G.; Trabelsi, T.; Francisco, J. S.; Zeng, X. The hypothiocyanite radical OSCN and its isomers. *Phys. Chem. Chem. Phys.* **2017**, *19*, 16713–16720.
- [34] Chen, C.; Wang, L.; Zhao, X.; Wu, Z.; Bernhardt, B.; Eckhardt, A. K.; Schreiner, P. R.; Zeng, X. Photochemistry of HNSO<sub>2</sub> in cryogenic matrices: spectroscopic identification of the intermediates and mechanism. *Phys. Chem. Chem. Phys.* **2020**, *22*, 7975–7983.
- [35] Ganapathi, K.; Venkataramen, A. Chemistry of thiazoles. *Proc. Indian Acad. Sci. Sect. A* **1945**, *22*, 362–378.
- [36] Patel, B. H.; Percivalle, C.; Ritson, D. J.; Duffy, C. D.; Sutherland, J. D. Common origins of RNA, protein and lipid precursors in a cyanosulfidic protometabolism. *Nat. Chem.* **2015**, *7*, 301–307.
- [37] Murai, T. Chemistry of Thioamides. **2019**, Springer.

- [38] Tull, R.; Weinstock, L. M. A new synthesis of thioformamide. *Angew. Chem. Int. Ed.* **1969**, *8*, 278–279.
- [39] Snyder, L. E.; Buhl, D. Observation of radio emission from interstellar hydrogen cyanide. *Astrophys. J.* **1971**, *163*, 47–52.
- [40] Thaddeus, P.; Kutner, M. L.; Penzias, A. A.; Wilson, R. W.; Jefferts, K. B. Interstellar hydrogen sulfide. *Astrophys. J.* **1972**, *176*, 73–76.
- [41] Willstätter, R.; Wirth, T. Über Thioformamid. *Ber. Dtsch. Chem. Ges.* **1909**, *42*, 1908–1922.
- [42] Bernhardt, B.; Dressler, F.; Eckhardt, A. K.; Becker, J.; Schreiner, P. R. Characterization of the simplest thiolimine: the higher energy tautomer of thioformamide. *Chem. Eur. J.* **2021**, *27*, 6732–6739.
- [43] Nowak, M. J.; Lapinski, L.; Rostkowska, H.; Leś, A.; Adamowicz, L. Theoretical and matrix-isolation experimental study on 2(1*H*)-pyridinethione/2-pyridinethiol. *J. Phys. Chem.* **1990**, *94*, 7406–7414.
- [44] Nowak, M. J.; Lapinski, L.; Fulara, J.; Leś, A.; Adamowicz, L. Theoretical and infrared matrix isolation study of 4(3*H*)-pyrimidinethione and 3(2*H*)-pyridazinethione. Tautomerism and phototautomerism. *J. Phys. Chem.* **1991**, *95*, 2404–2411.
- [45] Lapinski, L.; Rostkowska, H.; Khvorostov, A.; Yaman, M.; Fausto, R.; Nowak, M. J. Double-proton-transfer processes in dithioamide: UV-induced dithione → dithiol reaction and ground-state dithiol → dithione tunneling. *J. Phys. Chem. A* **2004**, *108*, 5551–5558.
- [46] Prusinowska, D.; Lapinski, L.; Nowak, M. J.; Adamowicz, L. Tautomerism, phototautomerism and infrared spectra of matrix-isolated 2-quinolinethione. *Spectrochim. Acta Part A Mol. Spectrosc.* **1995**, *51*, 1809–1826.
- [47] Brás, E. M.; Fausto, R. An insight into methimazole phototautomerism: central role of the thyl radical and effect of benzo substitution. *J. Mol. Struct.* **2018**, *1172*, 42–54.
- [48] Brás, E. M.; Fausto, R. Controlled light-driven switching in 2-thiobenzimidazole. *J. Photochem. Photobiol. A Chem.* **2018**, *357*, 185–192.
- [49] Rostkowska, H.; Lapinski, L.; Khvorostov, A.; Nowak, M. J. Proton-transfer processes in thiourea: UV induced thione → thiol reaction and ground state thiol → thione tunneling. *J. Phys. Chem. A* **2003**, *107*, 6373–6380.
- [50] Rostkowska, H.; Lapinski, L.; Nowak, M. J. Hydrogen-atom tunneling through a very high barrier; spontaneous thiol → thione conversion in thiourea isolated in low-temperature Ar, Ne, H<sub>2</sub> and D<sub>2</sub> matrices. *Phys. Chem. Chem. Phys.* **2018**, *20*, 13994–14002.
- [51] Lapinski, L.; Rostkowska, H.; Khvorostov, A.; Nowak, M. J. UV induced proton transfer in thioacetamide: first observation of thiol form of simple thioamide. *Phys. Chem. Chem. Phys.* **2003**, *5*, 1524–1529.
- [52] Góbi, S.; Nunes, C. M.; Reva, I.; Tarczay, G.; Fausto, R. S–H rotamerization via tunneling in a thiol form of thioacetamide. *Phys. Chem. Chem. Phys.* **2019**, *21*, 17063–17071.
- [53] Góbi, S.; Reva, I.; Csonka, I. P.; Nunes, C. M.; Tarczay, G.; Fausto, R. Selective conformational control by excitation of NH imino vibrational antennas. *Phys. Chem. Chem. Phys.* **2019**, *21*, 24935–24949.
- [54] Eyring, H. The activated complex and the absolute rate of chemical reactions. *Chem. Rev.* **1935**, *17*, 65–77.
- [55] Evans, M. G.; Polanyi, M. Some applications of the transition state method to the calculation of reaction velocities, especially in solution. *Trans. Faraday Soc.* **1935**, *31*, 875–894.
- [56] Evans, M. G.; Polanyi, M. Inertia and driving force of chemical reactions. *Trans. Faraday Soc.* **1938**, *34*, 11–24.
- [57] Jeffreys, H. On certain approximate solutions of linear differential equations of the second order. *Proc. London Math. Soc.* **1924**, *23*, 428–436.
- [58] Wentzel, G. Über strahlungslose Quantensprünge. *Z. Phys.* **1927**, *43*, 524–530.
- [59] Kramers, H. A. Wellenmechanik und halbzahlige Quantisierung. *Z. Phys.* **1926**, *39*, 828–840.
- [60] Brillouin, L. Remarques sur la mécanique ondulatoire. *J. Phys. le Radium* **1926**, *7*, 353–368.
- [61] Schrödinger, E. Quantisierung als Eigenwertproblem. *Ann. Phys.* **1926**, *80*, 437–590.
- [62] Kästner, J. Theory and simulation of atom tunneling in chemical reactions. *Wires. Comput. Mol. Sci.* **2014**, *4*, 158–168.
- [63] Meisner, J.; Kästner, J. Atom tunneling in chemistry. *Angew. Chem. Int. Ed.* **2016**, *55*, 5400–5413.
- [64] Borden, W. T. Reactions that involve tunneling by carbon and the role that calculations have played in their study. *Wires. Comput. Mol. Sci.* **2016**, *6*, 20–46.
- [65] Isaacson, A. D.; Truhlar, D. G.; Rai, S. N.; Steckler, R.; Hancock, G. C.; Garrett, B. C.; Redmon, M. J. POLYRATE: a general computer program for variational transition state theory and semiclassical tunneling calculations of chemical reaction rates. *Comput. Phys. Commun.* **1987**, *47*, 91–102.
- [66] Quanz, H.; Schreiner, P. R. TUNNEX: an easy-to-use Wentzel-Kramers-Brillouin (WKB) implementation to compute tunneling half-lives. *J. Comput. Chem.* **2019**, *40*, 543–547.
- [67] Ley, D.; Gerbig, D.; Schreiner, P. R. Tunnelling control of chemical reactions – the organic chemist’s perspective. *Org. Biomol. Chem.* **2012**, *10*, 3769–3956.
- [68] Gamow, G. The quantum theory of nuclear disintegration. *Nature* **1928**, *122*, 805–806.
- [69] Schreiner, P. R.; Reisenauer, H. P.; Ley, D.; Gerbig, D.; Wu, C.-H.; Allen, W. D. Methylhydroxycarbene: tunneling control of a chemical reaction. *Science* **2011**, *332*, 1300–1303.
- [70] Schreiner, P. R. Tunneling control of chemical reactions: the third reactivity paradigm. *J. Am. Chem. Soc.* **2017**, *139*, 15276–15283.
- [71] Schreiner, P. R. Quantum mechanical tunneling is essential to understanding chemical reactivity. *Trends Chem.* **2020**, *2*, 980–989.
- [72] Zuev, P. S.; Sheridan, R. S. Tunneling in the C–H insertion of a singlet carbene: *tert*-butylchlorocarbene. *J. Am. Chem. Soc.* **1994**, *116*, 4123–4124.
- [73] East, A. L. L.; Allen, W. D. The heat of formation of NCO. *J. Chem. Phys.* **1993**, *99*, 4638–4650.

- [74] Schuurman, M. S.; Muir, S. R.; Allen, W. D.; Schaefer III, H. F. Toward subchemical accuracy in computational thermochemistry: focal point analysis of the heat of formation of NCO and [H,N,C,O] isomers. *J. Chem. Phys.* **2004**, *120*, 11586–11599.
- [75] Bartlett, M. A.; Liang, T.; Pu, L.; Schaefer III, H. F.; Allen, W. D. The multichannel *n*-propyl + O<sub>2</sub> reaction surface: definitive theory on a model hydrocarbon oxidation mechanism. *J. Chem. Phys.* **2018**, *148*, 1–18.
- [76] Császár, A. G.; Allen, W. D.; Schaefer III, H. F. In pursuit of the ab initio limit for conformational energy prototypes. *J. Chem. Phys.* **1998**, *108*, 9751–9764.
- [77] Gonzales, J. M.; Allen, W. D.; Schaefer III, H. F. Model identity S<sub>N</sub>2 reactions CH<sub>3</sub>X + X<sup>-</sup> (X = F, Cl, CN, OH, SH, NH<sub>2</sub>, PH<sub>2</sub>): Marcus Theory analyzed. *J. Phys. Chem. A* **2005**, *109*, 10613–10628.
- [78] Stanton, J. F. Why CCSD(T) works: a different perspective. *Chem. Phys. Lett.* **1997**, *281*, 130–134.
- [79] Čížek, J. On the correlation problem in atomic and molecular systems. Calculation of wavefunction components in Ursell-type expansion using quantum-field theoretical methods. *J. Chem. Phys.* **1966**, *45*, 4256–4266.
- [80] Purvis, G. D.; Bartlett, R. J. A full coupled-cluster singles and doubles model: the inclusion of disconnected triples. *J. Chem. Phys.* **1982**, *76*, 1910–1918.
- [81] Raghavachari, K.; Trucks, G. W.; Pople, J. A.; Head-Gordon, M. A fifth-order perturbation comparison of electron correlation theories. *Chem. Phys. Lett.* **1989**, *157*, 479–483.
- [82] Crawford, T. D.; Schaefer III, H. F. An introduction to coupled cluster theory for computational chemists. *Rev. Comput. Chem.* **2000**, *14*, 33–136.
- [83] Dunning, T. H. Gaussian basis sets for use in correlated molecular calculations. I. The atoms boron through neon and hydrogen. *J. Chem. Phys.* **1989**, *90*, 1007–1023.
- [84] Woon, D. E.; Dunning, T. H. Gaussian basis sets for use in correlated molecular calculations. V. Core-valence basis sets for boron through neon. *J. Chem. Phys.* **1995**, *103*, 4572–4585.
- [85] Gerbig, D.; Schreiner, P. R. Formation of a tunneling product in the photorearrangement of *o*-nitrobenzaldehyde. *Angew. Chem. Int. Ed.* **2017**, *56*, 9445–9448.
- [86] Møller, C.; Plesset, M. S. Note on an approximation treatment for many-electron systems. *Phys. Rev.* **1934**, *46*, 618–622.
- [87] Nunes, C. M.; Eckhardt, A. K.; Reva, I.; Fausto, R.; Schreiner, P. R. Competitive nitrogen versus carbon tunneling. *J. Am. Chem. Soc.* **2019**, *141*, 14340–14348.
- [88] Castro, C.; Karney, W. L. Heavy-atom tunneling in organic reactions. *Angew. Chem. Int. Ed.* **2020**, *132*, 8355–8366.
- [89] Doubleday, C.; Armas, R.; Walker, D.; Cosgriff, C. V.; Greer, E. M. Heavy-atom tunneling calculations in thirteen organic reactions: tunneling contributions are substantial, and Bell's formula closely approximates multidimensional tunneling at ≥250 K. *Angew. Chem. Int. Ed.* **2017**, *56*, 13099–13102.
- [90] Inui, H.; Sawada, K.; Oishi, S.; Ushida, K.; McMahon, R. J. Aryl nitrene rearrangements: spectroscopic observation of a benzazirine and its ring expansion to a ketenimine by heavy-atom tunneling. *J. Am. Chem. Soc.* **2013**, *135*, 10246–10249.
- [91] Schleif, T.; Mieres-Perez, J.; Henkel, S.; Ertelt, M.; Borden, W. T.; Sander, W. The Cope rearrangement of 1,5-dimethylsemibullvalene-2(4)-d<sub>1</sub>: experimental evidence for heavy-atom tunneling. *Angew. Chem. Int. Ed.* **2017**, *56*, 10746–10749.
- [92] Schleif, T.; Tatchen, J.; Rowen, J. F.; Beyer, F.; Sanchez-Garcia, E.; Sander, W. Heavy-atom tunneling in semibullvalenes: how driving force, substituents, and environment influence the tunneling rates. *Chem. Eur. J.* **2020**, *26*, 10452–10458.
- [93] Whitman, D. W.; Carpenter, B. K. Limits on the activation parameters for automerization of cyclobutadiene-1,2-*d*<sub>2</sub>. *J. Am. Chem. Soc.* **1982**, *104*, 6473–6474.
- [94] Carpenter, B. K. Heavy-atom tunneling as the dominant pathway in a solution-phase reaction? Bond shift in antiaromatic annulenes. *J. Am. Chem. Soc.* **1983**, *105*, 1700–1701.
- [95] Wentrup, C. Carbenes and nitrenes: recent developments in fundamental chemistry. *Angew. Chem. Int. Ed.* **2018**, *57*, 11508–11521.
- [96] Nunes, C. M.; Knezz, S. N.; Reva, I.; Fausto, R.; McMahon, R. J. Evidence of a nitrene tunneling reaction: spontaneous rearrangement of 2-formyl phenylnitrene to an imino ketene in low-temperature matrixes. *J. Am. Chem. Soc.* **2016**, *138*, 15287–15290.
- [97] Michel, C. S.; Lampkin, P. P.; Shezaf, J. Z.; Moll, J. F.; Castro, C.; Karney, W. L. Tunneling by 16 carbons: planar bond shifting in [16]annulene. *J. Am. Chem. Soc.* **2019**, *141*, 5286–5293.
- [98] Kozuch, S. Heavy atom tunneling in the automerization of pentalene and other antiaromatic systems. *RSC Adv.* **2014**, *4*, 21650–21656.
- [99] Greer, E. M.; Cosgriff, C. V.; Doubleday, C. Computational evidence for heavy-atom tunneling in the Bergman cyclization of a 10-membered-ring enediyne. *J. Am. Chem. Soc.* **2013**, *135*, 10194–10197.
- [100] Curtin, D. Y. Stereochemical control of organic reactions differences in behaviour of diastereoisomers. *Rec. Chem. Prog.* **1954**, *15*, 111–128.
- [101] Seeman, J. I. Effect of conformational change on reactivity in organic chemistry. Evaluation, applications, and extensions of Curtin-Hammett/Winstein-Holness kinetics. *Chem. Rev.* **1983**, *83*, 84–134.
- [102] Seeman, J. I. The Curtin-Hammett principle and the Winstein-Holness equation: new definition and recent extensions to classical concepts. *J. Chem. Educ.* **1986**, *63*, 42–48.
- [103] Mardyukov, A.; Quanz, H.; Schreiner, P. R. Conformer-specific hydrogen atom tunnelling in trifluoromethylhydroxycarbene. *Nat. Chem.* **2017**, *9*, 71–76.
- [104] Eckhardt, A. K.; Erb, F. R.; Schreiner, P. R. Conformer-specific [1,2]H-tunnelling in captodatively-stabilized

- cyanohydroxycarbene (NC– $\ddot{C}$ –OH). *Chem. Sci.* **2019**, *10*, 802–808.
- [105] Bernhardt, B.; Ruth, M.; Eckhardt, A. K.; Schreiner, P. R. Ethynylhydroxycarbene (H–C $\equiv$ C– $\ddot{C}$ –OH). *J. Am. Chem. Soc.* **2021**, *143*, 3741–3746.
- [106] Roque, J. P. L.; Nunes, C. M.; Viegas, L. P.; Pereira, N. A. M.; Pinho, T. M. V. D.; Schreiner, P. R.; Fausto, R. Switching on H-tunneling through conformational control. *J. Am. Chem. Soc.* **2021**, *143*, 8266–8271.
- [107] Schleif, T.; Mieres-Perez, J.; Henkel, S.; Mendez-Vega, E.; Inui, H.; McMahon, R. J.; Sander, W. Conformer-specific heavy-atom tunneling in the rearrangement of benzazirines to ketenimines. *J. Org. Chem.* **2019**, *84*, 16013–16018.
- [108] Sarka, J.; Császár, A. G.; Schreiner, P. R. Do the mercaptocarbene (H–C–S–H) and selenocarbene (H–C–Se–H) congeners of hydroxycarbene (H–C–O–H) undergo 1,2-H-tunneling? *Collect. Czechoslov. Chem. Commun.* **2011**, *76*, 645–667.
- [109] Schreiner, P. R.; Reisenauer, H. P.; Pickard IV, F. C.; Simmonett, A. C.; Allen, W. D.; Mátyus, E.; Császár, A. G. Capture of hydroxymethylene and its fast disappearance through tunnelling. *Nature* **2008**, *453*, 906–909.
- [110] Gerbig, D.; Reisenauer, H. P.; Wu, C.; Ley, D.; Allen, W. D.; Schreiner, P. R. Phenylhydroxycarbene. *J. Am. Chem. Soc.* **2010**, *132*, 7273–7275.
- [111] Ley, D.; Gerbig, D.; Schreiner, P. R. Tunneling control of chemical reactions: C–H insertion versus H-tunneling in *tert*-butylhydroxycarbene. *Chem. Sci.* **2013**, *4*, 677–684.
- [112] Ley, D.; Gerbig, D.; Wagner, J. P.; Reisenauer, H. P.; Schreiner, P. R. Cyclopropylhydroxycarbene. *J. Am. Chem. Soc.* **2011**, *133*, 13614–13621.
- [113] Schreiner, P. R.; Reisenauer, H. P. Spectroscopic identification of dihydroxycarbene. *Angew. Chem. Int. Ed.* **2008**, *47*, 7071–7074.
- [114] Bernhardt, B.; Ruth, M.; Reisenauer, H. P.; Schreiner, P. R. Aminohydroxymethylene (H<sub>2</sub>N– $\ddot{C}$ –OH), the simplest aminooxycarbene. *J. Phys. Chem. A* **2021**, *125*, 7023–7028.
- [115] Hund, F. Zur Deutung der Molekelspektren. I. *Zeitschrift für Phys.* **1927**, *40*, 742–764.
- [116] Costa, P.; Sander, W. Hydrogen bonding switches the spin state of diphenylcarbene from triplet to singlet. *Angew. Chem. Int. Ed.* **2014**, *53*, 5122–5125.
- [117] Costa, P.; Fernandez-Oliva, M.; Sanchez-Garcia, E.; Sander, W. The highly reactive benzhydryl cation isolated and stabilized in water ice. *J. Am. Chem. Soc.* **2014**, *136*, 15625–15630.
- [118] Knorr, J.; Sokkar, P.; Schott, S.; Costa, P.; Thiel, W.; Sander, W.; Sanchez-Garcia, E.; Nuernberger, P. Competitive solvent-molecule interactions govern primary processes of diphenylcarbene in solvent mixtures. *Nat. Commun.* **2016**, *7*, 1–8.
- [119] Costa, P.; Lohmiller, T.; Trosien, I.; Savitsky, A.; Lubitz, W.; Fernandez-Oliva, M.; Sanchez-Garcia, E.; Sander, W. Light and temperature control of the spin state of bis(*p*-methoxyphenyl)carbene: a magnetically bistable carbene. *J. Am. Chem. Soc.* **2016**, *138*, 1622–1629.
- [120] Snyder, L. E.; Buhl, D.; Zuckerman, B.; Palmer, P. Microwave detection of interstellar formaldehyde. *Phys. Rev. Lett.* **1969**, *22*, 679–681.
- [121] Butlerow, A. Bildung einer zuckerartigen Substanz durch Synthese. *Justus Liebigs Ann. Chem.* **1861**, *120*, 295–298.
- [122] Breslow, R. On the mechanism of the formose reaction. *Tetrahedron Lett.* **1959**, *1*, 22–26.
- [123] Eckhardt, A. K.; Linden, M. M.; Wende, R. C.; Bernhardt, B.; Schreiner, P. R. Gas-phase sugar formation using hydroxymethylene as the reactive formaldehyde isomer. *Nat. Chem.* **2018**, *10*, 1141–1147.
- [124] Seebach, D. Methods of reactivity Umpolung. *Angew. Chem. Int. Ed.* **1979**, *18*, 239–258.
- [125] Eckhardt, A. K.; Schreiner, P. R. Spectroscopic evidence for aminomethylene (H– $\ddot{C}$ –NH<sub>2</sub>)—the simplest amino carbene. *Angew. Chem. Int. Ed.* **2018**, *57*, 5248–5252.
- [126] Ekern, S.; Szczepanski, J.; Vala, M. An ab initio study of the C<sub>3</sub>H<sub>2</sub>O potential surface: a mechanism for propynal formation and destruction. *J. Phys. Chem.* **1996**, *100*, 16109–16115.
- [127] Ekern, S.; Vala, M. Theoretical study of photochemical mechanisms of C<sub>3</sub>O formation. *J. Phys. Chem. A* **1997**, *101*, 3601–3606.
- [128] Ortman, B. J.; Hauge, R. H.; Margrave, J. L.; Kafafi, Z. H. Reactions of small carbon clusters with water in cryogenic matrices. The FTIR spectrum of hydroxyethynylcarbene. *J. Phys. Chem.* **1990**, *94*, 7973–7977.
- [129] Dibben, M.; Szczepanski, J.; Wehlburg, C.; Vala, M. Complexes of linear carbon clusters with water. *J. Phys. Chem. A* **2000**, *104*, 3584–3592.
- [130] Schreiner, P. R.; Reisenauer, H. P. The “non-reaction” of ground-state triplet carbon atoms with water revisited. *Chem. Phys. Chem.* **2006**, *7*, 880–885.
- [131] Liu, R.; Zhou, X.; Pulay, P. Ab initio study of the identity of the reaction product between C<sub>3</sub> and water in cryogenic matrices. *J. Phys. Chem.* **1992**, *96*, 5748–5752.
- [132] Szczepanski, J.; Ekern, S.; Vala, M. Spectroscopy and photochemistry of the C<sub>3</sub>-H<sub>2</sub>O complex in argon matrices. *J. Phys. Chem.* **1995**, *99*, 8002–8012.
- [133] Hammond, G. S. A correlation of reaction rates. *J. Am. Chem. Soc.* **1955**, *77*, 334–338.
- [134] Pettersson, M.; Lundell, J.; Khriachtchev, L.; Räsänen, M. IR spectrum of the other rotamer of formic acid, *cis*-HCOOH. *J. Am. Chem. Soc.* **1997**, *119*, 11715–11716.
- [135] Pettersson, M.; Maçôas, E. M. S.; Khriachtchev, L.; Lundell, J.; Fausto, R.; Räsänen, M. *Cis*→*trans* conversion of formic acid by dissipative tunneling in solid rare gases: influence of environment on the tunneling rate. *J. Chem. Phys.* **2002**, *117*, 9095–9098.
- [136] Khriachtchev, L.; Pettersson, M.; Räsänen, M. Conformational memory in photodissociation of formic acid. *J. Am. Chem. Soc.* **2002**, *124*, 10994–10995.

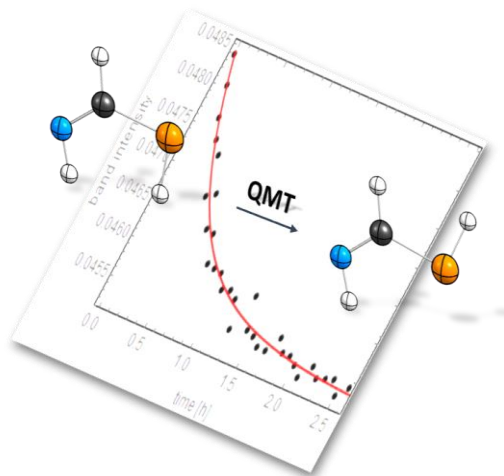
- [137] Maçôas, E. M. S.; Khriachtchev, L.; Pettersson, M.; Fausto, R.; Räsänen, M. Rotational isomerism in acetic acid: the first experimental observation of the high-energy conformer. *J. Am. Chem. Soc.* **2003**, *125*, 16188–16189.
- [138] Maçôas, E. M. S.; Khriachtchev, L.; Fausto, R.; Räsänen, M. Photochemistry and vibrational spectroscopy of the trans and cis conformers of acetic acid in solid Ar. *J. Phys. Chem. A* **2004**, *108*, 3380–3389.
- [139] Maçôas, E. M. S.; Khriachtchev, L.; Pettersson, M.; Fausto, R.; Räsänen, M. Rotational isomerism of acetic acid isolated in rare-gas matrices: effect of medium and isotopic substitution on IR-induced isomerization quantum yield and cis  $\rightarrow$  trans tunneling rate. *J. Chem. Phys.* **2004**, *121*, 1331–1338.
- [140] Maçôas, E. M. S.; Khriachtchev, L.; Pettersson, M.; Fausto, R.; Räsänen, M. Internal rotation in propionic acid: near-infrared-induced isomerization in solid argon. *J. Phys. Chem. A* **2005**, *109*, 3617–3625.
- [141] Gerbig, D.; Schreiner, P. R. Hydrogen-tunneling in biologically relevant small molecules: the rotamerizations of  $\alpha$ -ketocarboxylic acids. *J. Phys. Chem. B* **2015**, *119*, 693–703.
- [142] Apóstolo, R. F. G.; Bazsó, G.; Bento, R. R. F.; Tarczay, G.; Fausto, R. The first experimental observation of the higher-energy *trans* conformer of trifluoroacetic acid. *J. Mol. Struct.* **2016**, *1125*, 288–295.
- [143] Apóstolo, R. F. G.; Bento, R. R. F.; Fausto, R. Narrowband NIR-induced *in situ* generation of the high-energy *trans* conformer of trichloroacetic acid isolated in solid nitrogen and its spontaneous decay by tunneling to the low-energy *cis* conformer. *Croat. Chem. Acta* **2015**, *88*, 377–386.
- [144] Apóstolo, R. F. G.; Bazsó, G.; Ogruc-Ildiz, G.; Tarczay, G.; Fausto, R. Near-infrared *in situ* generation of the higher-energy *trans* conformer of tribromoacetic acid: observation of a large-scale matrix-site changing mediated by conformational conversion. *J. Chem. Phys.* **2018**, *148*, 1–12.
- [145] Lopes, S.; Nikitin, T.; Fausto, R. Propiolic acid in solid nitrogen: NIR- and UV-induced *cis*  $\rightarrow$  *trans* isomerization and matrix-site-dependent *trans*  $\rightarrow$  *cis* tunneling. *J. Phys. Chem. A* **2019**, *123*, 1581–1593.
- [146] Maier, G.; Endres, J.; Reisenauer, H. P. Interconversions between oxalic acid monoamide rotamers: photochemical process versus tunneling. *J. Mol. Struct.* **2012**, *1025*, 2–5.
- [147] Schreiner, P. R.; Wagner, J. P.; Reisenauer, H. P.; Gerbig, D.; Ley, D.; Sarka, J.; Császár, A. G.; Vaughn, A.; Allen, W. D. Domino tunneling. *J. Am. Chem. Soc.* **2015**, *137*, 7828–7834.
- [148] Reisenauer, H. P.; Wagner, J. P.; Schreiner, P. R. Gas-phase preparation of carbonic acid and its monomethyl ester. *Angew. Chem. Int. Ed.* **2014**, *53*, 11766–11771.
- [149] Wagner, J. P.; Reisenauer, H. P.; Hirvonen, V.; Wu, C.-H.; Tyberg, J. L.; Allen, W. D.; Schreiner, P. R. Tunneling in carbonic acid. *Chem. Commun.* **2016**, *52*, 7858–7861.
- [150] Linden, M. M.; Wagner, J. P.; Bernhardt, B.; Bartlett, M. A.; Allen, W. D.; Schreiner, P. R. Intricate conformational tunneling in carbonic acid monomethyl ester. *J. Phys. Chem. Lett.* **2018**, *9*, 1663–1667.
- [151] Pettersson, M.; Maçôas, E. M. S.; Khriachtchev, L.; Fausto, R.; Räsänen, M. Conformational isomerization of formic acid by vibrational excitation at energies below the torsional barrier. *J. Am. Chem. Soc.* **2003**, *125*, 4058–4059.
- [152] Liu, F.; Beames, J. M.; Petit, A. S.; McCoy, A. B.; Lester, M. I. Infrared-driven unimolecular reaction of CH<sub>3</sub>CHOO Criegee intermediates to OH radical products. *Science* **2014**, *345*, 1596–1598.
- [153] Barber, V. P.; Pandit, S.; Esposito, V. J.; McCoy, A. B.; Lester, M. I. CH stretch activation of CH<sub>3</sub>CHOO: deep tunneling to hydroxyl radical products. *J. Phys. Chem. A* **2019**, *123*, 2559–2569.
- [154] Ramos, R.; Spierings, D.; Racicot, I.; Steinberg, A. M. Measurement of the time spent by a tunnelling atom within the barrier region. *Nature* **2020**, *583*, 529–532.
- [155] Sainadh, U. S.; Xu, H.; Wang, X.; Atia-Tul-Noor, A.; Wallace, W. C.; Douguet, N.; Bray, A.; Ivanov, I.; Bartschat, K.; Kheifets, A.; Sang, R. T.; Litvinyuk, I. V. Attosecond angular streaking and tunnelling time in atomic hydrogen. *Nature* **2019**, *568*, 75–77.
- [156] Ryazantsev, S. V.; Feldman, V. I.; Khriachtchev, L. Conformational switching of HOCO radical: selective vibrational excitation and hydrogen-atom tunneling. *J. Am. Chem. Soc.* **2017**, *139*, 9551–9557.
- [157] Henkel, S.; Merini, M. P.; Mendez-Vega, E.; Sander, W. Lewis acid catalyzed heavy atom tunneling – the case of 1*H*-bicyclo[3.1.0]hexa-3,5-dien-2-one. *Chem. Sci.* **2021**, *12*, 11013–11019.
- [158] Lopes Jesus, A. J.; Reva, I.; Araujo-Andrade, C.; Fausto, R. Conformational switching by vibrational excitation of a remote NH bond. *J. Am. Chem. Soc.* **2015**, *137*, 14240–14243.
- [159] Halasa, A.; Reva, I.; Lapinski, L.; Rostkowska, H.; Fausto, R.; Nowak, M. J. Conformers of kojic acid and their near-IR-induced conversions: long-range intramolecular vibrational energy transfer. *J. Phys. Chem. A* **2016**, *120*, 2647–2656.
- [160] Lopes Jesus, A. J.; Nunes, C. M.; Fausto, R.; Reva, I. Conformational control over an aldehyde fragment by selective vibrational excitation of interchangeable remote antennas. *Chem. Commun.* **2018**, *54*, 4778–4781.
- [161] Nunes, C. M.; Pereira, N. A. M.; Viegas, L. P.; Pinho e Melo, T. M. V. D.; Fausto, R. Inducing molecular reactions by selective vibrational excitation of a remote antenna with near-infrared light. *Chem. Commun.* **2021**, *57*, 9570–9573.
- [162] Nunes, C. M.; Reva, I.; Fausto, R. Conformational isomerizations triggered by vibrational excitation of second stretching overtones. *Phys. Chem. Chem. Phys.* **2019**, *21*, 24993–25001.
- [163] Quanz, H.; Bernhardt, B.; Erb, F. R.; Bartlett, M. A.; Allen, W. D.; Schreiner, P. R. Identification and reactivity of *s-cis,s-cis*-dihydroxycarbene, a new [CH<sub>2</sub>O<sub>2</sub>] intermediate. *J. Am. Chem. Soc.* **2020**, *142*, 19457–19461.
- [164] Greer, E. M.; Kwon, K.; Greer, A.; Doubleday, C. Thermally activated tunneling in organic reactions. *Tetrahedron* **2016**, *72*, 7357–7373.
- [165] Schäfer, M.; Peckelsen, K.; Paul, M.; Martens, J.; Oomens, J.; Berden, G.; Berkessel, A.; Meijer, A. J. H. M. Hydrogen tunneling above room temperature evidenced by infrared ion spectroscopy. *J. Am. Chem. Soc.* **2017**, *139*, 5779–5786.

- [166] Veticatt, M. J.; Singleton, D. A. Isotope effects and heavy-atom tunneling in the Roush allylboration of aldehydes. *Org. Lett.* **2012**, *14*, 2370–2373.
- [167] Barman, P.; Upadhyay, P.; Faponle, A. S.; Kumar, J.; Nag, S. S.; Kumar, D.; Sastri, C. V.; de Visser, S. P. Deformylation reaction by a nonheme manganese(III)–peroxo complex via initial hydrogen-atom abstraction. *Angew. Chem. Int. Ed.* **2016**, *55*, 11091–11095.
- [168] Cantú Reinhard, F. G.; Barman, P.; Mukherjee, G.; Kumar, J.; Kumar, D.; Kumar, D.; Sastri, C. V.; de Visser, S. P. Keto-enol tautomerization triggers an electrophilic aldehyde deformylation reaction by a nonheme manganese(III)–peroxo complex. *J. Am. Chem. Soc.* **2017**, *139*, 18328–18338.
- [169] Bae, S. H.; Li, X.; Seo, M. S.; Lee, Y.; Fukuzumi, S.; Nam, W. Tunneling controls the reaction pathway in the deformylation of aldehydes by a nonheme iron(III)–hydroperoxo complex: hydrogen atom abstraction versus nucleophilic addition. *J. Am. Chem. Soc.* **2019**, *141*, 7675–7679.
- [170] Barman, P.; Cantú Reinhard, F. G.; Bagha, U. K.; Kumar, D.; Sastri, C.; de Visser, S. P. Hydrogen by deuterium substitution in an aldehyde tunes the regioselectivity by a nonheme manganese(III)–peroxo complex. *Angew. Chem. Int. Ed.* **2019**, 1–6.
- [171] Scheiner, S. Highly selective halide receptors based on chalcogen, pnicoen, and tetrel bonds. *Chem. Eur. J.* **2016**, *22*, 18850–18858.
- [172] Kozuch, S.; Nandi, A.; Sucher, A. Ping-pong tunneling reactions: can fluoride jump at absolute zero? *Chem. Eur. J.* **2018**, *24*, 16348–16355.
- [173] Nandi, A.; Sucher, A.; Tyomkin, A.; Kozuch, S. Ping-pong tunneling reactions, part 2: boron and carbon bell-clapper rearrangement. *Pure Appl. Chem.* **2020**, *92*, 39–47.
- [174] Solel, E.; Kozuch, S. Tuning the spin, aromaticity and quantum tunneling in computationally designed fulvalenes. *J. Org. Chem.* **2018**, *83*, 10826–10834.
- [175] Kozuch, S. Cyclopropenyl anions: carbon tunneling or diradical formation? A contest between Jahn-Teller and Hund. *J. Chem. Theory Comput.* **2015**, *11*, 3089–3095.
- [176] Martínez-Guajardo, G.; Donald, K. J.; Wittmaack, B. K.; Vazquez, M. A.; Merino, G. Shorter still: compressing C–C single bonds. *Org. Lett.* **2010**, *12*, 4058–4061.
- [177] Kozuch, S. A quantum mechanical “jack in the box”: rapid rearrangement of a tetrahydryl-tetrahydrane via heavy atom tunneling. *Org. Lett.* **2014**, *16*, 4102–4105.
- [178] Hoffmann, R.; Schleyer, P. v. R.; Schaefer III, H. F. Predicting molecules—more realism, please! *Angew. Chem. Int. Ed.* **2008**, *47*, 7164–7167.
- [179] Doddipatla, S.; He, C.; Kaiser, R. I.; Luo, Y.; Sun, R.; Galimova, G. R.; Mebel, A. M.; Millar, T. J. A chemical dynamics study on the gas phase formation of thioformaldehyde (H<sub>2</sub>CS) and its thiohydroxycarbene isomer (HCSH). *Proc. Natl. Acad. Sci. USA* **2020**, *117*, 22712–22719.
- [180] Nandi, A.; Gerbig, D.; Schreiner, P. R.; Borden, W. T.; Kozuch, S. Isotope-controlled selectivity by quantum tunneling: hydrogen migration versus ring expansion in cyclopropylmethylcarbenes. *J. Am. Chem. Soc.* **2017**, *139*, 9097–9099.
- [181] Isaev, S. D.; Yurchenko, A. G.; Stepanov, F. N.; Kolyada, G. G.; Novikov, S. S.; Karpenko, N. F. Synthesis and chemical reactions of adamantane-2-spiro-3'-diazirine. *Zh. Org. Khim.* **1973**, *9*, 724–727.
- [182] Marchand, A. P.; Kumar, K. A.; Mlinarić-Majerski, K.; Veljković, J. Intermolecular vs. intramolecular carbene reactions of a cage-functionalized cyclopentylcarbene. *Tetrahedron* **1998**, *54*, 15105–15112.
- [183] Šumanovac, T.; Alešković, M.; Šekutor, M.; Matković, M.; Baron, T.; Mlinarić-Majerski, K.; Bohne, C.; Basarić, N. Photoelimination of nitrogen from adamantane and pentacycloundecane (PCU) diazirines: spectroscopic study and supramolecular control. *Photochem. Photobiol. Sci.* **2019**, *18*, 1806–1822.
- [184] Kozuch, S. The reactivity game: theoretical predictions for heavy atom tunneling in adamantyl and related carbenes. *Phys. Chem. Chem. Phys.* **2014**, *16*, 7718–7727.
- [185] Bally, T.; Matzinger, S.; Truttmann, L.; Platz, M. S.; Morgan, S. Matrix spectroscopy of 2-adamantylidene, a dialkylcarbene with singlet ground state. *Angew. Chem. Int. Ed.* **1994**, *33*, 1964–1966.



## 2. Publications

### 2.1 Characterization of the Simplest Thiolimine: The Higher Energy Tautomer of Thioformamide



#### *Abstract:*

As sulfur containing organic molecules thioamides and their isomers are conceivable intermediates in prebiotic chemistry, *e. g.*, in the formation of amino acids and thiazoles and resemble viable candidates for detection in interstellar media. Here we report the characterization of parent thioformamide in the solid state *via* single crystal X-ray diffraction and its photochemical interconversion to its hitherto unreported higher energy tautomer thiolimine in inert argon and dinitrogen matrices. Upon photogeneration, four conformers of thiolimine form, whose ratio depends on the employed wavelength. One of these conformers interconverts due to quantum mechanical tunneling with a half-life of 30–45 min in both matrix materials at 3 and 20 K. A spontaneous reverse reaction from thiolimine to thioformamide is not observed. To support our experimental findings, we explored the potential energy surface of the system at the AE-CCSD(T)/aug-cc-pCVTZ level of theory and computed tunneling half-lives with the CVT/SCT approach applying DFT methods.

#### *Reference:*

Bastian Bernhardt, Friedemann Dressler, André K. Eckhardt, Jonathan Becker, and Peter R. Schreiner *Chem. Eur. J.* **2021**, 27, 6732–6739. (DOI: 10.1002/chem.202005188)

#### *Reproduced with permission from:*

© 2021, John Wiley & Sons, Inc.  
111 River Street  
Hoboken, NJ, 07030-5774  
United States of America

## Prebiotic Chemistry

# Characterization of the Simplest Thiolimine: The Higher Energy Tautomer of Thioformamide

Bastian Bernhardt,<sup>[a]</sup> Friedemann Dressler,<sup>[a]</sup> André K. Eckhardt,<sup>[a]</sup> Jonathan Becker,<sup>[b]</sup> and Peter R. Schreiner<sup>\*[a]</sup>

**Abstract:** As sulfur-containing organic molecules thioamides and their isomers are conceivable intermediates in prebiotic chemistry, for example, in the formation of amino acids and thiazoles and resemble viable candidates for detection in interstellar media. Here, we report the characterization of parent thioformamide in the solid state via single-crystal X-ray diffraction and its photochemical interconversion to its hitherto unreported higher energy tautomer thiolimine in inert argon and dinitrogen matrices. Upon photogeneration, four conformers of thiolimine form, whose ratio depends on

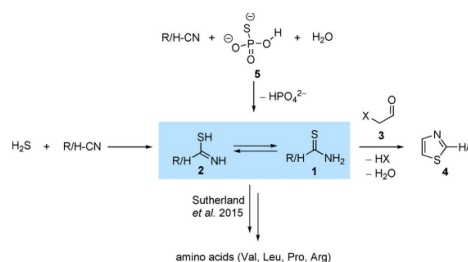
the employed wavelength. One of these conformers interconverts due to quantum mechanical tunneling with a half-life of 30–45 min in both matrix materials at 3 and 20 K. A spontaneous reverse reaction from thiolimine to thioformamide is not observed. To support our experimental findings, we explored the potential energy surface of the system at the AE-CCSD(T)/aug-cc-pCVTZ level of theory and computed tunneling half-lives with the CVT/SCT approach applying DFT methods.

## Introduction

Although thioformamide (**1**, methanethioamide, R=H) is the simplest thioamide, it is not as well characterized as one would assume. In nature as well as in synthetic chemistry<sup>[1]</sup> thioamides resemble building blocks for thiazoles (**4**), a unit that is present in various biologically important molecules (e.g., thiamin) and drugs.<sup>[2]</sup> General syntheses towards thiazoles build upon reacting thioamides with  $\alpha$ -halogenated aldehydes (**3**).<sup>[3]</sup> Parent thioformamide is an adduct of HCN and H<sub>2</sub>S,<sup>[4]</sup> both of which were detected in interstellar media.<sup>[5–7]</sup> This makes thioformamide a probable participant in the prebiotic synthesis of sulfur containing compounds important for the development of life (Scheme 1). Accordingly, Sutherland et al. demonstrated that various thioamide derivatives might play a role in the formation of amino acids through what has been termed “cyanosulfidic protometabolism”.<sup>[8]</sup> In a prebiotic context they can form from the reaction of nitriles with either H<sub>2</sub>S or thiophosphate (**5**).<sup>[9]</sup> This chemistry displays similarities to

that of HCN reacting with H<sub>2</sub>O, which has been investigated computationally recently.<sup>[10]</sup> The general idea of constructing organic molecules from simple building blocks has been widely accepted since the famous Urey–Miller experiments.<sup>[11]</sup> Mechanistically, addition of H<sub>2</sub>S to nitriles is expected to proceed via a thiolimine (**2**, methanimidothioic acid, R=H), which is the thermodynamically disfavored tautomer of **1**. To the best of our knowledge, no data exist for **2**, which prompted us to study the tautomerization between **1** and **2** in cryogenic argon (Ar) and dinitrogen (N<sub>2</sub>) matrices to provide first-hand evidence for the existence and spectral identity of **2**. We also report the first single-crystal X-ray diffraction structure of **1**.

Various thioamide derivatives have been isolated under cryogenic conditions and characterized by infrared (IR) spectroscopy



**Scheme 1.** Thioamides are considered key intermediates in the generation of some highly relevant biologically active molecules like amino acids and thiazoles (**4**) in prebiotic context. Their formation from nitriles and H<sub>2</sub>S or thiophosphate (**5**) has been described.<sup>[9]</sup> Here we focus on parent thioformamide (**1**, R=H) and its tautomerization to **2** (R=H).

[a] B. Bernhardt, F. Dressler, Dr. A. K. Eckhardt, Prof. Dr. P. R. Schreiner  
Institute of Organic Chemistry, Justus Liebig University  
Heinrich-Buff-Ring 17, 35390 Giessen (Germany)  
E-mail: prs@uni-giessen.de

[b] Dr. J. Becker  
Institute of Inorganic and Analytical Chemistry, Justus Liebig University  
Heinrich-Buff-Ring 17, 35390 Giessen (Germany)

Supporting information and the ORCID identification numbers for the authors of this article can be found under:  
<https://doi.org/10.1002/chem.202005188>.

© 2021 The Authors. Chemistry - A European Journal published by Wiley-VCH GmbH. This is an open access article under the terms of the Creative Commons Attribution License, which permits use, distribution and reproduction in any medium, provided the original work is properly cited.

py during the last decades. Several studies focused on the UV-induced thioamide→thiolimine tautomerization, which has been reported for 2(1*H*)-pyridinethione,<sup>[12]</sup> 4(3*H*)-pyrimidinethione and 3(2*H*)-pyridazinethione,<sup>[13]</sup> 2(1*H*)-quinolinethione,<sup>[14]</sup> methimazole,<sup>[15]</sup> 2-thiobenzimidazole,<sup>[16]</sup> thiourea,<sup>[17,18]</sup> and thioacetamide.<sup>[19–21]</sup> In the case of thiourea the reverse thiolimine → thioamide reaction has been observed even under cryogenic conditions and the results were interpreted as to involve quantum mechanical tunneling (QMT).<sup>[17,18]</sup> Dithiooxamide shows UV-induced double proton transfer forming the dithiolimine and the reverse reaction due to QMT.<sup>[22]</sup> Thioacetamide, on the other hand, does not display such a tunneling reaction under experimental laboratory conditions.<sup>[19,20]</sup> Generally speaking, QMT is an abundant, yet often underappreciated phenomenon in chemical reactions, and it is especially well observable under cryogenic matrix isolation conditions when first order tunneling half-lives range from a few seconds to several days.<sup>[23–26]</sup> Due to the similarities regarding cryogenic temperatures and very low concentrations, many of such reactions are also highly relevant in interstellar media.

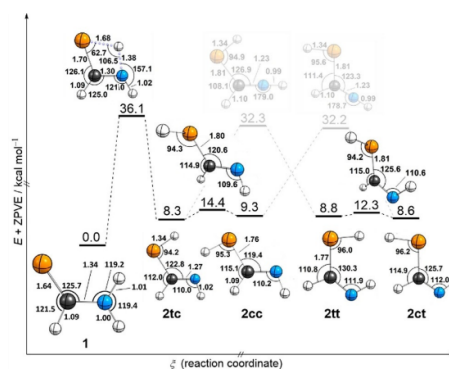
Owing to its quick decomposition at ambient conditions (see Supporting Information) reports on experimental data of **1** are rare.<sup>[27,28]</sup> Only two infrared studies on **1** in the liquid and solid phases exist, which provide IR spectra in good agreement with each other, but are controversial in the assignment of the observed bands.<sup>[29,30]</sup> However, no literature exists on the (photo-)reactivity of **1**. In stark contrast, the amide→enolimine interconversion of the congener formamide induced by irradiation with 248 nm in an Ar matrix at 10 K has been known since 2000<sup>[31]</sup> and its matrix IR spectra as early as 1970.<sup>[32,33]</sup> Irradiation with wavelengths >160 nm leads to its photodecomposition into complexes of HCN, HNC, HNCO, and H<sub>2</sub>O.<sup>[34]</sup> The tautomerizations of selenoformamide<sup>[35]</sup> and telluroformamide have been investigated only theoretically.<sup>[36]</sup> For all homologues this process has also been studied computationally by modelling aqueous hydration shells, which yielded significantly lower proton transfer barriers compared to the unimolecular gas phase reaction.<sup>[37]</sup>

The mechanism of the UV-induced tautomerization of thioamides has been discussed. Excited state intramolecular proton transfer (ESIPT) has been ruled out by Lapinski et al. due to the lack of intramolecular hydrogen bonds in these systems.<sup>[19]</sup> For methimazole<sup>[15]</sup> and 2-thiobenzimidazole<sup>[16]</sup> Brás and Fausto considered a photoinduced hydrogen-atom detachment-association (PIDA) mechanism, which has been described theoretically by Sobolewski et al.<sup>[38–41]</sup> Eventually, a study combining Raman spectroscopy and theory reconsidered the possibility of ESIPT to play a role in the tautomerization mechanism in thioacetamide.<sup>[42]</sup>

## Results and Discussion

### Computations and X-ray diffraction data

We computed the most significant part of the HC(S)NH<sub>2</sub> potential energy surface with density functional theory (DFT; see Supporting Information for details) as well as with coupled



**Scheme 2.** Potential energy surface of thioformamide (**1**) and its thiolimine tautomers (**2**) computed at the AE-CCSD(T)/aug-cc-pCVTZ level of theory. In our nomenclature for **2** the first letter represents *s-cis* or *s-trans* orientation of the S–H bond while the second letter represents *s-cis* or *s-trans* orientation of the N–H bond. Bond lengths are given in Å and angles in degrees of geometries optimized at the level of theory mentioned above. Only those internal coordinates that change throughout the displayed reactions are depicted, for exhaustive geometric data see the Supporting Information. Color code: Carbon—black, hydrogen—white, nitrogen—blue, sulfur—yellow.

cluster methods (Scheme 2). All computed minima shown in Scheme 2 display *C<sub>s</sub>* symmetry at all levels of theory applied in this study. According to the relative energies the ground state structure at cryogenic temperatures is the thioamide tautomer **1**, which is more than 8 kcal mol<sup>−1</sup> lower in energy than its thiolimine tautomers **2**. There are four conceivable conformers of **2** that are very close (within 1 kcal mol<sup>−1</sup>) in energy. The order of stability is **2cc** < **2tt** < **2ct** < **2tc** at every computational level applied here. The conformers can interconvert through C–S bond rotations or inversion of the C=N–H angle. The latter requires overcoming high lying *C<sub>s</sub>* symmetric transition states.

We obtained single crystals of **1** in ethyl acetate and solved their structure by X-ray diffraction and refined the data with the independent atom model and Hirshfeld atom refinement (Figure 1).<sup>[43]</sup> The excellent agreement of the computed geometry of **1** (Scheme 2) with the X-ray structure lends credibility to the theoretical approach. Within the crystal molecules of **1** are aligned in an array between ethyl acetate clusters. There are hydrogen bonding contacts within these arrays, but also between **1** and ethyl acetate. The structure of a single crystal of pure formamide has already been reported in 1954.<sup>[44]</sup> Formamide forms *C<sub>2h</sub>* symmetric dimers bounded with two N–H⋯O contacts. Gas-phase B3LYP/6–311++G(3df,3pd) computations predict that the analogous *C<sub>2h</sub>* dimer of **1** containing two N–H⋯S contacts is 2.0 kcal mol<sup>−1</sup> lower in energy than a *C<sub>s</sub>* dimer as depicted in Figure 1 containing only one such interaction. Note that the C–H⋯S contact in the crystal is 2.64 Å and, hence, cannot be accounted for a relevant binding contact.<sup>[45]</sup> The strong interaction between **1** and ethyl acetate (N–H⋯O contact of only 1.82 Å) is presumably the reason for the differ-

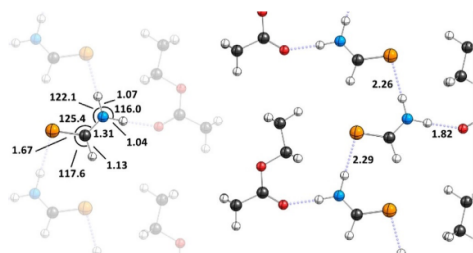


**Figure 1.** Slice through a crystal containing **1** and ethyl acetate. Left: Geometric details of a thioformamide molecule embedded in the crystal. Right: Intramolecular interactions between molecules of **1** with each other and ethyl acetate. Lengths are given in Å and angles in degrees. Color code: carbon—black, hydrogen—white, nitrogen—blue, oxygen—red, sulfur—yellow.

ence from the crystal structure in Figure 1 from the one of formamide and the computations. In a different vein, analogous S=C–N–H...O=C interactions resemble the central motif in thiourea catalysis.<sup>[46,47]</sup>

#### Matrix isolation and characterization of thioformamide

After deposition of a sample of freshly synthesized thioformamide (see Supporting Information for details) together with a large excess of Ar on the cold (3 K) matrix window, we measured IR and UV/Vis spectra of all matrix isolated species. The IR spectrum displayed in Figure 2 shows excellent agreement with the anharmonic spectrum computed at B3LYP/6–311++G(3df,3pd). Using Ar as the host material, the strongest bands are observed at 3519.4 (calc. 3507.2), 3402.2 (3391.1), 1597.6 (1596.7), 1432.0 (1424.2), 1287.6 (1283.3), and 393.1 (432.3) cm<sup>-1</sup>. We also recorded an IR spectrum of **1** in an N<sub>2</sub>

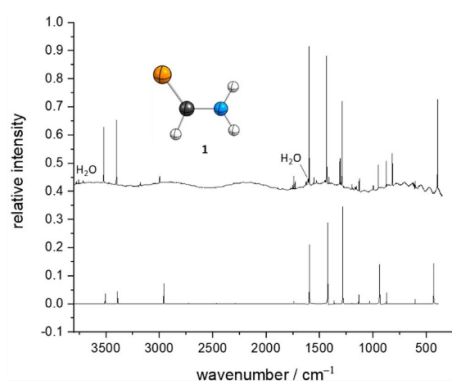


**Figure 2.** Top: IR spectrum of thioformamide (**1**) after deposition in an Ar matrix at 3 K. Bottom: Computed anharmonic IR spectrum of **1** at B3LYP/6–311++G(3df,3pd).

matrix. For the complete assignments see the Supporting Information. Our results are in good agreement with the experimental data by Davies and Jones<sup>[29]</sup> and Suzuki.<sup>[30]</sup> Additionally, there is a good match with a computational study by Kowal.<sup>[48]</sup> Our assignment is based on this latter study, which is in general accord with the one provided by Suzuki and in the computations conducted herein.

The recorded matrix UV/Vis spectrum (Figure 3) shows a strong absorption at ca. 260 nm. TD-B3LYP/6–311++G(3df,3pd) computations for thioformamide suggests two strong absorptions at 231 nm ( $f=0.2027$ ) and 225 nm ( $f=0.1517$  nm). After UV irradiation (vide infra) a small new feature at ca. 225 nm appears. This is in accord with the computational result that all thiolimine tautomers show absorptions between 210 nm and 215 nm ( $0.05 < f < 0.15$ ). For an analogous spectrum obtained in N<sub>2</sub> matrices as well as details of the nature of the transitions see the Supporting Information.

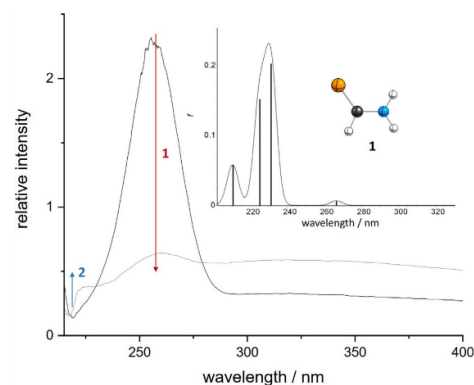


**Figure 3.** UV/Vis spectrum of the Ar matrix containing **1**. Black: After deposition of **1** in an Ar matrix. Grey: After irradiation with 254 nm for 10 min. Inset: Computed spectrum of **1** at TD-B3LYP/6–311++G(3df,3pd).

#### UV-induced thioamide to thiolimine interconversion

Irradiation of the matrix with UV light led to a decrease of the thioformamide bands. New bands appear in the IR spectra that can be assigned to **2**. The four conceivable conformers of this species can all be observed in these spectra. For ease of identification, we computed anharmonic IR spectra of **1** and **2** at B3LYP/6–311++G(3df,3pd). DFT in conjunction with a large Pople basis set generally reproduces matrix IR spectra very reasonably; recent precedence is provided in a study on thiotropolone.<sup>[49]</sup> Herein, the inclusion of anharmonicities leads to an overall good agreement between computations and measurements (see Supporting Information for details).

The computed intensities of the N–H and the S–H stretching vibrations of **2** are very low. The remainder of the simulated spectra is similar for all four conformers. The intensity pattern, especially in the C–H and N–H bending regions, turns

out to be very useful to distinguish between the two groups **2tc/2cc** and **2ct/2tt**. In the CN torsion region, the bands of **2ct** and **2tt** have nearly the same computed value. On the other hand, **2tc** and **2cc** display large shifts, such that this region is the most prominent for assignment (Figure 4). According to the anharmonic computations, only the CN torsion region in the IR spectrum differs significantly for the four conformers: two bands at 940.0 and 912.7  $\text{cm}^{-1}$  appear after UV irradiation and only **2tc** and **2cc** are computed to show IR absorptions. We assign the first band to **2cc** (calc. 944.2  $\text{cm}^{-1}$ ) and the second to **2tc** (calc. 902.5  $\text{cm}^{-1}$ ). The band at 1059  $\text{cm}^{-1}$  only has a computed counterpart in conformers **2ct** and **2tt**. As discussed below both conformers are present in the matrix and their IR bands can only be resolved in difference spectra (1058.9 and 1059.9  $\text{cm}^{-1}$ , see Figure 6). The computed values are 1048.8 and 1048.3  $\text{cm}^{-1}$  for **2ct** and **2tt**, respectively.

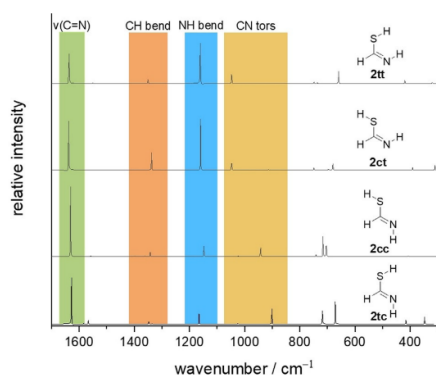


Figure 4. Computed anharmonic IR spectra of the four conceivable conformers of thiolimine 2 at B3LYP/6-311++G(3df,3pd).

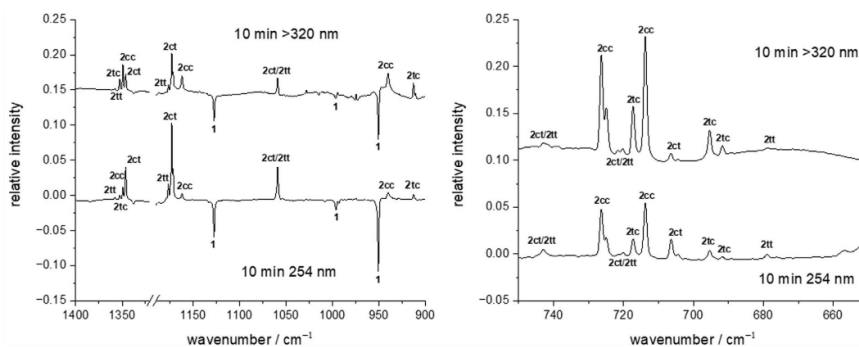


Figure 5. IR difference spectra of spectra measured before and after UV irradiation of the matrix. The ratio of the groups **2tc/2cc** and **2ct/2tt** is sensitive to the applied wavelength allowing for band assignment throughout the displayed spectral regions.

A study by Lapinski et al. demonstrated that the thioamide to thiolimine interconversion of thioacetamide yields different ratios of thiolimine conformers when the matrix is irradiated at different wavelengths.<sup>[19]</sup> Following this strategy we performed one experiment using 254 nm and another in which only wavelengths  $>320$  nm could pass through a cut-off filter installed in front of the matrix window. The difference spectra of the spectra recorded before and after 10 min of irradiation are presented in Figure 5. The intensity ratio of the new bands is indeed sensitive to the applied wavelength. At lower energies ( $>320$  nm) **2tc** and **2cc** are the main products after UV excitation while **2ct** and **2tt** are more easily accessible at lower wavelengths. This can be rationalized by taking into account the higher activation barriers for bending the N=C–S angle compared to rotating around the C–S bond (Scheme 2). This finding supports our assignment in the CN torsion region and allows to assign other bands to the groups **2tc/2cc** and **2ct/2tt**. Intensity patterns, comparing experimental with computational shifts, and interconversion of the conformers (see below) serve to resolve these two groups further and enables a confident assignment of each observed band to one conformer.

In the CH stretching region at around 1350  $\text{cm}^{-1}$  and the NH bending region at around 1170  $\text{cm}^{-1}$  four new bands appear after UV irradiation. Taking the described strategy into account we assign the strongest of these bands at 1346.2  $\text{cm}^{-1}$  to **2ct** (calc. 1338.4  $\text{cm}^{-1}$ ). With the same strategy the band at 1349.3  $\text{cm}^{-1}$  is assigned to **2cc** (calc. 1343.8  $\text{cm}^{-1}$ ), the band at 1352.7  $\text{cm}^{-1}$  to **2tc** (calc. 1349.1  $\text{cm}^{-1}$ ), and the band at 1358.0  $\text{cm}^{-1}$  to **2tt** (calc. 1352.2  $\text{cm}^{-1}$ ). The different shifts and intensities throughout the spectrum allow us to draw the conclusion that indeed **2ct** and **2tt** are both present. In the N–H bending region the band at 1162.2  $\text{cm}^{-1}$  can be assigned to **2cc**, the strong bands at 1171.8  $\text{cm}^{-1}$  and 1173.2  $\text{cm}^{-1}$  to **2ct**, and the band at 1176.9  $\text{cm}^{-1}$  to **2tt**. The computed values are 1149.7, 1161.3, and 1161.9  $\text{cm}^{-1}$  for **2cc**, **2ct**, and **2tt**, respectively, which reproduce the experimental spectra in good agreement.

Our assignment is further supported by the observation of a tunneling process from **2tt** to **2ct** and the rotamerization of **2tc** to **2cc** (vide infra). In the 670–750  $\text{cm}^{-1}$  range, all conformers are computed to show several characteristic bands as well. The assignment is possible by combining the above strategies. Analogously, we observed all four thiolimine conformers in  $\text{N}_2$  matrices. Spectra and assignments are available in the Supporting Information.

After prolonged UV irradiation the new bands assigned to the thiolimine tautomers vanished. The strongest bands after irradiation for 1 h are at 3361.8, 3202.3, 2091.2, 2026.2, 1233.4, 647.2, and 638.9  $\text{cm}^{-1}$ . These bands cannot be confidently assigned to the decomposition products  $\text{H}_2\text{S}$ ,  $\text{HCN}$ ,  $\text{HNC}$ ,  $\text{CS}$ ,  $\text{NH}_3$ ,  $\text{H}_2$ ,  $\text{HSCN}$ , or  $\text{HCNS}$  because in the present mixture significant shifts of the predicted bands of the pure compounds might occur due to the formation of complexes. Bands at 1624.1, 1553.0, and 1408.1  $\text{cm}^{-1}$  remain unchanged during UV irradiation and can thus be assigned to unknown impurities in our sample. The highest concentration of the thiolimine tautomers is observed after 10 min of irradiation when **1** is still among the main components.

#### Quantum mechanical tunneling (QMT)

After keeping the matrix for 2.5 h in the dark we observed a decay of bands belonging to **2tt** and a concomitant increase of those assigned to **2ct**. We measured the kinetics of this process by collecting IR spectra in 5 min intervals. Figure 6 shows that IR measurements without the use of a 4.5  $\mu\text{m}$  ( $\approx 2222 \text{ cm}^{-1}$ ) cut-off filter leads to the formation of **2cc** from **2tc**. This can be rationalized by the low activation barrier of only 6.1  $\text{kcal mol}^{-1}$ . We notice that wavelengths  $>4.5 \mu\text{m}$  ( $\approx 6.4 \text{ kcal mol}^{-1}$ ) would in principle suffice to initiate this process, however, we observe that when using such a cut-off filter only the reaction **2tt**  $\rightarrow$  **2ct** occurs. It is important to stress that even after longer times (up to 48 h) the intensities of bands of **2tt** do not reach zero. This might on the one hand be due to the IR Global irradiation from the spectrometer (the activation barrier for the reverse reaction **2ct**  $\rightarrow$  **2tt** is only 3.7  $\text{kcal mol}^{-1}$ ).

On the other hand, such phenomena have been assigned to matrix effects before, namely that specific matrix environments (or matrix sites) inhibit QMT.<sup>[50]</sup> Recent precedence is provided in a study on thioacetamide.<sup>[20]</sup> Furthermore, for the *N,N*-dideuterated isotopologue of thioformamide dark reactions of the thiolimine tautomers were not observed when installing the cut-off filter. This provides another hint that the reaction **2tt**  $\rightarrow$  **2ct** is due to QMT and resembles only the second example of conformational QMT leading to a rotation of a C–S bond.<sup>[20]</sup>

We obtained the experimental tunneling half-life of the reaction **2tt**  $\rightarrow$  **2ct** by following the decay (increase) of the strongest bands of **2tt** (**2ct**). A first-order kinetic model with the concentrations of **2ct** and **2tt** (that are proportional to the observed band intensities  $I$ ), the pre-exponential factor  $A$  (equal to the band intensity at  $t=0$ ) and the time  $t$  as in Figure 7 was used. The offset  $B$  needs to be included because the bands of **2tt** will not reach the asymptotical value of zero.

Especially when measuring the spectra with the 4.5  $\mu\text{m}$  cut-off filter the band intensities of **2** are rather small making an exact analysis difficult. However, changing the temperature from 3 to 20 K or placing the cut-off filter between the spectrometer and the matrix window does not change the results significantly neither in Ar nor in  $\text{N}_2$  (see the Supporting Information for details). The half-life remains between 25 and 45 min for both matrix materials.

We computed the tunneling half-lives for all conceivable reactions between the thiolimine conformers with canonical variational theory (CVT) in conjunction with small-curvature tunneling (SCT). This method has often been demonstrated to yield reliable results for matrix-isolated species.<sup>[24]</sup> Our results are shown in Table 1. In agreement with the experiment, **2tt**  $\rightarrow$  **2ct** is computed to be the fastest reaction. Even though according to the computations **2cc**  $\rightarrow$  **2tc** should be observable at laboratory time scales, we did not observe such a process. This becomes apparent when applying a scaling factor (219.5) to the computed half-lives accounting for the deviation of the experimental (ca. 30 min) and the computed value of the reaction **2tt**  $\rightarrow$  **2ct**. A somewhat more realistic value for **2cc**  $\rightarrow$  **2tc** results (1361 d), far outside reasonable experimental time

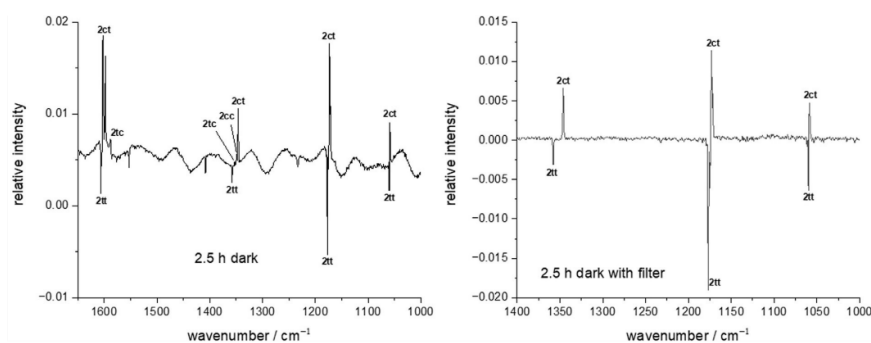


**Figure 6.** IR difference spectra of spectra measured before and after recording the kinetics for 2.5 h. Usage of a 4.5  $\mu\text{m}$  cut-off filter prevented the reaction **2tc**  $\rightarrow$  **2cc** induced by the Global of the spectrometer while **2tt**  $\rightarrow$  **2ct** proceeds due to QMT.

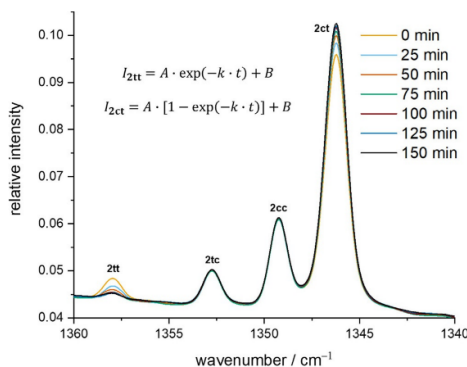


**Figure 7.** Kinetic evaluation of bands of the conformers of **2** in an Ar matrix at 3 K. A 4.5  $\mu\text{m}$  cut-off filter was used to limit photochemistry induced by the Globar of the spectrometer. The bands of **2tt** vanish with a half-life of ca. 30 min. Measurements were repeated every 5 min, but for clarity not all spectra are displayed here.

**Table 1.** Unscaled computed tunneling half-lives at the CVT/SCT/B3LYP/6-311++G(3df,3pd) level of theory. Experimentally, only **2tt**→**2ct** is observed.

Reaction	Symmetry number <sup>[a]</sup>	Tunneling half-life	
		Computation	Experiment
<b>2tt</b> → <b>2ct</b>	2	8.2 s	25–45 min
<b>2cc</b> → <b>2tc</b>	2	6.2 d	n.o. <sup>[b]</sup>
<b>2tt</b> → <b>2tc</b>	1	338 d	n.o. <sup>[b]</sup>
<b>2cc</b> → <b>2ct</b>	1	389 d	n.o. <sup>[b]</sup>

[a] Accounts for the degeneracy of the reaction coordinate  
[b] Not observed.

scales. Similar results were recently discussed for matrix isolated thioacetamide.<sup>[20]</sup> CVT/SCT underestimates tunneling half-lives probably because the matrix environment has a stabilizing effect on trapped species. As expected, for the reactions **2tt**→**2tc** and **2cc**→**2ct** the computed tunneling half-lives are much longer, due to the greater widths of the corresponding reaction barriers.

In contrast to the findings for thiourea<sup>[17,18]</sup> but in agreement with those for thioacetamide<sup>[20]</sup> no back-reaction to **1** was observed after keeping the matrix for several days in the dark.

Substitution apparently has a strong effect on the tunneling half-lives in thioamides. In this respect it is worth mentioning the different reactivities of amides, thioamides, and selenoamides. Such studies were carried out by Nowak et al. on thiourea<sup>[17,18]</sup> and selenourea.<sup>[51]</sup> The tunneling half-lives in Ar at 10 K are 52 h and 16 h with activation barriers of 25.1 kcal mol<sup>-1</sup> and 22.7 kcal mol<sup>-1</sup>, respectively, determined at the MP2/6-311++G(2d,p) level of theory.<sup>[51]</sup> At this level the minima are 14.8 kcal mol<sup>-1</sup> and 16.0 kcal mol<sup>-1</sup> apart from each other with the thioamide (selenoamide) form being more stable.<sup>[51]</sup> For matrix isolated urea such a reaction has not been reported, probably indicating a tunneling half-life too long to be observable. A very recent computational study employing the least-action tunneling (LAT) method and CVT/SCT supports the experimental trend in this series.<sup>[52]</sup>

As the tunneling rate increases for heavier homologues in this series, we aimed to determine whether this trend is also apparent in the parent structures. Table 2 shows the energies associated with the enolimine→amide tautomerization. The tunneling half-lives obtained with the Wentzel–Kramers–Brillouin (WKB) method are given in Table 2. Although the M06-2X/6-311++G(2d,p) level of theory predicts a decrease in the tunneling half-life, all values would be much too high to observe the corresponding reaction at laboratory time scales. This result is in agreement with our experimental findings reported herein as well as the absence of a tunneling reaction in the formamide system, which has been investigated by Maier and Endres.<sup>[31]</sup> We draw the conclusion that enolimine→amide tunneling is enabled by the effects of the (remote) substituent, whereas the parent systems themselves do not show such a reactivity intrinsically. This also implies that **1** and **2** might co-exist in interstellar media as quenching of **2** only seems possible through bimolecular reactivity, which is highly unlikely under interstellar conditions.

Substituent effects have been shown to affect tunneling rates before, most prominently in systematic studies on carboxylic acids<sup>[54–61]</sup> and highly reactive hydroxycarbenes.<sup>[62–69]</sup> In hydroxycarbenes + I-donating substituents like methyl result in reduced tunneling half-lives for [1,2]H-shifts towards the corresponding aldehyde.<sup>[69]</sup> Contradicting results are obtained for rotamerizations in carbonic acid<sup>[70]</sup> and its monomethyl ester.<sup>[71]</sup> When comparing our result for the reaction **2tt**→**2ct** (ca. 30 min) with the analogue reaction in thioacetamide (ca. 80 min)<sup>[20]</sup> a similar opposing trend is apparent. The absence of thiolimine→thioamide tunneling in thioacetamide<sup>[19]</sup> and thioformamide in contrast to thiourea<sup>[18]</sup> is puzzling, since  $\pi$ -donat-

**Table 2.** Relative energies, barriers, and tunneling half-lives of the enol→ketone tautomerization at B3LYP/6-311++G(3df,3pd) (M06-2X/6-311++G(2d,p) in brackets). The WKB method implemented in Tunnex<sup>[53]</sup> was used.

	Formamide	Thioformamide	Selenoformamide
$\Delta\Delta H_0$ between minima [kcal mol <sup>-1</sup> ]	12.8 (11.1)	10.0 (9.7)	10.4 (11.1)
$\Delta\Delta H_0^\ddagger$ enolimine→amide [kcal mol <sup>-1</sup> ]	26.4 (33.6)	27.1 (28.0)	25.4 (25.5)
computed QMT half-life [years]	2057 (44 210)	2307 (7079)	4703 (1315)

ing substituents incorporating heteroatoms (like  $\text{NH}_2$ ) lead to prolonged tunneling half-lives for [1,2]H-shifts in hydroxycarbenes.<sup>[69]</sup> Hence, substituent effects apparently do not affect QMT in a systematic way when comparing distinct compound classes with one another. On the one hand, barrier heights (and in this regard also barrier widths) are dependent on remote substitution. Also, the matrix material might interact differently with various derivatives of the same compound class. A very recent study in the realm of heavy-atom tunneling<sup>[72]</sup> addresses the interplay of these effects.<sup>[73]</sup> Disentangling the influences on tunneling half-lives to draw a clearer picture how to effectively control QMT remains an ongoing endeavor.

## Conclusions

We isolated thioformamide in Ar and  $\text{N}_2$  matrices and generated four conceivable conformers of the energetically higher lying thiolimine tautomer by UV excitation. One of these conformers (**2tt**) vanished with a half-life of ca. 30 min to form **2ct**. This process can be ascribed to QMT and is analogous to the findings reported recently on thioacetamide.<sup>[20]</sup>

In contrast to thiourea a tunneling reaction back to the thioamide tautomer has not been observed. This illustrates that (remote) substitution can enhance or inhibit QMT as it has already been shown in previous studies. As the effect of the substituent on QMT is intricate, further research is planned in our laboratories to fine-tune QMT and further establish its role as the 'third reactivity paradigm'.<sup>[26]</sup>

## Experimental Section

Thioformamide and its *N*-deuterated isotopologues were prepared according to the procedure by Willstätter and Wirth.<sup>[74]</sup> For details see the Supporting Information. A typical matrix isolation experiment is described in the Supporting Information. Computational details can be found there as well.

Deposition numbers 2033186, and 2032761 contain the supplementary crystallographic data for this paper. These data are provided free of charge by the joint Cambridge Crystallographic Data Centre and Fachinformationszentrum Karlsruhe Access Structures service.

## Acknowledgements

We thank Henrik Quanz and Dennis Gerbig (both JLU Giessen) for fruitful discussions. B.B. and A.K.E. thank the Fonds der Chemischen Industrie for scholarships. Open access funding enabled and organized by Projekt DEAL.

## Conflict of interest

The authors declare no conflict of interest.

**Keywords:** conformational interconversion · matrix isolation · prebiotic chemistry · tautomerism · tunneling

- [1] T. S. Jagodziński, *Chem. Rev.* **2003**, *103*, 197–228.
- [2] S. J. Kashyap, V. K. Garg, P. K. Sharma, N. Kumar, R. Dudhe, J. K. Gupta, *Med. Chem. Res.* **2012**, *21*, 2123–2132.
- [3] K. Ganapathi, A. Venkataramen, *Proc. Indian Acad. Sci. Sect. A* **1945**, *22*, 362–378.
- [4] R. Tull, L. M. Weinstock, *Angew. Chem. Int. Ed. Engl.* **1969**, *8*, 278–279; *Angew. Chem.* **1969**, *81*, 291–292.
- [5] D. Despois, *Earth Moon Planets* **1997**, *79*, 103–124.
- [6] P. G. J. Irwin, D. Toledo, R. Garland, N. A. Teanby, L. N. Fletcher, G. A. Orton, B. Bézard, *Nat. Astron.* **2018**, *2*, 420–427.
- [7] L. E. Snyder, D. Buhl, *Astrophys. J.* **1971**, *163*, L47–L52.
- [8] B. H. Patel, C. Percivalle, D. J. Ritson, C. D. Duffy, J. D. Sutherland, *Nat. Chem.* **2015**, *7*, 301–307.
- [9] D. J. Ritson, J. Xu, J. D. Sutherland, *Synlett* **2017**, *28*, 64–67.
- [10] T. Das, S. Ghule, K. Vanka, *ACS Cent. Sci.* **2019**, *5*, 1532–1540.
- [11] S. L. Miller, *Science* **1953**, *117*, 528–529.
- [12] M. J. Nowak, L. Lapinski, H. Rostkowska, A. Leś, L. Adamowicz, *J. Phys. Chem.* **1990**, *94*, 7406–7414.
- [13] M. J. Nowak, L. Lapinski, J. Fulara, A. Leś, L. Adamowicz, *J. Phys. Chem.* **1991**, *95*, 2404–2411.
- [14] D. Prusinowska, L. Lapinski, M. J. Nowak, L. Adamowicz, *Spectrochim. Acta Part A* **1995**, *51*, 1809–1826.
- [15] E. M. Brás, R. Fausto, *J. Mol. Struct.* **2018**, *1172*, 42–54.
- [16] E. M. Brás, R. Fausto, *J. Photochem. Photobiol. A* **2018**, *357*, 185–192.
- [17] H. Rostkowska, L. Lapinski, A. Khvorostov, M. J. Nowak, *J. Phys. Chem. A* **2003**, *107*, 6373–6380.
- [18] H. Rostkowska, L. Lapinski, M. J. Nowak, *Phys. Chem. Chem. Phys.* **2018**, *20*, 13994–14002.
- [19] L. Lapinski, H. Rostkowska, A. Khvorostov, M. J. Nowak, *Phys. Chem. Chem. Phys.* **2003**, *5*, 1524–1529.
- [20] S. Göbi, C. M. Nunes, I. Reva, G. Tarczay, R. Fausto, *Phys. Chem. Chem. Phys.* **2019**, *21*, 17063–17071.
- [21] S. Göbi, I. Reva, I. P. Csonka, C. M. Nunes, G. Tarczay, R. Fausto, *Phys. Chem. Chem. Phys.* **2019**, *21*, 24935–24949.
- [22] L. Lapinski, H. Rostkowska, A. Khvorostov, M. Yaman, R. Fausto, M. J. Nowak, *J. Phys. Chem. A* **2004**, *108*, 5551–5558.
- [23] D. Ley, D. Gerbig, P. R. Schreiner, *Org. Biomol. Chem.* **2012**, *10*, 3781–3790.
- [24] W. T. Borden, *WIREs Comput. Mol. Sci.* **2016**, *6*, 20–46.
- [25] J. Meisner, J. Kästner, *Angew. Chem. Int. Ed.* **2016**, *55*, 5400–5413; *Angew. Chem.* **2016**, *128*, 5488–5502.
- [26] P. R. Schreiner, *J. Am. Chem. Soc.* **2017**, *139*, 15276–15283.
- [27] R. Sugisaki, T. Tanaka, E. Hirota, *J. Mol. Spectrosc.* **1974**, *49*, 241–250.
- [28] R. H. Judge, D. C. Moule, J. D. Goddard, *Can. J. Chem.* **1987**, *65*, 2100–2105.
- [29] M. Davies, W. J. Jones, *J. Chem. Soc.* **1958**, 955–958.
- [30] I. Suzuki, *Bull. Chem. Soc. Jpn.* **1962**, *35*, 1286–1293.
- [31] G. Maier, J. Endres, *Eur. J. Org. Chem.* **2000**, 1061–1063.
- [32] S. T. King, *J. Phys. Chem.* **1971**, *75*, 405–410.
- [33] M. Räsänen, *J. Mol. Struct.* **1983**, *101*, 275–286.
- [34] F. Duvernay, A. Trivella, F. Borget, S. Coussan, J. P. Aycard, T. Chiavassa, *J. Phys. Chem. A* **2005**, *109*, 11155–11162.
- [35] W. Manz, G. Gattow, *Z. Anorg. Allg. Chem.* **1994**, *620*, 151–154.
- [36] S. Dapprich, G. Frenking, *Chem. Phys. Lett.* **1993**, *205*, 337–342.
- [37] N. Markova, V. Enchev, *J. Mol. Struct.* **2004**, *679*, 195–205.
- [38] A. L. Sobolewski, W. Domcke, *Chem. Phys.* **2000**, *259*, 181–191.
- [39] A. L. Sobolewski, W. Domcke, C. Dedonder-Lardeux, C. Jouvet, *Phys. Chem. Chem. Phys.* **2002**, *4*, 1093–1100.
- [40] B. Chmura, M. F. Rode, A. L. Sobolewski, L. Lapinski, M. J. Nowak, *J. Phys. Chem. A* **2008**, *112*, 13655–13661.
- [41] J. Jankowska, M. Barbatti, J. Sadlej, A. L. Sobolewski, *Phys. Chem. Chem. Phys.* **2017**, *19*, 5318–5325.
- [42] X. Chen, Y. Zhao, H. Zhang, J. Xue, X. Zheng, *J. Phys. Chem. A* **2015**, *119*, 832–842.
- [43] S. C. Capelli, H. B. Bürgi, B. Ditttrich, S. Grabowsky, D. Jayatilaka, *IUCrJ* **2014**, *1*, 361–379.
- [44] J. Ladell, B. Post, *Acta Crystallogr.* **1954**, *7*, 559–564.
- [45] R. Taylor, O. Kennard, *J. Am. Chem. Soc.* **1982**, *104*, 5063–5070.
- [46] P. R. Schreiner, A. Wittkopp, *Org. Lett.* **2002**, *4*, 217–220.
- [47] P. R. Schreiner, *Chem. Soc. Rev.* **2003**, *32*, 289–296.
- [48] A. T. Kowal, *J. Chem. Phys.* **2006**, *124*, 014304.

- [49] C. M. Nunes, N. A. M. Pereira, I. Reva, P. S. M. Amado, M. L. S. Cristiano, R. Fausto, *J. Phys. Chem. Lett.* **2020**, *11*, 8034–8039.
- [50] P. R. Schreiner, J. P. Wagner, H. P. Reisenauer, D. Gerbig, D. Ley, J. Sarka, A. G. Császár, A. Vaughn, W. D. Allen, *J. Am. Chem. Soc.* **2015**, *137*, 7828–7834.
- [51] H. Rostkowska, L. Lapinski, A. Khvorostov, M. J. Nowak, *Chem. Phys.* **2004**, *298*, 223–232.
- [52] I. Mosquera-Lois, D. Ferro-Costas, A. Fernandez-Ramos, *Phys. Chem. Chem. Phys.* **2020**, *22*, 24951–24963.
- [53] H. Quanz, P. R. Schreiner, *J. Comput. Chem.* **2019**, *40*, 543–547.
- [54] M. Pettersson, E. M. S. Maçõas, L. Khriachtchev, J. Lundell, R. Fausto, M. Räsänen, *J. Chem. Phys.* **2002**, *117*, 9095–9098.
- [55] E. M. S. Maçõas, L. Khriachtchev, M. Pettersson, R. Fausto, M. Räsänen, *J. Chem. Phys.* **2004**, *121*, 1331–1338.
- [56] E. M. S. Maçõas, L. Khriachtchev, M. Pettersson, R. Fausto, M. Räsänen, *J. Phys. Chem. A* **2005**, *109*, 3617–3625.
- [57] R. F. G. Apóstolo, G. Bazsó, R. R. F. Bento, G. Tarczay, R. Fausto, *J. Mol. Struct.* **2016**, *1125*, 288–295.
- [58] B. Kovács, N. Kuş, G. Tarczay, R. Fausto, *J. Phys. Chem. A* **2017**, *121*, 3392–3400.
- [59] G. Bazsó, S. Góbi, G. Tarczay, *J. Phys. Chem. A* **2012**, *116*, 4823–4832.
- [60] R. F. G. Apóstolo, G. Bazsó, G. Ogruc-İldiz, G. Tarczay, R. Fausto, *J. Chem. Phys.* **2018**, *148*, 044303.
- [61] S. Lopes, T. Nikitin, R. Fausto, *J. Phys. Chem. A* **2019**, *123*, 1581–1593.
- [62] P. R. Schreiner, H. P. Reisenauer, F. C. Pickard IV, A. C. Simmonett, W. D. Allen, E. Mátys, A. G. Császár, *Nature* **2008**, *453*, 906–909.
- [63] P. R. Schreiner, H. P. Reisenauer, *Angew. Chem. Int. Ed.* **2008**, *47*, 7071–7074; *Angew. Chem.* **2008**, *120*, 7179–7182.
- [64] D. Gerbig, H. P. Reisenauer, C. Wu, D. Ley, W. D. Allen, P. R. Schreiner, *J. Am. Chem. Soc.* **2010**, *132*, 7273–7275.
- [65] P. R. Schreiner, H. P. Reisenauer, D. Ley, D. Gerbig, C.-H. Wu, W. D. Allen, *Science* **2011**, *332*, 1300–1304.
- [66] D. Ley, D. Gerbig, J. P. Wagner, H. P. Reisenauer, P. R. Schreiner, *J. Am. Chem. Soc.* **2011**, *133*, 13614–13621.
- [67] D. Ley, D. Gerbig, P. R. Schreiner, *Chem. Sci.* **2013**, *4*, 677–684.
- [68] A. Mardyukov, H. Quanz, P. R. Schreiner, *Nat. Chem.* **2017**, *9*, 71–76.
- [69] A. K. Eckhardt, F. R. Erb, P. R. Schreiner, *Chem. Sci.* **2019**, *10*, 802–808.
- [70] J. P. Wagner, H. P. Reisenauer, V. Hirvonen, C.-H. Wu, J. L. Tyberg, W. D. Allen, P. R. Schreiner, *Chem. Commun.* **2016**, *52*, 7858–7861.
- [71] M. M. Linden, J. P. Wagner, B. Bernhardt, M. A. Bartlett, W. D. Allen, P. R. Schreiner, *J. Phys. Chem. Lett.* **2018**, *9*, 1663–1667.
- [72] C. Castro, W. L. Karney, *Angew. Chem. Int. Ed.* **2020**, *59*, 8355–8366; *Angew. Chem.* **2020**, *132*, 8431–8442.
- [73] T. Schleich, J. Tatchen, J. F. Rowen, F. Beyer, E. Sanchez-Garcia, W. Sander, *Chem. Eur. J.* **2020**, *26*, 10452–10458.
- [74] R. Willstätter, T. Wirth, *Ber. Dtsch. Chem. Ges.* **1909**, *42*, 1908–1922.

Manuscript received: December 3, 2020

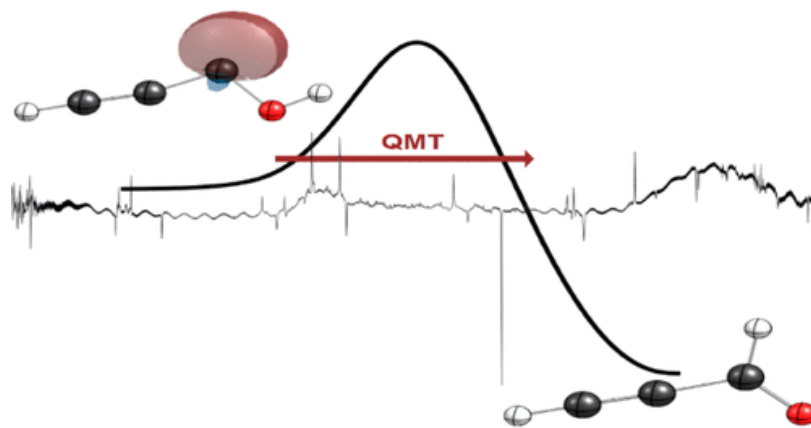
Revised manuscript received: January 21, 2021

Accepted manuscript online: January 26, 2021

Version of record online: March 12, 2021



## 2.2 Ethynylhydroxycarbene (H–C≡C– $\ddot{C}$ –OH)



### Abstract:

The species on the  $C_3H_2O$  potential energy surface have long been known to play a vital role in extraterrestrial chemistry. Here we report on the hitherto uncharacterized isomer ethynylhydroxycarbene (H–C≡C– $\ddot{C}$ –OH, **1**) generated by high-vacuum flash pyrolysis of ethynylglyoxylic acid ethyl ester and trapped in solid argon matrices at 3 and 20 K. Upon irradiation at 436 nm *trans*-**1** rearranges to its higher lying *cis*-conformer. Prolonged irradiation leads to the formation of propynal. When the matrix is kept in the dark, **1** reacts within a half-life of ca. 70 h to propynal in a conformer-specific [1,2]H-tunneling process. Our results are fully consistent with computations at the CCSD(T)/cc-pVTZ and the B3LYP/def2-QZVPP levels of theory.

### Reference:

Bastian Bernhardt, Marcel Ruth, André K. Eckhardt, and Peter R. Schreiner, *J. Am. Chem. Soc.* **2021**, *143*, 3741–3746. (DOI: 10.1021/jacs.1c00897)

### Highlight:

Ethynylhydroxycarbene—A New  $C_3H_2O$  Species, *Chemistry Views* **2021**. ([https://www.chemistryviews.org/details/news/11292097/EthynylhydroxycarbeneA\\_New\\_C3H2O\\_Species.html](https://www.chemistryviews.org/details/news/11292097/EthynylhydroxycarbeneA_New_C3H2O_Species.html))

### Reproduced with permission from:

© 2021, American Chemical Society  
1155 16<sup>th</sup> Street NW  
Washington, DC, 20036  
United States of America

# Ethynylhydroxycarbene (H–C≡C– $\ddot{C}$ –OH)

Bastian Bernhardt, Marcel Ruth, André K. Eckhardt, and Peter R. Schreiner\*

 Cite This: *J. Am. Chem. Soc.* 2021, 143, 3741–3746

 Read Online

ACCESS

 Metrics & More

 Article Recommendations

 Supporting Information

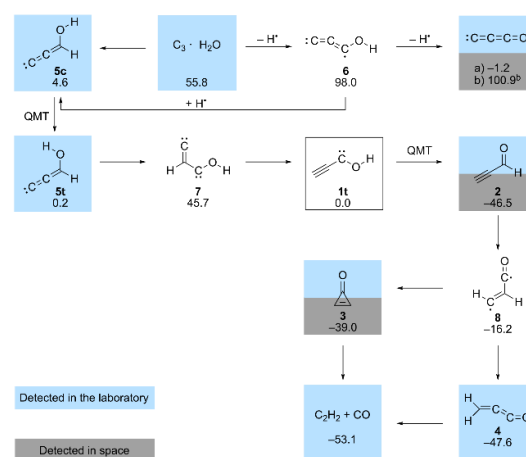
**ABSTRACT:** The species on the  $C_3H_2O$  potential energy surface have long been known to play a vital role in extraterrestrial chemistry. Here we report on the hitherto uncharacterized isomer ethynylhydroxycarbene (H–C≡C– $\ddot{C}$ –OH, **1**) generated by high-vacuum flash pyrolysis of ethynylglyoxylic acid ethyl ester and trapped in solid argon matrices at 3 and 20 K. Upon irradiation at 436 nm *trans*-**1** rearranges to its higher lying *cis*-conformer. Prolonged irradiation leads to the formation of propynal. When the matrix is kept in the dark, **1** reacts within a half-life of ca. 70 h to propynal in a conformer-specific [1,2]H-tunneling process. Our results are fully consistent with computations at the CCSD(T)/cc-pVTZ and the B3LYP/def2-QZVPP levels of theory.

Reactions of complexes of small carbon clusters with water resemble conceivable entrance channels for the formation of small oxygenated organic molecules in interstellar media.<sup>1–3</sup> It has been shown that carbon atoms in their triplet ground state are unreactive toward water,<sup>4</sup> and only for  $C_n \cdot H_2O$  with  $n \geq 3$  these complexes exist and show photoreactivity under laboratory conditions.<sup>5,6</sup> Hence, the simplest conceivable addition products all bear the formula  $C_3H_2O$ . Among these, readily prepared propynal (**2**, propionaldehyde)<sup>7,8</sup> and cyclopropenone (**3**)<sup>9–11</sup> have been also detected in space, while propadienone (**4**),<sup>12,13</sup> which lies comparably low in energy (Scheme 1),<sup>14</sup> has only been detected under cryogenic laboratory conditions.<sup>15</sup> Herein, we characterize a hitherto unreported species on the  $C_3H_2O$  potential energy surface (PES), namely ethynylhydroxycarbene (H–C≡C– $\ddot{C}$ –OH, **1**).

The  $C_3H_2O$  PES has been subject to computational and experimental research during the past four decades.<sup>14</sup> In 1990 Ortman et al. conducted photolysis of matrix-isolated carbon clusters complexed with water and found the reaction  $C_3H_2O \rightarrow 2 + C_3O$ .<sup>5</sup> A reactive intermediate detected by IR spectroscopy was assigned to the title compound **1**. Only two years later, however, Liu et al. suggested that the observed reactive intermediate is actually 3-hydroxypropadienyldiene (**5**) according to computed IR spectral data.<sup>16</sup> Eventually, Szczepanski et al. repeated the experiments of Ortman et al. and confirmed this computational conclusion.<sup>17</sup> The controversial IR bands were assigned to *cis*-3-hydroxypropadienyldiene (**5c**) and its *trans*-conformer (**5t**). Additionally, the **5c**  $\rightarrow$  **5t** interconversion in the absence of external stimuli was observed, which was interpreted on the basis of quantum mechanical tunneling (QMT). While the reaction sequence shown in Scheme 1 was later proposed on the basis of experimental and computational results,<sup>18,19</sup> **1** remains elusive.

In recent years we isolated and characterized several members of the hydroxycarbene family using high-vacuum flash pyrolysis (HVFP) of  $\alpha$ -keto acids and esters in conjunction with matrix isolation techniques.<sup>20–22</sup> Most

## Scheme 1. Proposed Mechanism<sup>18,19</sup> of the Observed Photoinduced Reactions of $C_3H_2O$ to $C_3O$ , **2**, and Acetylene + CO<sup>17a</sup>



“Ethynylhydroxycarbene (**1**) has not been detected; **2** and **3** are commodity chemicals. All compounds that have been found in space have as well been characterized under cryogenic laboratory conditions. Relative energies in kcal mol<sup>-1</sup> of singlet geometries were computed at the CCSD(T)/cc-pVTZ level of theory. <sup>b</sup>The relative energy of **6** is corrected for loss of H: a) refers to  $C_3O + H_2$  and b) refers to  $C_3O + 2 H$ .”

Received: January 24, 2021

Published: March 5, 2021

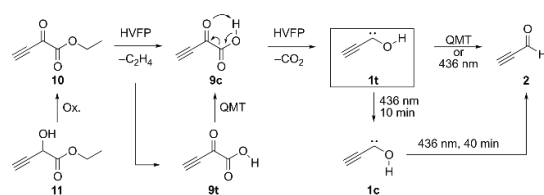


hydroxycarbenes display QMT to the corresponding aldehyde. The tunneling half-life depends on the substituent R, which in the case of R = OH, OMe, and NH<sub>2</sub> inhibits QMT.

In general, ethynylcarbenes are relevant in astrochemical processes<sup>23,24</sup> and can even be used synthetically.<sup>25–29</sup> The electronic structure of parent ground-state triplet propynylidene (HCCCH) has been explored in numerous experimental and computational studies with the result that both terminal carbons are equivalent in terms of their reactivity.<sup>30–32</sup> The photoreaction of propynylidene with triplet dioxygen provides another entrance channel to the C<sub>3</sub>H<sub>2</sub>O PES as shown in a study by Wierlacher et al., who observed **2** besides the corresponding dioxirane and carbonyl oxide.<sup>33</sup> Other triplet ground-state derivatives of propynylidene have been investigated spectroscopically and they display similarly delocalized electronic structures.<sup>34–36</sup> In contrast, singlet ethynylcarbenes (such as **1**) can best be represented by a localized carbene center in  $\alpha$ -position to a localized C $\equiv$ C bond.<sup>37</sup>

Herein we answer the following questions: (1) Can **1** be generated via pyrolysis of ethynylglyoxylic acid ethyl ester (**10**, Scheme 2) and (2) if so, does **1** undergo [1,2]H-tunneling to **2**? We support our experiments with computations at the CCSD(T)/cc-pVTZ and B3LYP/def2-QZVPP levels of theory and discuss our findings in the context of previous studies.

**Scheme 2. High-Vacuum Flash Pyrolysis (HVFP) of 10 Yields 1 via 9<sup>t</sup>**



<sup>a</sup> **1t** undergoes QMT to **2**. There is a second tunneling reaction from **9t** to **9c**, both of which are present after pyrolysis. Irradiation of the matrix at 436 nm leads to an increase of the concentrations of **1c** and **2** while **1t** vanishes nearly completely over the course of 40 min. Carbene **1c** is not photostable and vanishes after prolonged irradiation to form **2**.

We synthesized ethynylglyoxylic acid ethyl ester (**10**) via oxidation of 2-hydroxybut-3-ynoic acid ethyl ester (**11**) with Dess-Martin periodinane (see the Supporting Information for details). Precursor **10** was obtained as a yellow to brown liquid, which was stable for several weeks in a Schlenk tube connected to the matrix apparatus under reduced pressure (ca.  $3 \times 10^{-6}$  mbar). Gaseous **10** was pyrolyzed at 900 °C, and all pyrolysis products were co-condensed with an excess of argon onto the cold matrix window for IR measurements.

Mid-IR measurements of the resulting matrix revealed the formation of CO<sub>2</sub> and ethylene<sup>38</sup> during the pyrolysis. Additionally, we detected **2**, acetylene,<sup>39</sup> CO, and unreacted **10**. Bands from hitherto unreported species are discussed below. Conceivable species that are literature known (Scheme 1) like **3**,<sup>40,41</sup> **4**,<sup>15</sup> and C<sub>3</sub>O<sup>42</sup> were not observed based on comparison with published data.

After pyrolysis, a strong band at 1249.4 cm<sup>-1</sup> coincides well with the strongest band of **1t** computed at 1238.4 cm<sup>-1</sup> (determined anharmonically at B3LYP/def2-QZVPP). When irradiating the matrix at 436 nm for 40 min (Figure 1A) this

band vanishes almost completely along with bands at 3545.0 (theor. 3563.1), 3306.9 (3333.6), 2036.2 (2069.9), 1327.1 (1335.2), 797.7 (806.3), and 539.0 (533.2) cm<sup>-1</sup> all of which can be assigned to **1t**. Concomitantly, bands that can be assigned to **2** in accordance with literature data<sup>5,17</sup> at 2868.0 (theor. 2833.4), 2107.5 (2160.5), 1688.5 (1720.0), and 940.1 (940.9) cm<sup>-1</sup> increase in intensity.

Shorter irradiation times at 436 nm led to an increase of three bands that cannot be assigned to propynal (**2**). These bands at 2029.1, 1263.0, and 792.1 cm<sup>-1</sup> are barely visible after pyrolysis, reach a maximum after 10 min of irradiation at 436 nm, and decrease before they finally vanish completely after prolonged irradiation times (40 min). We assign these bands to *cis*-ethynylhydroxycarbene (**1c**) based on computed bands at 2064.3, 1265.9, and 796.8 cm<sup>-1</sup> (Figure 1B). This result is in analogy to previous studies on *trans*-trifluoromethylhydroxycarbene (F<sub>3</sub>C–C–OH, **12**) and *trans*-cyano-hydroxycarbene (NC–C–OH, **13**), which undergo photo-induced rotamerizations to their corresponding *cis*-conformers.<sup>43,44</sup> Both *cis*-hydroxycarbenes also vanish after prolonged irradiation.

In order to complement our photochemical experiments we checked for QMT reactivity by keeping the as-deposited matrix in the dark and measuring IR spectra in intervals of 1 h. We performed three such experiments: (1) at 3 K, (2) at 20 K, and (3) at 3 K and a 4.5  $\mu$ m cutoff filter installed between the spectrometer's light source and the matrix window. In all three experiments we observed a slow decay of the bands of **1t** and a simultaneous increase of those of **2** (Figure 1C). Additionally, another such set of bands is apparent, which we assign to *trans*-ethynylglyoxylic acid (**9t**) and its more stable *cis*-conformer (**9c**; Figure 1D), both of which are present due to incomplete pyrolysis of **10**. Both **9c** and **9t** can be assigned in a spectrum measured directly after pyrolysis as minor components (see the Supporting Information for complete band assignments).

We evaluated the kinetics of both QMT reactions by integrating over the strongest IR bands of all four species (**1t**, **2**, **9t**, and **9c**) and following their increase (decrease) over time. The obtained curves were fitted to monoexponential functions (first-order rate law) from which tunneling half-lives were calculated (Figure 2); see the Supporting Information for details, error estimates, and the data for **9t**  $\rightarrow$  **9c**. The kinetic profile of the reaction **1t**  $\rightarrow$  **2** is not temperature dependent, and the spectrometer beam does not seem to have a significant impact on the associated tunneling half-life of ca. 70 h taking the estimated relative error of ca. 12% into account. This result clearly points toward a QMT reaction from **1t** to **2**, which is further supported by CVT/SCT computations (*vide infra*).

We computed the potential energy surface around **1** at the CCSD(T)/cc-pVTZ level of theory (Figure 3). Similar to other hydroxycarbenes the **1t**  $\rightarrow$  **2** reaction is associated with a substantial barrier of 31.8 kcal mol<sup>-1</sup> and, hence, cannot be initiated solely by excitation from the IR spectrometer in a single photon process. IR spectra were recorded up to 7000 cm<sup>-1</sup> corresponding to a maximum energy output of only 20.0 kcal mol<sup>-1</sup>.

Tunneling computations using canonical variational theory in conjunction with small curvature tunneling (CVT/SCT) at the B3LYP/def2-QZVPP level of theory yield a QMT half-life of 62.1 h for **1t**  $\rightarrow$  **2** in excellent agreement with our experiment. The QMT half-life of **1t** nicely fits in the series of hydroxycarbenes (Figure 4). Ethynyl (sp hybridized) as a moderate  $\sigma$  acceptor ( $-I$ )<sup>45,46</sup> is expected to captodatively

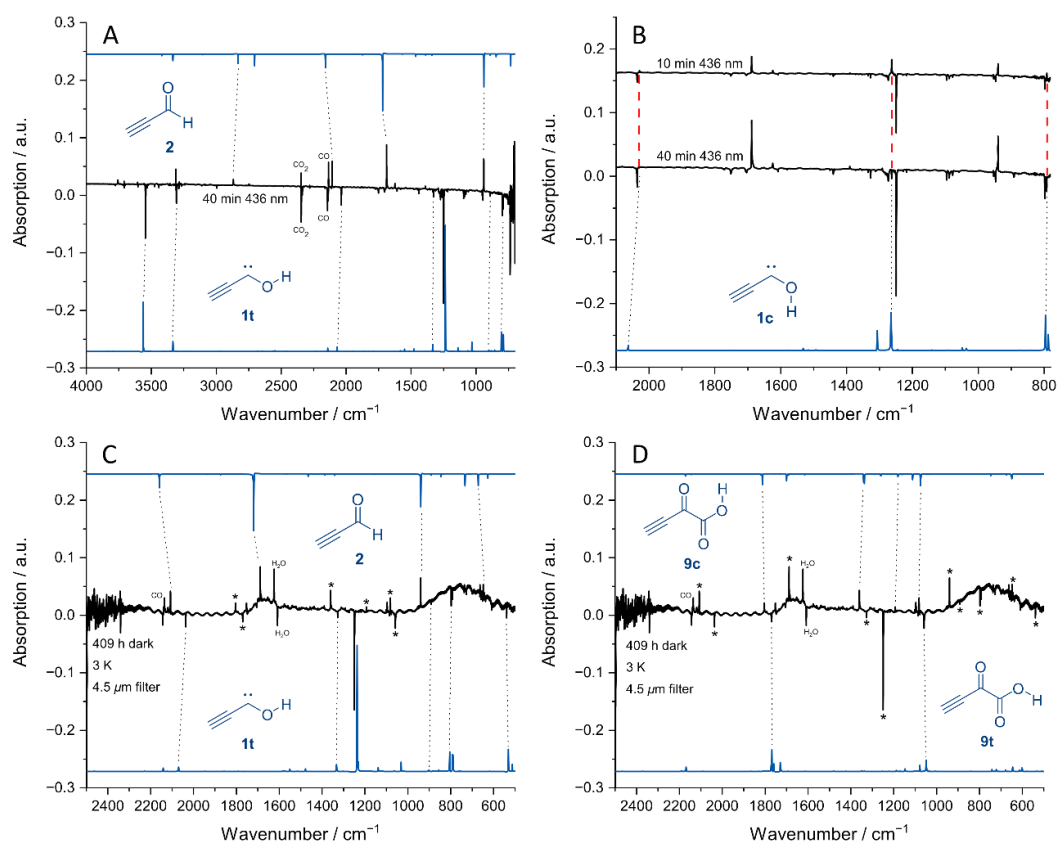


**Figure 1.** Experimental matrix IR difference spectra (black) and anharmonic spectra computed at the B3LYP/def2-QZVPP level of theory (blue). (A) After 40 min of irradiation at 436 nm bands of **1t** decrease while those of **2** increase in intensity. (B) Three bands that increase after 10 min irradiation at 436 nm and decrease after prolonged irradiation (red dashed lines) are assigned to **1c**. (C and D) By keeping the matrix in the dark for 409 h at 3 K using a 4.5  $\mu\text{m}$  cutoff filter the reactions **1t**  $\rightarrow$  **2** (C) and **9t**  $\rightarrow$  **9c** (D) were observed. Note that C and D display the same experimental difference spectrum. Bands that are assigned in C are marked with an asterisk in D and *vice versa*.

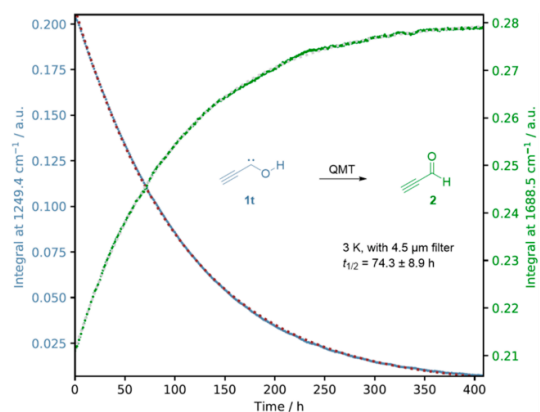


**Figure 2.** Evaluation of the tunneling half-life of the reaction from **1t** (blue data points, red fit) to **2** (green, gray) at 3 K using a 4.5  $\mu\text{m}$  cutoff filter.

stabilize the carbene center ( $\text{sp}^2$ ) in **1**, resulting in its longer half-life compared to parent hydroxymethylene (**16**).<sup>47</sup> As expected, the effect of the substituent in **1** is smaller than in trifluoromethylhydroxycarbene (**12**)<sup>43</sup> and cyanohydroxycarbene (**13**),<sup>44</sup> both of which also resemble cases of captodatively stabilized hydroxycarbenes. However, the effect is stronger than in cyclopropylhydroxycarbene (**18**),<sup>48</sup> in which the carbene center is stabilized by  $\pi$  donation (+M). The natural bond orbitals (NBO; Figure 3) of **1** support its carbene character (HOMO) and show the stabilizing effect of the adjacent oxygen lone pairs (HOMO-3). The NBOs do not provide hints for the ethynyl's  $\pi$  system to interact with the carbene center (see the SI for details).

Carbene **1** is the only hydroxycarbene without further heteroatom substituents for which the higher lying *cis*-conformer (**1c**) could be observed, which is another sign of its increased stability. According to CCSD(T)/cc-pVTZ computations **1c** lies 2.3 kcal mol<sup>-1</sup> above **1t**. Recently, we reported the spontaneous rotamerization of *cis-cis*-dihydroxycarbene to its *cis-trans*-conformer, resembling the first tunneling rotamerization in a hydroxycarbene.<sup>49</sup> However, here we could not observe the analogous reaction **1c**  $\rightarrow$  **1t**.

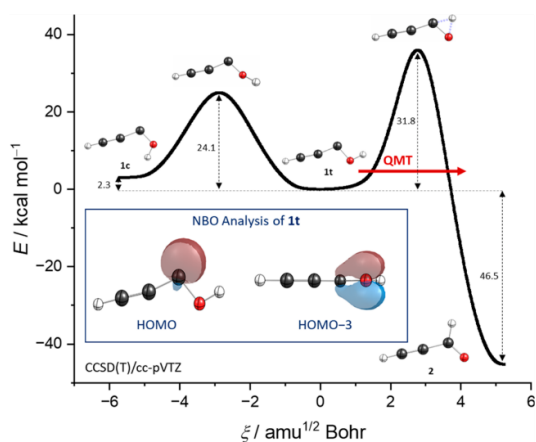


**Figure 3.** Intrinsic reaction coordinates (IRC) of  $1t \rightarrow 2$  and  $1c \rightarrow 1t$ . The IRC curve was determined at B3LYP/def2-QZVPP, and the relative energies of the stationary points are given at the CCSD(T)/cc-pVTZ level of theory. Inset: Highest occupied molecular orbital (HOMO) and HOMO-3 of  $1t$  obtained at B3LYP/def2-QZVPP. The HOMO-1 and HOMO-2 (Supporting Information) resemble the  $\pi$ -system at the alkyne moiety. Color code: Carbon, black; hydrogen, white; oxygen, red.

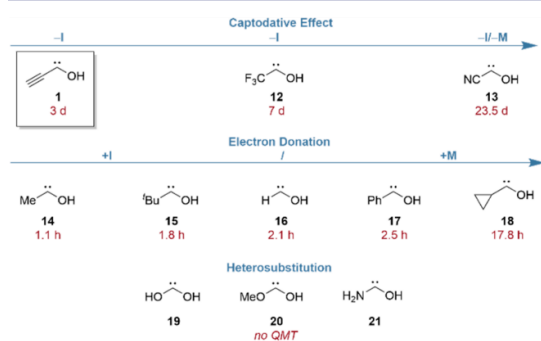


**Figure 4.** Comparison of experimental QMT half-lives of matrix isolated hydroxycarbenes.<sup>44</sup>

This is in line with the computed tunneling half-life of 60.8 d (CVT/SCT//B3LYP/def2-QZVPP) for this reaction. Note that the  $1c \rightarrow 1t$  activation barrier amounts to 21.8 kcal mol<sup>-1</sup> at the CCSD(T)/cc-pVTZ level of theory (Figure 3) while the corresponding barrier of *cis-cis*-dihydroxycarbene is only 9.4 kcal mol<sup>-1</sup>. As only  $1t$  undergoes QMT to  $2$  while  $1c$  is persistent under cryogenic conditions, the Curtin–Hammett principle is not applicable here. Similar cases of conformer-specific QMT have been reported for  $12$ <sup>43</sup> and  $13$ .<sup>44</sup>

The feasibility of  $1t \rightarrow 2$  supports the mechanism of the astrochemical formation of small organic molecules from  $C_3H_2O$  in Scheme 1.<sup>18</sup> Additionally, the intermediacy of  $1$  might open a channel for the generation of more complex sugar-like molecules via carbonyl ene reactions with carbonyls, as has been demonstrated for other hydroxycarbenes.<sup>50</sup> As noted before,<sup>17</sup> QMT is a crucial element on the  $C_3H_2O$  PES and astrochemical reactions in general, as they usually occur at diluted and low temperature (matrix isolation-like) conditions.

We isolated, characterized, and investigated the reactivity of  $1$  in argon matrices at 3 and 20 K. This complements and expands previous studies on the  $C_3H_2O$  potential energy surface and ethynylcarbenes in general. Carbene  $1$  is a viable intermediate in astrochemistry (Scheme 1). Upon irradiation at 436 nm  $1t$  reacts to afford  $2$ ;  $1c$  forms as well, but vanishes upon prolonged irradiation. The  $1t \rightarrow 2$  reaction also occurs spontaneously when keeping the matrix in the dark via QMT with a tunneling half-life of ca. 70 h in accord with theory and the general trend of hydroxycarbene QMT half-lives. Exploiting substituent effects to influence QMT reactivity and half-lives in a predictable fashion is therefore possible.

## ■ ASSOCIATED CONTENT

### Supporting Information

The Supporting Information is available free of charge at <https://pubs.acs.org/doi/10.1021/jacs.1c00897>.

Synthetic details, matrix IR and UV/Vis spectra, matrix IR band assignments, details on the kinetic analyses, and computational details (PDF)

## ■ AUTHOR INFORMATION

### Corresponding Author

Peter R. Schreiner – Institute of Organic Chemistry, Justus Liebig University Giessen, 35392 Giessen, Germany; [orcid.org/0000-0002-3608-5515](https://orcid.org/0000-0002-3608-5515); Email: [prs@uni-giessen.de](mailto:prs@uni-giessen.de)

### Authors

Bastian Bernhardt – Institute of Organic Chemistry, Justus Liebig University Giessen, 35392 Giessen, Germany; [orcid.org/0000-0002-7734-6427](https://orcid.org/0000-0002-7734-6427)  
 Marcel Ruth – Institute of Organic Chemistry, Justus Liebig University Giessen, 35392 Giessen, Germany  
 André K. Eckhardt – Institute of Organic Chemistry, Justus Liebig University Giessen, 35392 Giessen, Germany; [orcid.org/0000-0003-1029-9272](https://orcid.org/0000-0003-1029-9272)

Complete contact information is available at: <https://pubs.acs.org/10.1021/jacs.1c00897>

### Funding

B.B. and A.K.E. thank the Fonds der Chemischen Industrie for doctoral scholarships.

### Notes

The authors declare no competing financial interest.

## ■ ACKNOWLEDGMENTS

We thank our colleagues Fumito Saito, Dennis Gerbig, Artur Mardyukov, Henrik Quanz, Felix Keul, Jan M. Schümann, and Friedemann Dressler for fruitful discussions.

## ■ REFERENCES

- Federman, S. R.; Huntress, W. T. Diffuse Interstellar Clouds as Chemical Laboratory: The Chemistry of Diatomic Carbon Species. *Astrophys. J.* **1989**, *338*, 140–146.
- Bernath, P. F.; Hinkle, K. H.; Keady, J. J. Detection of  $C_5$  in the Circumstellar Shell of IRC+10216. *Science* **1989**, *244*, 562–564.
- Gredel, R. Molecular abundances in translucent clouds. *AIP Conf. Proc.* **1993**, *312*, 47.
- Schreiner, P. R.; Reisenauer, H. P. The “Non-Reaction” of Ground-State Triplet Carbon Atoms with Water Revisited. *Chem. Phys. Chem.* **2006**, *7*, 880–885.

- (5) Ortman, B. J.; Hauge, R. H.; Margrave, J. L.; Kafafi, Z. H. Reactions of Small Carbon Clusters with Water in Cryogenic Matrices. The FTIR Spectrum of Hydroxyethynylcarbene. *J. Phys. Chem.* **1990**, *94*, 7973–7977.
- (6) Dibben, M.; Szczepanski, J.; Wehlburg, C.; Vala, M. Complexes of Linear Carbon Clusters with Water. *J. Phys. Chem. A* **2000**, *104*, 3584–3592.
- (7) Irvine, W. M.; Brown, R. D.; Cragg, D. M.; Friberg, P.; Godfrey, P. D.; Kaifu, N.; Matthews, H. E.; Ohishi, M.; Suzuki, H.; Takeo, H. A new interstellar polyatomic molecule - Detection of propynal in the cold cloud TMC-1. *Astrophys. J.* **1988**, *335*, 89–93.
- (8) Sauer, J. C. Propiolaldehyde. *Org. Synth.* **1956**, *36*, 66.
- (9) Hollis, J. M.; Remijan, A. J.; Jewell, P. R.; Lovas, F. J. Cyclopropenone (c-H<sub>2</sub>C<sub>3</sub>O): A New Interstellar Ring Molecule. *Astrophys. J.* **2006**, *642*, 933–939.
- (10) Loison, J. C.; Agúndez, M.; Marcelino, N.; Wakelam, V.; Hickson, K. M.; Cernicharo, J.; Gerin, M.; Roueff, E.; Guélin, M. The interstellar chemistry of H<sub>2</sub>C<sub>3</sub>O isomers. *Mon. Not. R. Astron. Soc.* **2016**, *456*, 4101–4110.
- (11) Breslow, R.; Pecoraro, J.; Sugimoto, T. Cyclopropenone. *Org. Synth.* **1977**, *57*, 41.
- (12) Brown, R. D.; Godfrey, P. D.; Champion, R.; McNaughton, D. Microwave Spectrum and Unusual Geometry of Propadienone (Methylene Ketene). *J. Am. Chem. Soc.* **1981**, *103*, 5711–5715.
- (13) Brown, R. D.; Champion, R.; Elmes, P. S.; Godfrey, P. D. The Structure of Propadienone. *J. Am. Chem. Soc.* **1985**, *107*, 4109–4112.
- (14) Komornicki, A.; Dykstra, C. E.; Vincent, M. A.; Radom, L. A Theoretical Study of Propadienone and Its Isomers Propynal and Cyclopropenone. *J. Am. Chem. Soc.* **1981**, *103*, 1652–1656.
- (15) Chapman, O. L.; Miller, M. D.; Pitznerberger, S. M. Infrared Spectroscopy of Matrix-Isolated Propadienone. *J. Am. Chem. Soc.* **1987**, *109*, 6867–6868.
- (16) Liu, R.; Zhou, X.; Pulay, P. Ab Initio Study of the Identity of the Reaction Product between C<sub>3</sub> and Water in Cryogenic Matrices. *J. Phys. Chem.* **1992**, *96*, 5748–5752.
- (17) Szczepanski, J.; Ekern, S.; Vala, M. Spectroscopy and Photochemistry of the C<sub>3</sub>H<sub>2</sub>O Complex in Argon Matrices. *J. Phys. Chem.* **1995**, *99*, 8002–8012.
- (18) Ekern, S.; Szczepanski, J.; Vala, M. An ab Initio Study of the C<sub>3</sub>H<sub>2</sub>O Potential Surface: A Mechanism for Propynal Formation and Destruction. *J. Phys. Chem.* **1996**, *100*, 16109–16115.
- (19) Ekern, S.; Vala, M. Theoretical Study of Photochemical Mechanisms of C<sub>3</sub>O Formation. *J. Phys. Chem. A* **1997**, *101*, 3601–3606.
- (20) Ley, D.; Gerbig, D.; Schreiner, P. R. Tunneling control of chemical reactions - the organic chemist's perspective. *Org. Biomol. Chem.* **2012**, *10*, 3769–3956.
- (21) Schreiner, P. R. Tunneling Control of Chemical Reactions: The Third Reactivity Paradigm. *J. Am. Chem. Soc.* **2017**, *139*, 15276–15283.
- (22) Schreiner, P. R. Quantum Mechanical Tunneling Is Essential to Understanding Chemical Reactivity. *Trends Chem.* **2020**, *2*, 980–989.
- (23) Kaiser, R. I.; Ochsenfeld, C.; Stranges, D.; Head-Gordon, M.; Lee, Y. T. Combined crossed molecular beams and ab initio investigation of the formation of carbon-bearing molecules in the interstellar medium via neutral-neutral reactions. *Faraday Discuss.* **1998**, *109*, 183–204.
- (24) Smith, I. W. M.; Herbst, E.; Chang, Q. Rapid neutral-neutral reactions at low temperatures: a new network and first results for TMC-1. *Mon. Not. R. Astron. Soc.* **2004**, *350*, 323–330.
- (25) Shavrin, K. N.; Gvozdev, V. D.; Nefedov, O. M. (Alk-1-ynyl) oxiranes in the Reaction of (Alk-1-ynyl) chlorocarbenes with Alkali Metal Alkoxides. *Mendeleev Commun.* **1995**, *5*, 181–182.
- (26) Shavrin, K. N.; Gvozdev, V. D.; Nefedov, O. M. A new general method for the generation of (alk-1-ynyl)halocarbenes by base solvolysis of 3-substituted 1,1,1,3-tetrahalopropanes. *Mendeleev Commun.* **1997**, *7*, 144–145.
- (27) Shavrin, K. N.; Gvozdev, V. D.; Nefedov, O. M. Alkynylhalocarbenes 4. Generation of (alk-1-ynyl)halocarbenes from 3-substituted 1,1,1,3-tetrahalopropanes under the action of bases. *Russ. Chem. Bull.* **2002**, *51*, 1237–1253.
- (28) Shavrin, K. N.; Gvozdev, V. D.; Nefedov, O. M. Generation of previously unknown (alk-1-ynyl)organylthiocarbenes by the  $\gamma$ -elimination of HCl from 1-substituted 3-organyl-1-chloropropadienes under the action of bases. *Mendeleev Commun.* **2003**, *13*, 52–53.
- (29) Shavrin, K. N.; Gvozdev, V. D.; Pinus, I. Y.; Dotsenko, I. P.; Nefedov, O. M. (Alk-1-ynyl)organylthiocarbenes: generation and reactions with olefins. *Russ. Chem. Bull.* **2004**, *53*, 2546–2553.
- (30) Seburg, R. A.; Patterson, E. V.; Stanton, J. F.; McMahon, R. J. Structures, Automerizations, and Isomerizations of C<sub>3</sub>H<sub>2</sub> Isomers. *J. Am. Chem. Soc.* **1997**, *119*, 5847–5856.
- (31) Seburg, R. A.; Patterson, E. V.; McMahon, R. J. Structure of Triplet Propynylidene (HCCCH) as Probed by IR, UV/vis, and EPR Spectroscopy of Isotopomers. *J. Am. Chem. Soc.* **2009**, *131*, 9442–9455.
- (32) Osborn, D. L.; Vogelhuber, K. M.; Wren, S. W.; Miller, E. M.; Lu, Y. J.; Case, A. S.; Sheps, L.; McMahon, R. J.; Stanton, J. F.; Harding, L. B.; Ruscic, B.; Lineberger, W. C. Electronic States of the Quasilinear Molecule Propargylene (HCCCH) from Negative Ion Photoelectron Spectroscopy. *J. Am. Chem. Soc.* **2014**, *136*, 10361–10372.
- (33) Wierlacher, S.; Sander, W.; Marquardt, C.; Kraka, E.; Cremer, D. Propinal O-oxide. *Chem. Phys. Lett.* **1994**, *222*, 319–324.
- (34) Bogdanov, S. E.; Faustov, V. I.; Shavrin, K. N.; Gvozdev, V. D.; Promyslov, V. M.; Egorov, M. P.; Nefedov, O. M. A Highly Delocalized Triplet Carbene, 5-Methylhexa-1,2,4-triene-1,3-diyl: Matrix IR Identification, Structure, and Reactions. *J. Am. Chem. Soc.* **2009**, *131*, 14688–14698.
- (35) Misochko, E. Y.; Akimov, A. V.; Korchagin, D. V.; Masitov, A. A.; Shavrin, K. N. Matrix isolation ESR spectroscopy and quantum chemical calculations on 5-methylhexa-1,2,4-triene-1,3-diyl, a highly delocalized triplet “hybrid” carbene. *Phys. Chem. Chem. Phys.* **2012**, *14*, 2032–2039.
- (36) Knezz, S. N.; Waltz, T. A.; Haenni, B. C.; Burmann, N. J.; McMahon, R. J. Spectroscopy and Photochemistry of Triplet 1,3-Dimethylpropynylidene (MeC<sub>3</sub>Me). *J. Am. Chem. Soc.* **2016**, *138*, 12596–12604.
- (37) Baskir, E. G.; Gvozdev, V. D.; Shavrin, K. N.; Egorov, M. P.; Nefedov, O. M. Infrared-Spectroscopic Study of (4-Methylpent-3-en-1-ynyl)methylthiocarbene, Its Photochemical Transformations, and Reactions in an Argon Matrix. *J. Phys. Chem. A* **2019**, *123*, 9175–9184.
- (38) Cowieson, D. R.; Barnes, A. J.; Orville-Thomas, W. J. The Vibrational Spectra of Ethylene Monomer and Dimer in Argon Matrices. *J. Raman Spectrosc.* **1981**, *10*, 224–226.
- (39) Jovan Jose, K. V.; Gadre, S. R.; Sundararajan, K.; Viswanathan, K. S. Effect of matrix on IR frequencies of acetylene and acetylene-methanol complex: Infrared matrix isolation and ab initio study. *J. Chem. Phys.* **2007**, *127*, 1–10.
- (40) Breslow, R.; Ryan, G. Cyclopropenone. *J. Am. Chem. Soc.* **1967**, *89*, 3073.
- (41) Brown, F. R.; Finseth, D. H.; Miller, F. A.; Rhee, K. H. The Vibrational Spectra of Cyclopropenone and Cyclopropenone-d<sub>2</sub>. *J. Am. Chem. Soc.* **1975**, *97*, 1011–1017.
- (42) Brown, R. D.; Pullin, D. E.; Rice, E. H. N.; Rodler, M. The Infrared Spectrum and Force Field of C<sub>3</sub>O. *J. Am. Chem. Soc.* **1985**, *107*, 7877–7880.
- (43) Mardyukov, A.; Quanz, H.; Schreiner, P. R. Conformer-specific hydrogen atom tunnelling in trifluoromethylhydroxycarbene. *Nat. Chem.* **2017**, *9*, 71–76.
- (44) Eckhardt, A. K.; Erb, F. R.; Schreiner, P. R. Conformer-specific [1,2]H-tunnelling in captodatively-stabilized cyanohydroxycarbene (NC–C̄–OH). *Chem. Sci.* **2019**, *10*, 802–808.
- (45) Landgrebe, J. A.; Rynbrandt, R. H. Synthesis and Solvolysis of o-, m-, and p-Ethynylbenzyl Chloride and Closely Related Structures. The Electronic Nature of the Acetylene Group. *J. Org. Chem.* **1966**, *31*, 2585–2593.

(46) Lucas, X.; Quiñonero, D.; Frontera, A.; Deyà, P. M. Counterintuitive Substituent Effect of the Ethynyl Group in Ion- $\pi$  Interactions. *J. Phys. Chem. A* **2009**, *113*, 10367–10375.

(47) Schreiner, P. R.; Reisenauer, H. P.; Pickard, F. C., IV; Simmonett, A. C.; Allen, W. D.; Mátyus, E.; Császár, A. G. Capture of hydroxymethylene and its fast disappearance through tunnelling. *Nature* **2008**, *453*, 906–909.

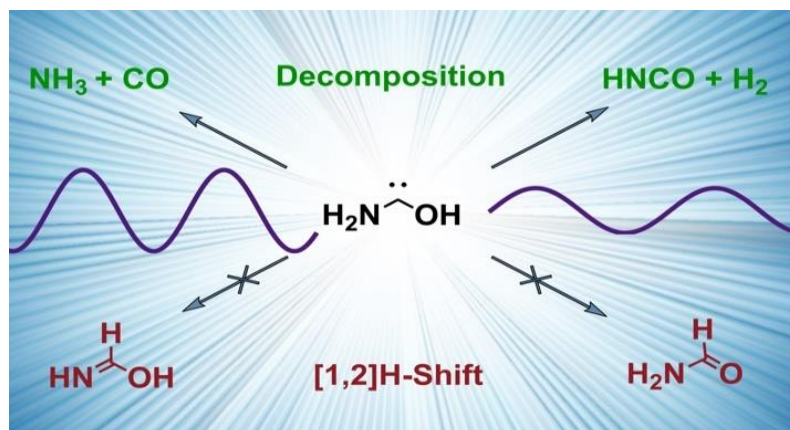
(48) Ley, D.; Gerbig, D.; Wagner, J. P.; Reisenauer, H. P.; Schreiner, P. R. Cyclopropylhydroxycarbene. *J. Am. Chem. Soc.* **2011**, *133*, 13614–13621.

(49) Quanz, H.; Bernhardt, B.; Erb, F. R.; Bartlett, M. A.; Allen, W. D.; Schreiner, P. R. Identification and Reactivity of *s*-cis, *s*-cis-Dihydroxycarbene, a New [CH<sub>2</sub>O<sub>2</sub>] Intermediate. *J. Am. Chem. Soc.* **2020**, *142*, 19457–19461.

(50) Eckhardt, A. K.; Linden, M. M.; Wende, R. C.; Bernhardt, B.; Schreiner, P. R. Gas-phase sugar formation using hydroxymethylene as the reactive formaldehyde isomer. *Nat. Chem.* **2018**, *10*, 1141–1147.



## 2.3 Aminohydroxymethylene ( $\text{H}_2\text{N}-\ddot{\text{C}}-\text{OH}$ ), the Simplest Aminooxycarbene



### Abstract:

We generated and isolated hitherto unreported aminohydroxymethylene (**1**, aminohydroxycarbene) in solid Ar *via* pyrolysis of oxalic acid monoamide (**2**). Astrochemically relevant carbene **1** is persistent under cryogenic conditions and only decomposes to  $\text{HNCO} + \text{H}_2$  and  $\text{NH}_3 + \text{CO}$  upon irradiation of the matrix at 254 nm. This photoreactivity is contrary to other hydroxycarbenes and aminomethylene, which undergo [1,2]H shifts to the corresponding carbonyls or imine. The experimental data are well supported by the results of CCSD(T)/cc-pVTZ and B3LYP/6-311++G(3df,3pd) computations.

### Reference:

Bastian Bernhardt, Marcel Ruth, Hans Peter Reisenauer, and Peter R. Schreiner *J. Phys. Chem. A* **2021**, *125*, 7023–7028. (DOI: 10.1021/acs.jpca.1c06151)

Underline denotes shared first authors.

### Highlight:

Aminohydroxymethylene, *Chemistry Views* **2021**.  
(<https://www.chemistryviews.org/details/news/11313638/Aminohydroxymethylene.html>)

*Reproduced with permission from:*

© 2021, American Chemical Society  
1155 16<sup>th</sup> Street NW  
Washington, DC, 20036  
United States of America

# Aminohydroxymethylene ( $\text{H}_2\text{N}-\ddot{\text{C}}-\text{OH}$ ), the Simplest Aminooxycarbene

Published as part of *The Journal of Physical Chemistry virtual special issue "10 Years of the ACS PHYS Astrochemistry Subdivision"*.

Bastian Bernhardt,<sup>#</sup> Marcel Ruth,<sup>#</sup> Hans Peter Reisenauer, and Peter R. Schreiner<sup>\*</sup>



Cite This: *J. Phys. Chem. A* 2021, 125, 7023–7028



Read Online

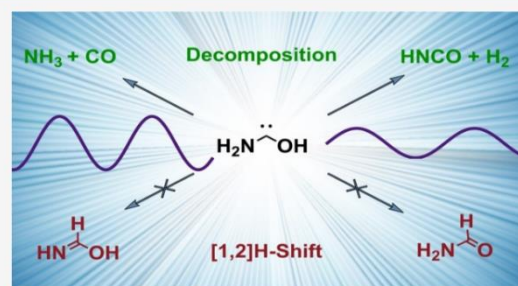
ACCESS |

Metrics & More

Article Recommendations

Supporting Information

**ABSTRACT:** We generated and isolated hitherto unreported aminohydroxymethylene (**1**, aminohydroxycarbene) in solid Ar via pyrolysis of oxalic acid monoamide (**2**). Astrochemically relevant carbene **1** is persistent under cryogenic conditions and only decomposes to HNCO + H<sub>2</sub> and NH<sub>3</sub> + CO upon irradiation of the matrix at 254 nm. This photoreactivity is contrary to other hydroxycarbenes and aminomethylene, which undergo [1,2]H shifts to the corresponding carbonyls or imine. The experimental data are well supported by the results of CCSD(T)/cc-pVTZ and B3LYP/6-311++G(3df,3pd) computations.

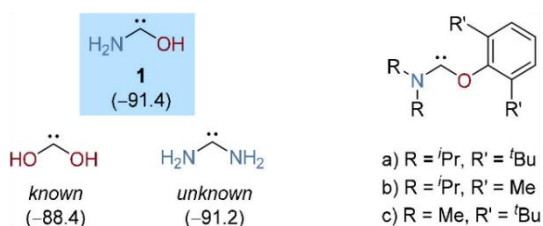


## INTRODUCTION

Aminohydroxymethylene (**1**, aminohydroxycarbene) is a prototypical electron donor stabilized carbene,<sup>1–3</sup> which has, however, never been spectroscopically identified. While diaminocarbenes and especially *N,N*-heterocyclic carbenes are ubiquitously used as ligands and catalysts,<sup>4–6</sup> aminooxycarbenes are far less popular.<sup>7,8</sup> This is surprising considering the very large isodesmic stabilization enthalpy of the corresponding parent species (Scheme 1)<sup>9,10</sup> but can be explained by their suspected high reactivity. The first

generation of *N,O*-heterocyclic carbenes (oxazolidin-2-ylidenes) was achieved 1996 by pyrolysis of 2-alkoxy-2-amino- $\Delta^3$ -1,3,4-oxadiazolines.<sup>11,12</sup> Only two years later Alder et al. reported several persistent aminooxycarbenes (Scheme 1), enabled by steric blocking of the carbene center by the *O*-substituent,<sup>13</sup> which is absent in cyclic systems. Since then, only a few examples of aminooxycarbenes appeared in the literature; they have mostly been used as metal ligands.<sup>14–17</sup> Here we report on the generation, characterization, and reactivity of the simplest aminooxycarbene **1**.

Scheme 1<sup>a</sup>



<sup>a</sup>Left: Aminohydroxymethylene (**1**) and structural analogues. Dihydroxycarbene is a known and surprisingly stable CH<sub>2</sub>O<sub>2</sub> isomer (cf. Criegee intermediate);<sup>18,19</sup> diaminocarbene is unknown. Iso-desmic stabilizations in kcal mol<sup>-1</sup> relative to methylene (0.0 kcal mol<sup>-1</sup>) obtained from ref 10 are given in parentheses. Right: Experimentally reported persistent aminooxycarbenes bearing bulky *O*-substituents.<sup>13</sup>

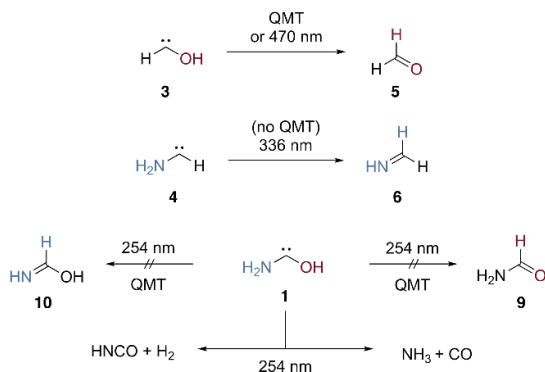
Carbene **1** is an isomer of formamide (**9**) and formimidic acid (**10**; Scheme 2). H<sub>2</sub>NCOH species have been discussed in the context of interstellar and prebiotic chemistry as they may form in the reactions of HCN with H<sub>2</sub>O.<sup>20</sup> Indeed, **1** has been implied in the on-surface isomerization of formamide.<sup>21,22</sup> The radical cation of **1** has been identified in mass spectrometric studies,<sup>23</sup> and it readily adds to alkenes.<sup>24,25</sup> A deprotonated derivative of **1**, namely, lithium *N,N*-dicyclohexylmethylenolate (C<sub>2</sub>NCOLi), has recently been proposed as an intermediate in transition-metal-free Fischer–Tropsch chemistry.<sup>26</sup> 1-Aminoethanol<sup>27</sup> may be considered the dimerization product of **1** and methylene.

Received: July 9, 2021

Revised: July 30, 2021

Published: August 10, 2021

**Scheme 2. Reaction Products of Hydroxymethylene (3) and Aminomethylene (4) and the Absence of These Products in Their “Hybrid” Aminohydroxymethylene (1)<sup>a</sup>**

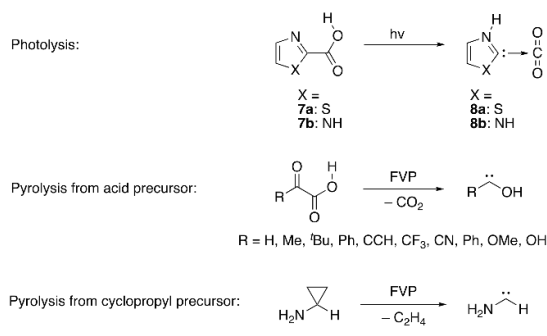


<sup>a</sup>Carbene 1 instead decomposes to HNCO + H<sub>2</sub> and NH<sub>3</sub> + CO.

Structurally, **1** combines the functionalities of hydroxymethylene (**3**)<sup>28</sup> and aminomethylene (**4**),<sup>10</sup> both of which have been studied under matrix isolation conditions (Scheme 2). As most hydroxycarbenes,<sup>29–31</sup> **3** undergoes a [1,2]H shift to yield formaldehyde (**5**) via quantum mechanical tunneling (QMT) or photochemical excitation.<sup>28</sup> Carbene **4** reacts in a similar fashion to methanimine **6** but only when the matrix is irradiated with UV light.<sup>10</sup> Herein we demonstrate that **1** does not follow either of these reaction paths but instead decomposes photochemically to NH<sub>3</sub> + CO and HNCO + H<sub>2</sub>.

Earlier studies demonstrated that the irradiation of thiazole-2-carboxylic acid (**7a**)<sup>32</sup> and imidazole-2-carboxylic acid (**7b**)<sup>33</sup> in an Ar matrix at 10 K yields the corresponding carbenes **8a** and **8b** complexed with CO<sub>2</sub> (Scheme 3). In

**Scheme 3. Examples of Strategies To Generate and Isolate Carbenes from Various Precursors under Matrix Conditions**



contrast, **1** cannot be detected directly upon photolysis of oxalic acid monoamide (**2**) but presumably is an intermediate during photodecomposition of **2** into HNCO + H<sub>2</sub> and NH<sub>3</sub> + CO.<sup>34</sup> As we have demonstrated in multiple cases (Scheme 3),<sup>29–31</sup> decarboxylation via flash vacuum pyrolysis (FVP) of α-keto carboxylic acids is the method of choice for the generation, matrix isolation, and structural elucidation of hydroxycarbenes. Accordingly, we generated **1** via pyrolysis of oxalic acid monoamide (**2**).

A gas phase study by Terlouw et al.<sup>35</sup> hints toward the possibility to isolate **1** under matrix isolation conditions but also toward its facile isomerization to formamide (**9**) and/or formimidic acid (**10**), because all three species were detected after one-electron reduction of their cations in collision induced dissociation mass spectra. The relationship between **1**, **9**, and **10** has been the subject of several computational studies.<sup>36–38</sup> The spectroscopic properties of **10** were elucidated in an investigation on the photoreactivity of **9** in an Ar matrix.<sup>39</sup> According to this study, irradiation with a KrF excimer laser (λ = 248 nm) induces a [1,3]H shift of **9** to yield **10**.<sup>39</sup> In contrast, irradiation of **9** at 193 nm yields the photodecomposition products NH<sub>3</sub> + CO as well as HNCO + H<sub>2</sub>.<sup>40</sup> These findings are also in fair agreement with a study by Duvernay et al., which shows that irradiation of formamide at 240 nm leads to **10** while broad-band UV irradiation (λ > 160 nm) results in dehydrogenation and dehydration of **10**.<sup>41</sup>

## EXPERIMENTAL SECTION

Details of the compound syntheses and characterizations are described in the Supporting Information. A Sumitomo cryostat system consisting of an RDK 408D2 closed-cycle refrigerator cold head and an F-70 compressor unit was used for matrix isolation experiments. A polished CsI window was mounted in the cold head's sample holder. The sample holder, connected with silicon diodes for temperature measurements, was covered by the vacuum shroud, which was equipped with KBr windows to allow for IR measurements. In some experiments BaF<sub>2</sub> windows were used due to their higher transparency when measuring UV/vis spectra. The sample and the host gas (Ar, purity of 99.999%) were co-deposited at 15 K. All spectral data were collected at 3 K except for two kinetic experiments, which were performed at 20 K. The pyrolysis zone was equipped with a heatable 90 mm long quartz tube (inner diameter 7 mm), controlled by a Ni/CrNi thermocouple. The travel distance of the sample from the pyrolysis zone to the matrix was ~45 mm. Ar was stored in a 2 L gas balloon, which was evacuated and filled three times before every experiment. The sample was evaporated from a Schlenk tube at 55 °C (water) and reduced pressure (~3 × 10<sup>-6</sup> mbar) and co-deposited with a high excess of argon on both sides of the matrix window in the dark (preventing unwanted photochemistry) at a rate of ~1 mbar min<sup>-1</sup>, based on the pressure inside the Ar balloon. Pyrolyses were carried out at 700 °C. IR spectra were recorded between 7000 and 350 cm<sup>-1</sup> with a resolution of 0.7 cm<sup>-1</sup> with a Bruker Vertex 70 FTIR spectrometer. A spectrum of the cold matrix window before deposition was used as background spectrum for the subsequent IR measurements. UV/vis spectra were recorded between 200 and 800 nm with a resolution of 1 nm with a Jasco V-760 spectrophotometer. A high-pressure-mercury lamp equipped with a monochromator (LOT Quantum Design) or a low-pressure-mercury lamp (Grüntzel) fitted with a Vycor filter were used for irradiation of the matrix during photochemical experiments. Computational details are provided in the Supporting Information.

## RESULTS AND DISCUSSION

**Experimental Results.** We pyrolyzed **2** at 700 °C in high vacuum prior to trapping the resulting products in an Ar matrix. Under the applied conditions the thermal fragmentation of **2** was not complete and complex IR spectra resulted

(Figures S12–S15). The main components formed in such experiments are  $\text{CO}_2$ ,<sup>42</sup> formamide (9),<sup>43,44</sup> the two most stable conformers of formimidic acid (10),<sup>39</sup> HCN,<sup>45</sup>  $\text{H}_2\text{O}$ ,<sup>46</sup>  $\text{CO}$ ,<sup>47</sup>  $\text{NH}_3$ ,<sup>48</sup> and  $\text{HNCO}$ ,<sup>49</sup> whose bands agree with published reference data as well as with our own reference spectra of the respective matrix-isolated pure compounds. In addition, hitherto unreported bands at 3661.8, 3654.3, 3537.0, 3529.9, 1608.0, 1605.4, 1250.6, 1247.7, 602.5, 598.2, 551.5, and  $545.0\text{ cm}^{-1}$  (only the strongest bands are listed; for an exhaustive list see Table S1) can be assigned to *trans*-aminohydroxymethylene (1t). Upon short-time irradiation (1–15 min) at 254 nm these IR bands vanish and the signals of  $\text{CO}$ ,  $\text{NH}_3$ , and  $\text{HNCO}$  increase in intensity. Due to the interaction with the co-product  $\text{H}_2$ , the band of the latter is shifted to significantly higher frequencies than that of the undisturbed molecule present after pyrolysis ( $2264$  vs  $2259\text{ cm}^{-1}$ ).<sup>40</sup> Besides a small decrease of IR absorptions of unreacted 2t and the corresponding growth of those of the *cis*-rotamer 2c due to photochemical isomerization (see the Supporting Information for details),<sup>34</sup> the IR bands of all other pyrolysis products remain unchanged. Hence, subtraction of spectra measured before and after photolysis provides an excellent tool for monitoring the photolytical reactions and evaluating the IR absorption bands of 1t (Figure 1). Due to

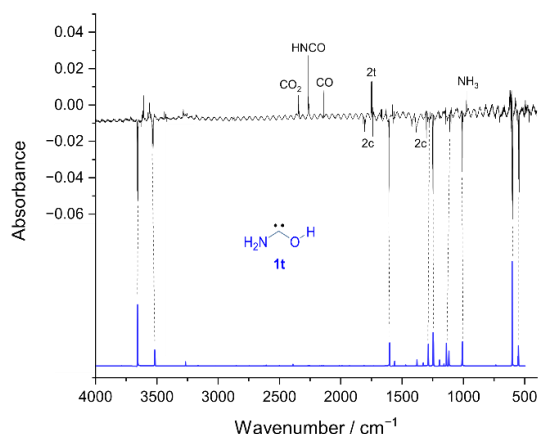


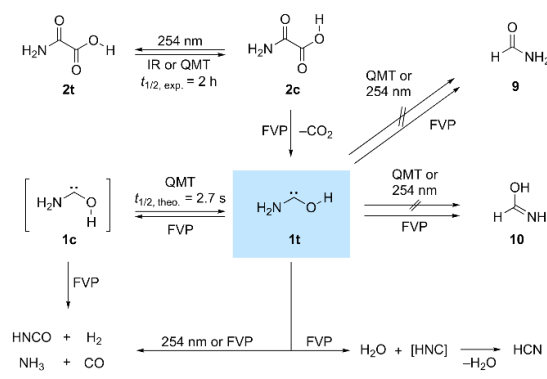
**Figure 1.** Black: Experimental matrix IR difference spectrum of spectra measured before and after irradiation of the pyrolysate at 254 nm for 15 min. Blue: Anharmonic B3LYP/6-311++G(3df,3pd) spectrum of 1t, which reacts to  $\text{HNCO} + \text{H}_2$  and  $\text{CO} + \text{NH}_3$  upon photolysis. Note that the rotamerization  $2c \rightarrow 2t$  occurs under the same conditions.<sup>34</sup>

matrix effects, all bands are split in mainly two components separated by a few wavenumbers. The excellent agreement between the experimental and computed IR absorption bands provides convincing evidence for the successful preparation of 1t and allows for band assignments. Nine of the twelve fundamental vibrations of 1t can be assigned in the experimental difference spectrum. For example, a strong band of the OH stretching vibration appears at  $3661.8/3654.3\text{ cm}^{-1}$  and that of the asymmetric stretching of the  $\text{NH}_2$  group at  $3537.0/3529.9\text{ cm}^{-1}$ . A very intense band ( $1608.0/1605.4\text{ cm}^{-1}$ ) is assigned to the  $\text{NH}_2$  scissoring vibration, while a couple of CO stretching and  $\text{NH}_2$  rocking vibrations give rise to another very strong band at  $1250.6/1247.7\text{ cm}^{-1}$ . Further

band assignments are provided in Table S1. Spectra of the pyrolysis products of *d*<sub>3</sub>-2 support our assignments through excellent matching of the experimentally observed and computed shifts in vibrational frequencies upon deuteration (see Tables S2, S3 and Figure S18).

Scheme 4 summarizes the reaction network also including the results of earlier photolysis experiments with 2.<sup>34</sup> The

#### Scheme 4. Reaction Network around Aminohydroxymethylene (1)



observed photobehavior of 1 is different from that of hydroxymethylene<sup>28</sup> and aminomethylene,<sup>10</sup> which undergo  $[1,2]\text{H}$  shifts to form the corresponding aldehyde (here 9) and imine (here 10; Scheme 2), respectively. Keeping a matrix containing 1t for one day in the dark did not lead to any changes in the recorded IR spectra. In agreement with other heteroatom-stabilized hydroxycarbenes ( $\text{HO}-\dot{\text{C}}-\text{OH}$  and  $\text{MeO}-\dot{\text{C}}-\text{OH}$ )<sup>18</sup> and aminomethylene,<sup>10</sup> 1t is persistent under cryogenic conditions and does not undergo QMT.

UV/vis measurements provide additional evidence for the successful isolation of 1t (Figure 2). The recorded very weak absorption with a maximum at 248 nm is in good agreement with the EOM-CCSD/aug-cc-pVTZ//CCSD(T)/cc-pVTZ

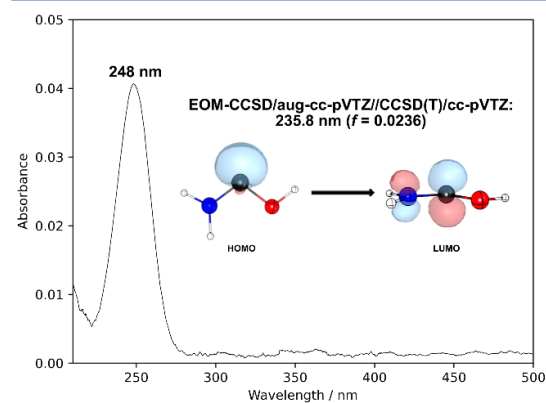


**Figure 2.** Experimental matrix UV/vis difference spectrum of spectra measured before and after irradiation of the pyrolysate at 254 nm for 15 min. Natural bond orbitals (NBOs) of 1t corresponding to the  $\text{HOMO} \rightarrow \text{LUMO}$  transition were computed at the B3LYP/6-311++G(3df,3pd) level of theory (see the Supporting Information for details).

computed HOMO → LUMO transition at 235.8 nm with a low oscillator strength of  $f = 0.0236$ . Furthermore, the measured UV absorption maximum fits well with those of dimethoxycarbene (257 nm)<sup>50</sup> and dihydroxycarbene (256 nm).<sup>18</sup> Apparently, a second donor substituent attached to the carbene center causes a remarkable large hypsochromic band shift (cf. H–C̣–OH:  $\lambda_{\text{max}} = 428$  nm). This means that the  $S_0$ – $S_1$  energy gap in **1t** of roughly 100 kcal mol<sup>-1</sup> is nearly twice as large as in parent hydroxymethylene. This high value not only exceeds all bond dissociation energies in **1t** (cf. Scheme S13) but makes an internal conversion process from  $S_1$  to  $S_0$  preceding a reaction from  $S_1$  highly improbable. This may account for the differences in the photochemical reactivity of **1t**.

**Computational Results.** Carbene **1** possesses a singlet ground state with an adiabatic singlet/triplet energy separation of 66.9 kcal mol<sup>-1</sup> at B3LYP/6-311++G(3df,3pd). This value clearly indicates a strong stabilizing effect of the heteroatom substituents (OH and NH<sub>2</sub>) on the carbene center, which is further demonstrated when comparing bond lengths in **1t** with those in aminohydroxymethane (**11**; Figure 3). Interactions of

the empty p-orbital at the carbene center with the heteroatom lone pairs result in a shortage of the CN bond (by 0.127 Å) and the CO bond (by 0.066 Å). This stabilization manifests in two resonance structures provided by natural resonance theory (NRT). According to these, the stabilizing effect of N is larger than of O, in line with their atomic properties.<sup>51</sup> Our natural bond orbital (NBO) analysis even suggests a CN  $\pi$ -bond in **1t**. A similar NBO resembling a CO  $\pi$ -bond is absent. The concentration of negative charge on the carbene carbon indicates that **1t** is expected to be highly nucleophilic. Additional information about the NBO and NRT analyses can be found in the Supporting Information.

The PES around **1** is depicted in Figure 4. Its global minimum is **9**, which is among the main products after pyrolysis of **2**. The computed activation barrier of only 35.4 kcal mol<sup>-1</sup> of the [1,2]H shift connecting **1** and **9** is the lowest of all conceivable reaction paths of **1**. Other pathways lead to the second rearrangement product **10** or to fragmentation into NH<sub>3</sub> + CO, HNC + H<sub>2</sub>, or HCN (via HNC) + H<sub>2</sub>O. The computed enthalpies of the respective transition states (TS1–TS7) are considerably higher in energy. Nevertheless, all these products could be detected in low concentrations by their characteristic absorption bands in the IR spectrum of the pyrolysate, thus providing additional strong chemical evidence for the generation of **1**. Note that HCN can form by rearrangement of HNC under the pyrolysis conditions as this process is associated with a barrier of 30.0 kcal mol<sup>-1</sup> and an exothermicity of 14.7 kcal mol<sup>-1</sup> (cf. Scheme S11).

It should be noted that the thermal H<sub>2</sub> elimination leading to HCNO as well as the fragmentation into NH<sub>3</sub> + CO requires the intermediacy of the *cis*-conformer **1c**, which could not be detected directly by spectroscopy neither as pyrolysis product nor after photolysis. This is in contrast to other stabilized hydroxycarbenes (R = OH,<sup>18</sup> OMe,<sup>18</sup> CN,<sup>52</sup> and CCH<sup>53</sup>) for which the *trans*- and the *cis*-conformers have been spectroscopically detected. *cis*-Aminohydroxymethylene (**1c**) is computed to be 5.2 kcal mol<sup>-1</sup> higher in energy than **1t**, separated from the latter by an activation barrier of only 9.2 kcal mol<sup>-1</sup>. The reason for the nonobservability of **1c** is

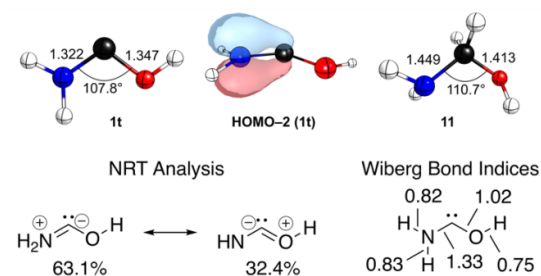


**Figure 3.** Top: Computed B3LYP/6-311++G(3df,3pd) distances (in Å) and angles in **1t** and aminohydroxymethane (**11**). The HOMO-2 of **1t** resembles a  $\pi$  interaction between the nitrogen lone pair and the carbene center. Bottom: This interaction is also apparent in the NRT analysis and Wiberg bond indices of **1t**.

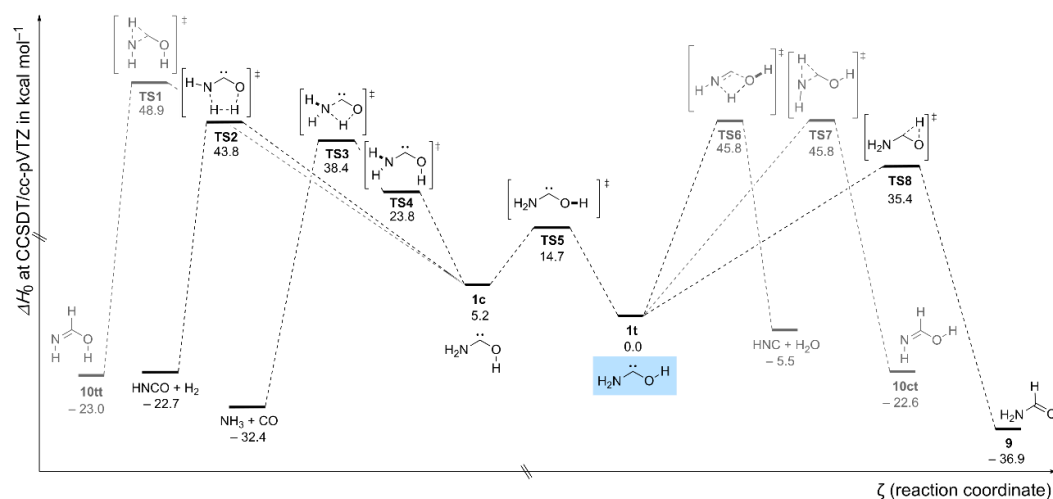


**Figure 4.** PES around **1** computed at the CCSD(T)/cc-pVTZ level of theory including zero-point vibrational energies (ZPVEs) at the same level. Note that only conformers of **10** directly linked to **1** are depicted. We refer to Scheme S10 for details of the PES around **10**.

provided by canonical variational theory (CVT) in conjunction with small curvature tunneling (SCT)<sup>54</sup> at B3LYP/6-311++G(3df,3pd), which predicts that **1c** would undergo QMT with a half-life of only 2.7 s to **1t**. An analogous QMT reaction with an experimental half-life of 15 min (in a much more stabilizing N<sub>2</sub> matrix) has recently been reported for *cis-cis*-dihydroxycarbene.<sup>19</sup> Note that we cannot detect *d*<sub>3</sub>-**1c** in the corresponding experiments even though its QMT half-life is expected to be much longer (cf. Table S14). The computed QMT half-life of **1t** → **9** amounts to 170 d at CVT/SCT//B3LYP/6-311++G(3df,3pd) in agreement with the persistence of **1t** at cryogenic temperatures, because it is stabilized through the OH and the NH<sub>2</sub> substituents (*vide supra*).

## CONCLUSIONS

We prepared, isolated, and characterized aminohydroxymethylene (**1**), the simplest aminoxy carbene, in an Ar matrix via pyrolysis of oxalic acid monoamide (**2**). Irradiation of its observed *trans*-conformer **1t** at 254 nm leads to the formation of HNCO + H<sub>2</sub> and NH<sub>3</sub> + CO. This result is in contrast to other hydroxycarbenes and aminomethylene, which undergo [1,2]H shifts to the corresponding carbonyls or imine. Due to very significant heteroatom stabilization, QMT from **1t** to formamide (**9**) or formimidic acid (**10**) does not take place on laboratory time-scales but may be relevant in astrochemical processes. The above-mentioned products together with HCN + H<sub>2</sub>O, **9**, and **10** are also present after pyrolysis of **2** and, hence, provide chemical evidence for the generation of **1** and hint toward the intermediate presence of the higher energy *cis*-conformer **1c**. This species is not persistent even at 3 K due to its fast QMT reaction to **1t**.

## ASSOCIATED CONTENT

### Supporting Information

The Supporting Information is available free of charge at <https://pubs.acs.org/doi/10.1021/acs.jpca.1c06151>.

Synthetic details, matrix IR and UV/vis spectra, matrix IR band assignments, details on the kinetic analyses, and computational details (PDF)

## AUTHOR INFORMATION

### Corresponding Author

Peter R. Schreiner – Institute of Organic Chemistry, Justus Liebig University, 35392 Giessen, Germany; [orcid.org/0000-0002-3608-5515](https://orcid.org/0000-0002-3608-5515); Email: [prs@uni-giessen.de](mailto:prs@uni-giessen.de)

### Authors

Bastian Bernhardt – Institute of Organic Chemistry, Justus Liebig University, 35392 Giessen, Germany  
 Marcel Ruth – Institute of Organic Chemistry, Justus Liebig University, 35392 Giessen, Germany  
 Hans Peter Reisenauer – Institute of Organic Chemistry, Justus Liebig University, 35392 Giessen, Germany

Complete contact information is available at: <https://pubs.acs.org/doi/10.1021/acs.jpca.1c06151>

### Author Contributions

<sup>#</sup>B.B. and M.R. contributed equally. The manuscript was written and the research conducted through contributions of all authors. All authors have given approval to the final version of the manuscript.

## Notes

The authors declare no competing financial interest.

## ACKNOWLEDGMENTS

B.B. thanks the Fonds der Chemischen Industrie for a doctoral scholarship. We thank our colleagues Dr. Dennis Gerbig, Henrik Quanz, Markus Schauermaier, and Dr. Ephraim Solel for fruitful discussions.

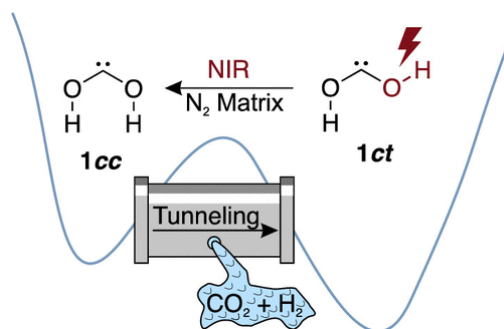
## REFERENCES

- Moss, R. A.; Zdrojewski, T.; Ho, G.-J. Push–Pull Carbenes: Methoxytrifluoromethylcarbene. *J. Chem. Soc., Chem. Commun.* **1991**, 946–947.
- Moss, R. A.; Zdrojewski, T.; Krogh-Jespersen, K.; Wlostowski, M.; Matro, A. Push-Pull Carbenes: Alkoxyoxycarbenes. *Tetrahedron Lett.* **1991**, 32, 1925–1928.
- Buron, C.; Gornitzka, H.; Romanenko, V.; Bertrand, G. Stable Versions of Transient Push-Pull Carbenes: Extending Lifetimes from Nanoseconds to Weeks. *Science* **2000**, 288, 834–836.
- Yang, L.; Wang, H. Recent Advances in Carbon Dioxide Capture, Fixation, and Activation by using N-Heterocyclic Carbenes. *ChemSusChem* **2014**, 7, 962–998.
- Flanigan, D. M.; Romanov-Michailidis, F.; White, N. A.; Rovis, T. Organocatalytic Reactions Enabled by N-Heterocyclic Carbenes. *Chem. Rev.* **2015**, 115, 9307–9387.
- Peris, E. Smart N-Heterocyclic Carbene Ligands in Catalysis. *Chem. Rev.* **2018**, 118, 9988–10031.
- Melaimi, M.; Soleilhavoup, M.; Bertrand, G. Stable Cyclic Carbenes and Related Species beyond Diaminocarbenes. *Angew. Chem., Int. Ed.* **2010**, 49, 8810–8849.
- Slaughter, L. M. Acyclic Aminocarbenes in Catalysis. *ACS Catal.* **2012**, 2, 1802–1816.
- Kelemen, Z.; Hollóczki, O.; Oláh, J.; Nyulászi, L. Oxazol-2-ylidenes. A New Class of Stable Carbenes? *RSC Adv.* **2013**, 3, 7970–7978.
- Eckhardt, A. K.; Schreiner, P. R. Spectroscopic Evidence for Aminomethylene (H–C–NH<sub>2</sub>)—The Simplest Amino Carbene. *Angew. Chem., Int. Ed.* **2018**, 57, 5248–5252.
- Couture, P.; Terlouw, J. K.; Warkentin, J. 2-Alkoxy-2-amino-Δ<sup>3</sup>-1,3,4-oxadiazolines as Novel Sources of Alkoxyaminocarbenes. *J. Am. Chem. Soc.* **1996**, 118, 4214–4215.
- Couture, P.; Warkentin, J. Spiro-fused 2-alkoxy-2-amino-Δ<sup>3</sup>-1,3,4-oxadiazolines. Synthesis and thermolysis to corresponding aminoxy-carbenes. *Can. J. Chem.* **1997**, 75, 1264–1280.
- Alder, R. W.; Butts, C. P.; Orpen, A. G. Stable Aminoxy- and Aminothiocarbenes. *J. Am. Chem. Soc.* **1998**, 120, 11526–11527.
- Klementyeva, S. V.; Abramov, P. A.; Somov, N. V.; Dudkina, Y. B.; Budnikova, Y. H.; Poddel'sky, A. I. Deprotonation of Benzoxazolium Salt: Trapping of a Radical-Cation Intermediate. *Org. Lett.* **2019**, 21, 946–950.
- Hahn, F. E.; Hein, P.; Lügger, T. Synthesis of Heterobimetallic Metal Derivatives: a Carbene Complex as Chelate Ligand. *Z. Anorg. Allg. Chem.* **2003**, 629, 1316–1321.
- Ruiz, J.; Perandones, B. F.; García, G.; Mosquera, M. E. G. Synthesis of N-Heterocyclic Carbene Complexes of Manganese(I) by Coupling Isocyanide Ligands with Propargylamines and Propargylic Alcohols. *Organometallics* **2007**, 26, 5687–5695.
- Seo, H.; Snead, D. R.; Abboud, K. A.; Hong, S. Bulky Acyclic Aminoxy carbene Ligands. *Organometallics* **2011**, 30, 5725–5730.
- Schreiner, P. R.; Reisenauer, H. P. Spectroscopic Identification of Dihydroxycarbene. *Angew. Chem., Int. Ed.* **2008**, 47, 7071–7074.
- Quanz, H.; Bernhardt, B.; Erb, F. R.; Bartlett, M. A.; Allen, W. D.; Schreiner, P. R. Identification and Reactivity of *s-cis,s-cis*-Dihydroxycarbene, a New [CH<sub>2</sub>O<sub>2</sub>] Intermediate. *J. Am. Chem. Soc.* **2020**, 142, 19457–19461.
- Heikkilä, A.; Pettersson, M.; Lundell, J.; Khriachtchev, L.; Räsänen, M. Matrix Isolation and ab Initio Studies of 1:1 Hydrogen-

- Bonded Complexes HCN–H<sub>2</sub>O and HNC–H<sub>2</sub>O Produced by Photolysis of Formaldoxime. *J. Phys. Chem. A* **1999**, *103*, 2945–2951.
- (21) Nguyen, H. T.; Nguyen, M. T. Effects of Water Molecules on Rearrangements of Formamide on the Kaolinite Basal (001) Surface. *J. Phys. Chem. A* **2014**, *118*, 7017–7023.
- (22) Nguyen, H. T.; Nguyen, M. T. Effects of Sulfur-Deficient Defect and Water on Rearrangements of Formamide on Pyrite (100) Surface. *J. Phys. Chem. A* **2014**, *118*, 4079–4086.
- (23) Ruttink, P. J. A.; Burgers, P. C.; Terlouw, J. K. The decarbonylation of ionized formamide, H–C(=O)–NH<sub>2</sub><sup>+</sup>, and aminohydroxycarbene, HO–C–NH<sub>2</sub><sup>+</sup>: decay via an excited state. A quantum chemical investigation. *Int. J. Mass Spectrom. Ion Processes* **1995**, *145*, 35–43.
- (24) Bouchoux, G.; Espagne, A. Ionized Aminohydroxycarbene and its Isomers: Relative Stability and Unimolecular Reactivity. *Chem. Phys. Lett.* **2001**, *348*, 329–336.
- (25) Bouchoux, G.; Chamot-Rooke, J. Electrophilic and Radical Reactivity of Ionized Aminohydroxycarbene Toward Alkenes. *Int. J. Mass Spectrom.* **2002**, *219*, 625–641.
- (26) Xu, M.; Qu, Z.-w.; Grimme, S.; Stephan, D. W. Lithium Dicyclohexylamide in Transition-Metal-Free Fischer–Tropsch Chemistry. *J. Am. Chem. Soc.* **2021**, *143*, 634–638.
- (27) Marduykov, A.; Keul, F.; Schreiner, P. R. Preparation and Characterization of the Enol of Acetamide: 1-Aminoethanol, a High-Energy Prebiotic Molecule. *Chem. Sci.* **2020**, *11*, 12358–12363.
- (28) Schreiner, P. R.; Reisenauer, H. P.; Pickard IV, F. C.; Simmonett, A. C.; Allen, W. D.; Mátyus, E.; Császár, A. G. Capture of Hydroxymethylene and its Fast Disappearance Through Tunneling. *Nature* **2008**, *453*, 906–909.
- (29) Ley, D.; Gerbig, D.; Schreiner, P. R. Tunneling Control of Chemical Reactions – the Organic Chemist’s Perspective. *Org. Biomol. Chem.* **2012**, *10*, 3781–3790.
- (30) Schreiner, P. R. Tunneling Control of Chemical Reactions: The Third Reactivity Paradigm. *J. Am. Chem. Soc.* **2017**, *139*, 15276–15283.
- (31) Schreiner, P. R. Quantum Mechanical Tunneling Is Essential to Understanding Chemical Reactivity. *Trends Chem.* **2020**, *2*, 980–989.
- (32) Maier, G.; Endres, J.; Reisenauer, H. P. 2,3-Dihydrothiazol-2-ylidene. *Angew. Chem., Int. Ed. Engl.* **1997**, *36*, 1709–1712.
- (33) Maier, G.; Endres, J. 2,3-Dihydroimidazol-2-ylidene. *Eur. J. Org. Chem.* **1998**, *1998*, 1517–1520.
- (34) Maier, G.; Endres, J.; Reisenauer, H. P. Interconversions Between Oxalic Acid Monoamide Rotamers: Photochemical Process Versus Tunneling. *J. Mol. Struct.* **2012**, *1025*, 2–5.
- (35) McGibbon, G. A.; Burgers, P. C.; Terlouw, J. K. The Imidic Acids H–N=C(H)–OH and CH<sub>3</sub>–N=C(H)–OH and Their Tautomeric Carbenes H<sub>2</sub>N–Ċ–OH and CH<sub>3</sub>–N(H)–Ċ–OH: Stable Species in the Gas Phase Formed by One-Electron Reduction of Their Cations. *Int. J. Mass Spectrom. Ion Processes* **1994**, *136*, 191–208.
- (36) Nguyen, V. S.; Abbott, H. L.; Dawley, M. M.; Orlando, T. M.; Leszczynski, J.; Nguyen, M. T. Theoretical Study of Formamide Decomposition Pathways. *J. Phys. Chem. A* **2011**, *115*, 841–851.
- (37) Gahlaut, A.; Paranjothy, M. Unimolecular Decomposition of Formamide via Direct Chemical Dynamics Simulations. *Phys. Chem. Chem. Phys.* **2018**, *20*, 8498–8505.
- (38) Vichiotti, R. M.; da Silva, A. B. F.; Haiduke, R. L. A. Providing Theoretical Data for Detection of Four Formimidic Acid Isomers in Astrophysical Media. *Mol. Astrophys.* **2018**, *10*, 1–10.
- (39) Maier, G.; Endres, J. Isomerization of Matrix-Isolated Formamide: IR-Spectroscopic Detection of Formimidic Acid. *Eur. J. Org. Chem.* **2000**, *2000*, 1061–1063.
- (40) Lundell, J.; Krajewska, M.; Räsänen, M. Matrix Isolation Fourier Transform Infrared and Ab Initio Studies of the 193-nm-Induced Photodecomposition of Formamide. *J. Phys. Chem. A* **1998**, *102*, 6643–6650.
- (41) Duvernay, F.; Trivella, A.; Borget, F.; Coussan, S.; Aycard, J.-P.; Chiavassa, T. Matrix Isolation Fourier Transform Infrared Study of Photodecomposition of Formimidic Acid. *J. Phys. Chem. A* **2005**, *109*, 11155–11162.
- (42) Schriver, A.; Schriver-Mazzuoli, L.; Vigasin, A. A. Matrix Isolation Spectra of the Carbon Dioxide Monomer and Dimer Revisited. *Vib. Spectrosc.* **2000**, *23*, 83–94.
- (43) King, S.-T. Infrared Study of the NH<sub>2</sub> ‘Inversion’ Vibration for Formamide in the Vapor Phase and in an Argon Matrix. *J. Phys. Chem.* **1971**, *75*, 405–410.
- (44) Räsänen, M. A Matrix Infrared Study of Monomeric Formamide. *J. Mol. Struct.* **1983**, *101*, 275–286.
- (45) Pacansky, J.; Calder, G. V. The Infrared Spectra of HCN Isotopes in Argon Matrices: An Examination of the Assumptions of Matrix Isolation Spectroscopy. *J. Mol. Struct.* **1972**, *14*, 363–383.
- (46) Ayers, G. P.; Pullin, A. D. E. The i.r. Spectra of Matrix Isolated Water Species—I. Assignment of Bands to (H<sub>2</sub>O)<sub>2</sub>, (D<sub>2</sub>O)<sub>2</sub> and HDO Dimer Species in Argon Matrices. *Spectrochim. Acta, Pt. A: Mol. Spectrosc.* **1976**, *32*, 1629–1639.
- (47) Leroi, G. E.; Ewing, G. E.; Pimentel, G. C. Infrared Spectra of Carbon Monoxide in an Argon Matrix. *J. Chem. Phys.* **1964**, *40*, 2298–2303.
- (48) Cugley, J. A.; Pullin, A. D. E. The Infrared Spectrum of Ammonia Isolated in Argon and Nitrogen Matrices. *Spectrochim. Acta, Pt. A: Mol. Spectrosc.* **1973**, *29*, 1665–1672.
- (49) Teles, J. H.; Maier, G.; Andes Hess, B., Jr; Schaad, L. J.; Winnewisser, M.; Winnewisser, B. P. The CHNO Isomers. *Chem. Ber.* **1989**, *122*, 753–766.
- (50) Reisenauer, H. P.; Romański, J.; Młostoń, G.; Schreiner, P. R. Dimethoxycarbene: Conformational Analysis of a Reactive Intermediate. *Eur. J. Org. Chem.* **2006**, *2006*, 4813–4818.
- (51) Kapp, J.; Schade, C.; El-Nahasa, A. M.; von Ragué Schleyer, P. Heavy Element  $\pi$  Donation is not Less Effective. *Angew. Chem., Int. Ed. Engl.* **1996**, *35*, 2236–2238.
- (52) Eckhardt, A. K.; Erb, F. R.; Schreiner, P. R. Conformer-Specific [1,2]H-Tunneling in Captodatively-Stabilized Cyanohydroxycarbene (NC–Ċ–OH). *Chem. Sci.* **2019**, *10*, 802–808.
- (53) Bernhardt, B.; Ruth, M.; Eckhardt, A. K.; Schreiner, P. R. Ethynylhydroxycarbene (H–C≡C–Ċ–OH). *J. Am. Chem. Soc.* **2021**, *143*, 3741–3746.
- (54) Bao, J. L.; Truhlar, D. G. Variational Transition State Theory: Theoretical Framework and Recent Developments. *Chem. Soc. Rev.* **2017**, *46*, 7548–7596.



## 2.4 Identification and Reactivity of *s-cis,s-cis*-Dihydroxycarbene, a New [CH<sub>2</sub>O<sub>2</sub>] Intermediate



### Abstract:

We report the first preparation of the *s-cis,s-cis* conformer of dihydroxycarbene (**1cc**) by means of pyrolysis of oxalic acid, isolation of the lower-energy *s-trans,s-trans* (**1tt**) and *s-cis,s-trans* (**1ct**) product conformers at cryogenic temperatures in a N<sub>2</sub> matrix, and subsequent narrow-band near-infrared (NIR) laser excitation to give **1cc**. Carbene **1cc** converts quickly to **1ct** via quantum-mechanical tunneling with an effective half-life of 22 min at 3 K. The potential energy surface features around **1** were pinpointed by convergent focal point analysis targeting the AE-CCSDT(Q)/CBS level of electronic structure theory. Computations of the tunneling kinetics confirm the time scale of the **1cc** → **1ct** rotamerization and suggest that direct **1cc** → H<sub>2</sub> + CO<sub>2</sub> decomposition may also be a minor pathway. The intriguing latter possibility cannot be confirmed spectroscopically, but hints of it may be present in the measured kinetic profiles.

### Reference:

Henrik Quanz, Bastian Bernhardt, Frederik R. Erb, Marcus A. Bartlett, Wesley D. Allen, and Peter R. Schreiner *J. Am. Chem. Soc.* **2020**, *142*, 19457–19461. (DOI: 10.1021/jacs.0c09317)

Underline denotes shared first authors.

### Highlight:

Spotlights on Recent *JACS* Publications: Attabey R. Benítez *J. Am. Chem. Soc.* **2020**, *142*, 20913–20914. (DOI: 10.1021/jacs.0c12720)

Reproduced with permission from:

© 2020, American Chemical Society  
1155 16<sup>th</sup> Street NW  
Washington, DC, 20036  
United States of America

## Identification and Reactivity of *s-cis,s-cis*-Dihydroxycarbene, a New [CH<sub>2</sub>O<sub>2</sub>] Intermediate

Henrik Quanz,<sup>||</sup> Bastian Bernhardt,<sup>||</sup> Frederik R. Erb, Marcus A. Bartlett, Wesley D. Allen,<sup>\*</sup> and Peter R. Schreiner<sup>\*</sup>

Cite This: *J. Am. Chem. Soc.* 2020, 142, 19457–19461

Read Online

ACCESS |

Metrics & More

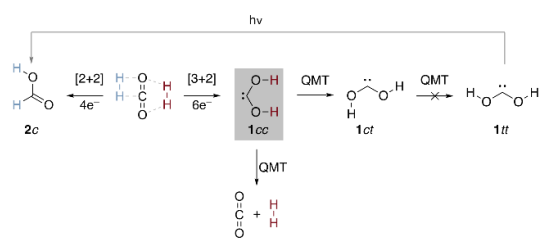
Article Recommendations

Supporting Information

**ABSTRACT:** We report the first preparation of the *s-cis,s-cis* conformer of dihydroxycarbene (**1cc**) by means of pyrolysis of oxalic acid, isolation of the lower-energy *s-trans,s-trans* (**1tt**) and *s-cis,s-trans* (**1ct**) product conformers at cryogenic temperatures in a N<sub>2</sub> matrix, and subsequent narrow-band near-infrared (NIR) laser excitation to give **1cc**. Carbene **1cc** converts quickly to **1ct** via quantum-mechanical tunneling with an effective half-life of 22 min at 3 K. The potential energy surface features around **1** were pinpointed by convergent focal point analysis targeting the AE-CCSDT(Q)/CBS level of electronic structure theory. Computations of the tunneling kinetics confirm the time scale of the **1cc** → **1ct** rotamerization and suggest that direct **1cc** → H<sub>2</sub> + CO<sub>2</sub> decomposition may also be a minor pathway. The intriguing latter possibility cannot be confirmed spectroscopically, but hints of it may be present in the measured kinetic profiles.

The fundamental chemistry of the [CH<sub>2</sub>O<sub>2</sub>] system is paramount to the grand challenges of energy storage and transportation as well as control of global warming. Moreover, as highly abundant molecules in space, H<sub>2</sub> and CO<sub>2</sub> may provide access to simple organic molecules in the atmosphere of prebiotic earth and extraterrestrial environments.<sup>1–3</sup> Although the direct reduction of CO<sub>2</sub> with H<sub>2</sub> has a prodigious activation barrier (>80 kcal mol<sup>-1</sup>), McCarthy et al.<sup>4</sup> formed both *s-cis,s-trans*-dihydroxycarbene (**1ct**) (Scheme 1) and *s-*

**Scheme 1. Formal Electrocyclic Reactions of H<sub>2</sub> + CO<sub>2</sub> Leading to *s-cis,s-cis*-Dihydroxycarbene (**1cc**), *s-cis*-Formic Acid (**2c**), and the Lower-Lying Rotamers of **1****



*trans*-formic acid (**2t**) by electric discharge of gaseous H<sub>2</sub> + CO<sub>2</sub> mixtures. This alternative route complements our original synthesis of **1ct** and *s-trans,s-trans*-dihydroxycarbene (**1tt**) based on pyrolysis of oxalic acid.<sup>5</sup>

The formation of **1** and subsequently **2** from H<sub>2</sub> + CO<sub>2</sub> potentially plays a role in the origin of life by trapping of H<sub>2</sub> from volcanic or other origins before its rapid escape into the atmosphere.<sup>6</sup> As **2** is present in volcanic eruptions and black smokers,<sup>7</sup> one viable route may involve **1** as a reactive intermediate. In a different vein, we have shown recently that

dihydroxycarbenes react with carbonyl compounds to form sugars in the gas phase.<sup>8</sup> Analogously, **1** may be a C<sub>1</sub> building block for amino acids through its reactions with imines.

In contrast to most hydroxycarbenes, at cryogenic temperatures **1** does not undergo a [1,2]-H shift via quantum-mechanical tunneling (QMT) to the associated carbonyl product<sup>9</sup> **2** because strong oxygen lone-pair electron donation increases the accompanying barrier.<sup>4</sup> Of the three possible dihydroxycarbene rotamers,<sup>10</sup> **1tt** and **1ct** have been identified spectroscopically,<sup>4,5,11</sup> but the higher-energy species *s-cis,s-cis*-dihydroxycarbene (**1cc**) has not been reported. Here we isolate and spectroscopically characterize **1cc**, document its conformational QMT to **1ct**, and explore the possibility of its direct dissociation into H<sub>2</sub> + CO<sub>2</sub> at very low temperatures.

The direct formation of **1** from H<sub>2</sub> and CO<sub>2</sub><sup>4</sup> seems feasible only through the **1cc** rotamer, elevating the need to fully characterize this species. While **2c** is 44.6 kcal mol<sup>-1</sup> lower in energy than **1cc** (Figure 1), the activation barriers to form **1** and **2** from H<sub>2</sub> + CO<sub>2</sub> differ by less than 8 kcal mol<sup>-1</sup>. Although the formation of **2** is formally a thermally forbidden<sup>12,13</sup> four-electron [2 + 2] cycloaddition,<sup>14,15</sup> it is kinetically favored in the absence of QMT over the allowed six-electron [3 + 2] reaction to give **1cc** (Scheme 1). However, the situation might change when QMT is taken into account, as this phenomenon leads to increased reaction rates, i.e., effectively lower activation barriers. The possible involvement of **1** in fundamental [CH<sub>2</sub>O<sub>2</sub>] chemistry has long been

Received: August 30, 2020  
 Published: November 9, 2020



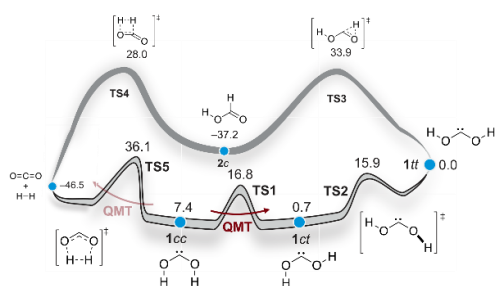
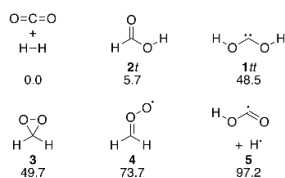


**Figure 1.** Pictorial presentation (not drawn to scale) of the converged FPA relative energies ( $\Delta H_0$ , in kcal mol<sup>-1</sup>) of key species connected to **1**. Details of the computations are given in the SI.

**Scheme 2. Relative Energies of the Experimentally Identified Species (Lowest-Energy Conformers) on the [CH<sub>2</sub>O<sub>2</sub>] Potential Energy Surface (Computed FPA Relative Energies Are Given in kcal mol<sup>-1</sup>)**



overlooked, as studies have mostly emphasized the Criegee intermediate **4**<sup>16,17</sup> and dioxirane **3**,<sup>18</sup> which are actually *higher* in energy (Scheme 2).

Here we follow our established route employing high-vacuum flash pyrolysis (HVFP) of oxalic acid (**6**) to first produce and trap **1ff** and **1ct** in a N<sub>2</sub> matrix at 3 K.<sup>5</sup> To generate **1cc**, **1ff** and **1ct** were prepared first and then selectively irradiated with near-infrared (NIR) light from a narrow-band optical parametric oscillator (OPO) laser. Similar strategies have been used to detect higher-lying rotamers of other matrix-isolated compounds (e.g., formic acid).<sup>19–22</sup> New electronic structure computations employing focal point analysis (FPA)<sup>23–27</sup> were executed to obtain definitive energetics for the potential energy surface (PES) surrounding **1** (Figure 1) at the composite AE-CCSD(T)/CBS//AE-CCSD(T)<sup>28–32</sup>/aug-cc-pCVTZ<sup>33</sup> level of theory.<sup>34,35</sup> Tunneling half-lives were computed using both AE-CCSD(T)/aug-cc-pCVTZ reaction paths conjoined with the Wentzel–Kramers–Brillouin (WKB) method<sup>36–39</sup> as well as density functional theory (DFT)<sup>40–46</sup> curves treated with small-curvature tunneling (SCT) canonical variational theory (CVT).<sup>47,48</sup>

In our optically transparent matrices resulting from deposition of the pyrolysis products on a cold window, selective vibrational excitation of **1ff** at 7026 ± 4 cm<sup>-1</sup> gave **1ct** (Figures S2 and S3), while the back reaction was initiated with NIR irradiation at 6542 ± 4 cm<sup>-1</sup> (Figure S3). After NIR irradiation at either of these two absorptions, we also observed new IR bands that vanished over the course of 1.5 h when the matrix was kept in the dark (Figure S4). We assigned these bands to the **1cc** conformer with the help of VPT2//AE-CCSD(T)/aug-cc-pCVTZ<sup>49,50</sup> vibrational frequency computations (Figure 2); full details of the assignments, including total energy distributions,<sup>51–53</sup> can be found in Table S3. The

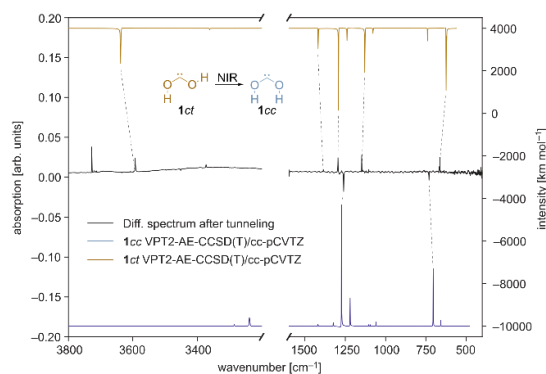


**Figure 2.** Dihydroxycarbene rotamers **1cc** and **1ct** identified in a N<sub>2</sub> matrix at 3 K. Bottom and top traces: computed VPT2//AE-CCSD(T)/aug-cc-pCVTZ spectra of **1cc** and **1ct**, respectively. Middle trace: difference spectrum obtained from spectra recorded before and after the matrix was irradiated at 7026.0 ± 4 cm<sup>-1</sup> (**1ff** band) for 15 min and then at 6542 ± 4 cm<sup>-1</sup> (**1ct** band) for 15 min and then kept in the dark for 1.5 h. The full spectrum is shown in Figure S4.<sup>54–56</sup>

multireference character of TS4 and TS5 is marginal (cf. Chapter 4.3 in the Supporting Information (SI)).<sup>25</sup>

While the bands of **1cc** vanished, the bands of **1ct** simultaneously grew. Because the barrier for this conformational interconversion is 9.4 kcal mol<sup>-1</sup> (Figure 1), QMT must be operative for this reaction to occur at 3 K. The disappearance of **1cc** over time (Figure 3) was monitored at

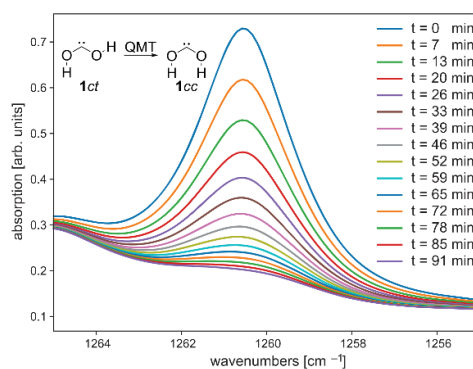


**Figure 3.** Temporal decay of the most intense IR band (1260.2 cm<sup>-1</sup>) of **1cc** over 138 min at 3.0 K in a N<sub>2</sub> matrix. Spectra were taken every 98 s with a 4.5 μm low-pass filter in front of the matrix to avoid photoreactions caused by the spectrometer global source. For clarity, only every fourth trace is shown. The temporal profile of the **1cc** band at 730.1 cm<sup>-1</sup> is shown in Figure S5.<sup>54–56</sup>

different temperatures, and our kinetic analyses revealed effective tunneling half-lives in the 17–22 min range over the 3–20 K interval (Table 1). The relative insensitivity of the reaction rate to temperature is also indicative of QMT.

In solid Ar and Ne matrices, we could interconvert **1ff** and **1ct** by NIR irradiation, but the **1cc** rotamer remained undetected (Figures S7–S11). However, the bands of **1ct** could not be depleted completely even after prolonged irradiation, which might hint that **1cc** formed but has an inherent lifetime of less than 2 min in these environments. Our

**Table 1. Tunneling Kinetics of *s-cis,s-cis*-Dihydroxycarbene (1cc) in a N<sub>2</sub> Matrix<sup>a</sup>**

T/K	$\tau_{ci}$ /h	$\tau_{leak}$ /h	$\tau_{eff}$ /h <sup>b</sup>	leak fraction	initial 1cc:1ct population ratio
3.0	0.331(1)	0.78(10)	0.363	0.13(2)	2.797(3)
7.5	0.331(1)	0.73(9)	0.359	0.14(3)	2.106(3)
12.5	0.312(1)	0.48(12)	0.325	0.10(7)	3.483(3)
15.0	0.307(1)	0.82(22)	0.331	0.09(3)	4.255(5)
20.0	0.278(1)	0.35(7)	0.291	0.19(18)	3.133(3)

<sup>a</sup>Standard errors of the least-squares fits are shown in parentheses in multiples of the last significant digit. See the text and SI for a description of the fitting parameters. <sup>b</sup> $\tau_{eff}$  = effective half-life for overall 1cc decay.

best theoretical prediction for the 1cc → 1ct tunneling half-life in the gas phase is 1.2 min, which was derived as follows: (a) uniform scaling of the optimized AE-CCSD(T)/aug-cc-pCVTZ potential energy curve (Table S30) by 1.024 to reproduce the converged FPA rotamerization barrier; (b) WKB evaluation of the tunneling half-life on this scaled curve; and (c) application of the SCT correction factor of 0.0363 given by the B3LYP/cc-pVTZ level of theory (Table S29). The resulting prediction is consistent with both the observed lack of 1cc bands in the Ar and Ne matrices and the measured 1cc half-life of 17–22 min in solid N<sub>2</sub>, whose appreciable polarizability is known to stabilize reactive intermediates. Khriachtchev et al. reported a similar stabilization of the high-lying HOCO-conformer in N<sub>2</sub>.<sup>19</sup> To investigate this effect, we computed N<sub>2</sub> complexes of all three rotamers of 1 (SI Chapter 4.2), similar to those reported for formic acid.<sup>20</sup> The AE-CCSD(T)/aug-cc-pCVTZ-optimized complexes display O–H···N<sub>2</sub> interactions that yield binding energies of 1.2–1.8 kcal mol<sup>-1</sup> and vibrational frequency shifts as large as 63 cm<sup>-1</sup>. Such substantial interactions are also evidenced in the experimental IR spectra of 1ct and 1tt, as both species display an O–H stretching frequency in N<sub>2</sub> that differs from the corresponding value in solid Ne (Tables S11 and S12) by almost 60 cm<sup>-1</sup>.

The QMT kinetics from 3 to 20 K was analyzed by means of a simultaneous nonlinear least-squares fit of two 1cc and three 1ct high-quality IR bands (Table 1). The simplest integrated rate equations capable of accurately fitting the entirety of the kinetic data for 1cc decay and 1ct growth required four adjustable parameters: the rotamerization half-life ( $\tau_{ci}$ ), the 1cc:1ct initial population ratio, a half-life for alternative 1cc decay ( $\tau_{leak}$ ), and a branching fraction for such secondary leaking. Unlike the cases of carbonic<sup>57</sup> and oxalic acid,<sup>58</sup> no evidence of frozen molecules or distinct fast and slow conformational tunneling was found. Figures S19–S28 show that if the rate constants for 1cc decay and 1ct growth are set equal to one another, the spectral data cannot be fit precisely, revealing the necessity of the “leak” component. As shown in Table 1, leaking is responsible for roughly 10% of the decay, which is too small to allow the parameters for this unknown process to be pinned down to a high degree. Nonetheless, we believe that the kinetic profiles provide compelling evidence for a secondary, minor process of decay with a half-life less than but on the same order of magnitude as  $\tau_{ci}$ .

One candidate for the leaking process is suggested by our CVT/SCT tunneling computations (Tables S29–S33) at several levels of theory, including CCSD(T)/aug-cc-pVTZ//B2-PLYP/aug-cc-pVTZ. To wit, the rate for the direct 1cc → H<sub>2</sub> + CO<sub>2</sub> decomposition is in the same time regime as the

rotamerization, in agreement with the kinetic analysis. Neither product can be monitored in our experiments because the CO<sub>2</sub> concentration after pyrolysis exceeds our spectrometer limits and H<sub>2</sub> is not IR-active. Continuously populating 1cc by laser irradiation of the other rotamers should lead to overall depletion of 1 to form H<sub>2</sub> and CO<sub>2</sub>, but this was not observed after 5 h (Figure S6).

We attempted to probe the behavior of the dideuterated species <sup>2</sup>H<sub>2</sub>-1 originating from the pyrolysis of <sup>2</sup>H<sub>2</sub>-oxalic acid<sup>5</sup> in order to further characterize 1cc and its tunneling decay (which should be quenched by dideuteration). However, bands of <sup>2</sup>H<sub>2</sub>-1cc were not observed after NIR excitation because the energy of the O–<sup>2</sup>H overtone of <sup>2</sup>H<sub>2</sub>-1tt is barely too low (5258 cm<sup>-1</sup> = 15.0 kcal mol<sup>-1</sup>) to overcome the rotamerization barriers (1tt → 1ct = 15.9 and 1ct → 1cc = 16.1 kcal mol<sup>-1</sup>).

We tried to prepare monodeuterated 1 through ester pyrolysis of several suitable precursors<sup>59</sup> (Scheme S1), hoping to use the OH group as an NIR antenna for remote rotamerization.<sup>60</sup> This would have allowed an indirect probe of the leak process because the heavier <sup>2</sup>H-1cc isotopomer could not dissociate by QMT while rotamerization would still occur at approximately 50% of the rate of the parent molecule. However, in all of our attempts the carbene yield was too low through this alternative generation method (see the SI for details).

To conclude, we have isolated and characterized in solid N<sub>2</sub> the higher-lying *s-cis,s-cis* rotamer of dihydroxycarbene, which may be the missing link in the reduction of CO<sub>2</sub> with H<sub>2</sub> to form 1ct<sup>1</sup> and subsequently formic acid. The 1cc species rapidly rotamerizes even at 3 K and could be identified only in stabilizing N<sub>2</sub> rather than noble gas cryogenic environments. A secondary QMT pathway involving dissociation of 1cc to H<sub>2</sub> + CO<sub>2</sub> is plausible according to theory and might be responsible for the biexponential characteristics measured in our decay profiles.

## ■ ASSOCIATED CONTENT

### SI Supporting Information

The Supporting Information is available free of charge at <https://pubs.acs.org/doi/10.1021/jacs.0c09317>.

Full-matrix IR spectra after pyrolysis of 6 in N<sub>2</sub>, Ar, and Ne; full matrix IR spectra after irradiation with NIR light in N<sub>2</sub>, Ar, and Ne; full assignments of 1 in Ne and N<sub>2</sub>; full PES around 1 at the FPA//AE-CCSD(T)/aug-cc-pCVTZ level of theory; geometries with all important bond lengths and angles; Cartesian coordinates of all molecules on the PES; detailed results of tunneling computations; details of the kinetic analysis; description of attempts to generate <sup>2</sup>H<sub>1</sub>-1 (PDF)

## ■ AUTHOR INFORMATION

### Corresponding Authors

Peter R. Schreiner – Institute of Organic Chemistry, Justus Liebig University, D-35392 Giessen, Germany; [orcid.org/0000-0002-3608-5515](https://orcid.org/0000-0002-3608-5515); Email: [prs@uni-giessen.de](mailto:prs@uni-giessen.de)

Wesley D. Allen – Center for Computational Quantum Chemistry and Department of Chemistry, University of Georgia, Athens, Georgia 30602, United States; Allen Heritage Foundation, Dickson, Tennessee 37055, United States; Email: [wdallen@uga.edu](mailto:wdallen@uga.edu)

## Authors

Henrik Quanz – Institute of Organic Chemistry, Justus Liebig University, D-35392 Giessen, Germany

Bastian Bernhardt – Institute of Organic Chemistry, Justus Liebig University, D-35392 Giessen, Germany; [orcid.org/0000-0002-7734-6427](https://orcid.org/0000-0002-7734-6427)

Frederik R. Erb – Institute of Organic Chemistry, Justus Liebig University, D-35392 Giessen, Germany

Marcus A. Bartlett – Center for Computational Quantum Chemistry and Department of Chemistry, University of Georgia, Athens, Georgia 30602, United States

Complete contact information is available at:

<https://pubs.acs.org/10.1021/jacs.0c09317>

## Author Contributions

<sup>†</sup>H.Q. and B.B. contributed equally.

## Notes

The authors declare no competing financial interest.

## ACKNOWLEDGMENTS

We thank Dennis Gerbig for maintaining our computer clusters and André K. Eckhardt and Hans P. Reisenauer for fruitful discussions. B.B. thanks the Bayer Fellowship Program and the Deutscher Akademischer Austauschdienst for financial support during a research visit at the University of Georgia and the Fonds der Chemischen Industrie for a doctoral scholarship. This work was supported by the Volkswagen Foundation (“What is Life” Grant 92 748 to P.R.S.).

## REFERENCES

- (1) Tian, F.; Toon, O. B.; Pavlov, A. A.; De Sterck, H. A Hydrogen-Rich Early Earth Atmosphere. *Science* **2005**, *308*, 1014–1017.
- (2) Kasting, J. F. Earth's early atmosphere. *Science* **1993**, *259*, 920–926.
- (3) Herbst, E. The chemistry of interstellar space. *Chem. Soc. Rev.* **2001**, *30*, 168–176.
- (4) Womack, C. C.; Crabtree, K. N.; McCaslin, L.; Martinez, O.; Field, R. W.; Stanton, J. F.; McCarthy, M. C. Gas-Phase Structure Determination of Dihydroxycarbene, One of the Smallest Stable Singlet Carbenes. *Angew. Chem. Int. Ed.* **2014**, *53*, 4089–4092.
- (5) Schreiner, P. R.; Reisenauer, H. P. Spectroscopic Identification of Dihydroxycarbene. *Angew. Chem. Int. Ed.* **2008**, *47*, 7071–7074.
- (6) Jeans, J. *The Dynamical Theory of Gases*; Cambridge University Press: London, 1916; Vol. 1, p 436.
- (7) Allen, A. G.; Baxter, P. J.; Ottley, C. J. Gas and particle emissions from Soufrière Hills Volcano, Montserrat, West Indies: characterization and health hazard assessment. *Bull. Volcanol.* **2000**, *62*, 8–19.
- (8) Eckhardt, A. K.; Linden, M. M.; Wende, R. C.; Bernhardt, B.; Schreiner, P. R. Gas-phase sugar formation using hydroxymethylene as the reactive formaldehyde isomer. *Nat. Chem.* **2018**, *10*, 1141–1147.
- (9) Schreiner, P. R. Tunneling Control of Chemical Reactions: The Third Reactivity Paradigm. *J. Am. Chem. Soc.* **2017**, *139*, 15276–15283.
- (10) Feller, D.; Borden, W. T.; Davidson, E. R. A theoretical study of paths for decomposition and rearrangement of dihydroxycarbene. *J. Comput. Chem.* **1980**, *1*, 158–166.
- (11) Broderick, B. M.; McCaslin, L.; Moradi, C. P.; Stanton, J. F.; Doublerly, G. E. Reactive intermediates in <sup>4</sup>He nanodroplets: Infrared laser Stark spectroscopy of dihydroxycarbene. *J. Chem. Phys.* **2015**, *142*, 144309–144316.
- (12) Hutschka, F.; Dedieu, A.; Leitner, W. Metathesis as a Critical Step for the Transition Metal Catalyzed Formation of Formic Acid from CO<sub>2</sub> and H<sub>2</sub>: An Ab Initio Investigation. *Angew. Chem. Int. Ed. Engl.* **1995**, *34*, 1742–1745.
- (13) Steigerwald, M. L.; Goddard, W. A., III The 2<sub>g</sub> + 2<sub>g</sub> Reactions at Transition Metals. 1. The Reactions of D<sub>2</sub> with Cl<sub>2</sub>TiH<sup>+</sup>, Cl<sub>2</sub>TiH, and Cl<sub>2</sub>ScH. *J. Am. Chem. Soc.* **1984**, *106*, 308–311.
- (14) Woodward, R. B.; Hoffmann, R. The Conservation of Orbital Symmetry. *Angew. Chem. Int. Ed. Engl.* **1969**, *8*, 781–853.
- (15) Woodward, R. B.; Hoffmann, R. Stereochemistry of Electrocyclic Reactions. *J. Am. Chem. Soc.* **1965**, *87*, 395–397.
- (16) Taatjes, C. A.; Meloni, G.; Selby, T. M.; Trevitt, A. J.; Osborn, D. L.; Percival, C. J.; Shallcross, D. E. Direct Observation of the Gas-Phase Criegee Intermediate (CH<sub>2</sub>OO). *J. Am. Chem. Soc.* **2008**, *130*, 11883–11885.
- (17) Wadt, W. R.; Goddard, W. A., III Electronic structure of the Criegee intermediate. Ramifications for the mechanism of ozonolysis. *J. Am. Chem. Soc.* **1975**, *97*, 3004–3021.
- (18) Lovas, F. J.; Suenram, R. D. Identification of dioxirane (H<sub>2</sub>COO) in ozone-olefin reactions via microwave spectroscopy. *Chem. Phys. Lett.* **1977**, *51*, 453–456.
- (19) Lopes, S.; Domanskaya, A. V.; Fausto, R.; Räsänen, M.; Khriachtchev, L. Formic and acetic acids in a nitrogen matrix: Enhanced stability of the higher-energy conformer. *J. Chem. Phys.* **2010**, *133*, 144507–144514.
- (20) Marushkevich, K.; Khriachtchev, L.; Lundell, J.; Domanskaya, A.; Räsänen, M. Matrix Isolation and Ab Initio Study of *Trans*–*Trans* and *Trans*–*Cis* Dimers of Formic Acid. *J. Phys. Chem. A* **2010**, *114*, 3495–3502.
- (21) Pettersson, M.; Lundell, J.; Khriachtchev, L.; Räsänen, M. IR Spectrum of the Other Rotamer of Formic Acid, *cis*-HCOOH. *J. Am. Chem. Soc.* **1997**, *119*, 11715–11716.
- (22) Gerbig, D.; Schreiner, P. R. Hydrogen-Tunneling in Biologically Relevant Small Molecules: The Rotamerizations of  $\alpha$ -Ketocarboxylic Acids. *J. Phys. Chem. B* **2015**, *119*, 693–703.
- (23) East, A. L. L.; Allen, W. D. The heat of formation of NCO. *J. Chem. Phys.* **1993**, *99*, 4638–4650.
- (24) Schuurman, M. S.; Muir, S. R.; Allen, W. D.; Schaefer, H. F., III Toward subchemical accuracy in computational thermochemistry: Focal point analysis of the heat of formation of NCO and [H<sub>2</sub>N,C,O] isomers. *J. Chem. Phys.* **2004**, *120*, 11586–11599.
- (25) Bartlett, M. A.; Liang, T.; Pu, L.; Schaefer, H. F., III; Allen, W. D. The multichannel *n*-propyl + O<sub>2</sub> reaction surface: Definitive theory on a model hydrocarbon oxidation mechanism. *J. Chem. Phys.* **2018**, *148*, 094303.
- (26) Császár, A. G.; Allen, W. D.; Schaefer, H. F., III In pursuit of the ab initio limit for conformational energy prototypes. *J. Chem. Phys.* **1998**, *108*, 9751–9764.
- (27) Gonzales, J. M.; Allen, W. D.; Schaefer, H. F., III Model Identity S<sub>N</sub>2 Reactions CH<sub>3</sub>X + X<sup>−</sup> (X = F, Cl, CN, OH, SH, NH<sub>2</sub>, PH<sub>2</sub>): Marcus Theory Analyzed. *J. Phys. Chem. A* **2005**, *109*, 10613–10628.
- (28) Stanton, J. F. Why CCSD(T) works: a different perspective. *Chem. Phys. Lett.* **1997**, *281*, 130–134.
- (29) Čížek, J. On the Correlation Problem in Atomic and Molecular Systems. Calculation of Wavefunction Components in Ursell-Type Expansion Using Quantum-Field Theoretical Methods. *J. Chem. Phys.* **1966**, *45*, 4256–4266.
- (30) Bartlett, R. J.; Watts, J. D.; Kucharski, S. A.; Noga, J. Non-iterative fifth-order triple and quadruple excitation energy corrections in correlated methods. *Chem. Phys. Lett.* **1990**, *165*, 513–522.
- (31) Purvis, G. D., III; Bartlett, R. J. A full coupled-cluster singles and doubles model: The inclusion of disconnected triples. *J. Chem. Phys.* **1982**, *76*, 1910–1918.
- (32) Raghavachari, K.; Trucks, G. W.; Pople, J. A.; Head-Gordon, M. A fifth-order perturbation comparison of electron correlation theories. *Chem. Phys. Lett.* **1989**, *157*, 479–483.
- (33) Woon, D. E.; Dunning, T. H., Jr. Gaussian basis sets for use in correlated molecular calculations. V. Core-valence basis sets for boron through neon. *J. Chem. Phys.* **1995**, *103*, 4572–4585.
- (34) Kállay, M.; Nagy, P. R.; Mester, D.; Rolik, Z.; Samu, G.; Csontos, J.; Csóka, J.; Szabó, P. B.; Gyevi-Nagy, L.; Hégyely, B.; Ladjánszki, L.; Szegedy, L.; Ladóczki, B.; Petrov, K.; Farkas, M.; Mezei,

- P. D.; Ganyecz, Á. MRCC, a Quantum-Chemical Program Suite. Available at <https://www.mrcc.hu>.
- (35) MOLPRO, a Package of Ab Initio Programs, ver. 2019.2 (see the SI for the full reference). Available at <https://www.molpro.net>.
- (36) Wentzel, G. Eine Verallgemeinerung der Quantenbedingungen für die Zwecke der Wellenmechanik. *Eur. Phys. J. A* **1926**, *38*, 518–529.
- (37) Kramers, H. A. Wellenmechanik und halbzahlige Quantisierung. *Eur. Phys. J. A* **1926**, *39*, 828–840.
- (38) Brillouin, L. La mécanique ondulatoire de Schrödinger: une méthode générale de résolution par approximations successives. *C. R. Acad. Sci.* **1926**, *183*, 24–26.
- (39) Quanz, H.; Schreiner, P. R. TUNNEX: An easy-to-use Wentzel-Kramers-Brillouin (WKB) implementation to compute tunneling half-lives. *J. Comput. Chem.* **2019**, *40*, 543–547.
- (40) Lee, C.; Yang, W.; Parr, R. G. Development of the Colle-Salvetti correlation-energy formula into a functional of the electron density. *Phys. Rev. B* **1988**, *37*, 785–789.
- (41) Becke, A. D. A new mixing of Hartree-Fock and local density-functional theories. *J. Chem. Phys.* **1993**, *98*, 1372–1377.
- (42) Becke, A. D. Density-functional exchange-energy approximation with correct asymptotic behavior. *Phys. Rev. A* **1988**, *38*, 3098–3100.
- (43) Kim, K.; Jordan, K. D. Comparison of Density Functional and MP2 Calculations on the Water Monomer and Dimer. *J. Phys. Chem.* **1994**, *98*, 10089–10094.
- (44) Stephens, P. J.; Devlin, F. J.; Chabalowski, C. F.; Frisch, M. J. Ab Initio Calculation of Vibrational Absorption and Circular Dichroism Spectra Using Density Functional Force Fields. *J. Phys. Chem.* **1994**, *98*, 11623–11627.
- (45) Grimme, S. Semiempirical hybrid density functional with perturbative second-order correlation. *J. Chem. Phys.* **2006**, *124*, 034108.
- (46) Bousquet, D.; Brémond, E.; Sancho-García, J. C.; Ciofini, I.; Adamo, C. Is There Still Room for Parameter Free Double Hybrids? Performances of PBE0-DH and B2PLYP over Extended Benchmark Sets. *J. Chem. Theory Comput.* **2013**, *9*, 3444–3452.
- (47) Fernandez-Ramos, A.; Ellingson, B. A.; Garrett, B. C.; Truhlar, D. G. Variational transition state theory with multidimensional tunneling. *Rev. Comput. Chem.* **2007**, *23*, 125–233.
- (48) Frisch, M. J.; et al. *Gaussian 16*, rev. B.01; Gaussian, Inc.: Wallingford, CT, 2016 (see the SI for the full reference). Available at <https://www.gaussian.com>.
- (49) Allen, W. D.; Császár, A. G. On the ab initio determination of higher-order force constants at nonstationary reference geometries. *J. Chem. Phys.* **1993**, *98*, 2983–3015.
- (50) Allen, W. D.; Császár, A. G.; Szalay, V.; Mills, I. M. General derivative relations for anharmonic force fields. *Mol. Phys.* **1996**, *89*, 1213–1221.
- (51) Pulay, P.; Török, F. *Acta Chim. Acad. Sci. Hungary* **1965**, *44*, 287.
- (52) Keresztury, G.; Jalsovszky, G. An alternative calculation of the vibrational potential energy distribution. *J. Mol. Struct.* **1971**, *10*, 304–305.
- (53) Allen, W. D.; Császár, A. G.; Horner, D. A. The Puckering Inversion Barrier and Vibrational Spectrum of Cyclopentene. A Scaled Quantum Mechanical Force Field Algorithm. *J. Am. Chem. Soc.* **1992**, *114*, 6834–6849.
- (54) Hunter, J.; Matplotlib, D. A 2D Graphics Environment. *Comput. Sci. Eng.* **2007**, *9*, 90–95.
- (55) Behnel, S.; Bradshaw, R.; Citro, C.; Dalcin, L.; Seljebotn, D. S.; Smith, K. Cython: The Best of Both Worlds. *Comput. Sci. Eng.* **2011**, *13*, 31–39.
- (56) van der Walt, S.; Colbert, S. C.; Varoquaux, G. The NumPy Array: A Structure for Efficient Numerical Computation. *Comput. Sci. Eng.* **2011**, *13*, 22–30.
- (57) Wagner, J. P.; Reisenauer, H. P.; Hirvonen, V.; Wu, C.-H.; Tyberg, J. L.; Allen, W. D.; Schreiner, P. R. Tunneling in carbonic acid. *Chem. Commun.* **2016**, *52*, 7858–7861.
- (58) Schreiner, P. R.; Wagner, J. P.; Reisenauer, H. P.; Gerbig, D.; Ley, D.; Sarka, J.; Császár, A. G.; Vaughn, A.; Allen, W. D. Domino Tunneling. *J. Am. Chem. Soc.* **2015**, *137*, 7828–7834.
- (59) Honda, K.; Ohkura, S.; Hayashi, Y.; Kawauchi, S.; Mikami, K. Cationic Chiral Pd-Catalyzed “Acetylenic” Diels–Alder Reaction: Computational Analysis of Reversal in Enantioselectivity. *Chem. Asian J.* **2018**, *13*, 2842–2846.
- (60) Halasa, A.; Reva, L.; Lapinski, L.; Nowak, M. J.; Fausto, R. Conformational Changes in Thiazole-2-carboxylic Acid Selectively Induced by Excitation with Narrowband Near-IR and UV Light. *J. Phys. Chem. A* **2016**, *120*, 2078–2088.

## 2.5 Further co-Authored Publications

Intricate Conformational Tunneling in Carbonic Acid Monomethyl Ester. Michael M. Linden, J. Philipp Wagner, Bastian Bernhardt, Marcus A. Bartlett, Wesley D. Allen, and Peter R. Schreiner *J. Phys. Chem. Lett.* **2018**, *9*, 1663–1667. (DOI: 10.1021/acs.jpcllett.8b00295)

Gas-phase sugar formation using hydroxymethylene as the reactive formaldehyde isomer. André K. Eckhardt, Michael M. Linden, Raffael C. Wende, Bastian Bernhardt, and Peter R. Schreiner *Nat. Chem.* **2018**, *10*, 1141–1147. (DOI: 10.1038/s41557-018-0128-2)

*Highlights:* a) Super-reactive molecule could solve space sugar mystery, *Chemistry World* **2018**, (<https://www.chemistryworld.com/news/super-reactive-molecule-could-solve-space-sugar-mystery/3009487.article>); b) Süßes Leben – einfachste Zucker ohne Biosynthese, *JLU news release* **2018**, (<https://www.uni-giessen.de/ueberuns/pressestelle/pm/pm158-18>); c) Einfachste Zucker ohne Biosynthese – *LABO Online* **2018**, (<https://www.labo.de/news/einfachste-zucker-ohne-biosynthese.htm>); d) Süßes Leben – einfachste Zucker ohne Biosynthese – *Innovations Report* **2018**, (<https://www.innovations-report.de/fachgebiete/biowissenschaften-chemie/suesses-leben-einfachste-zucker-ohne-biosynthese/>).

Photochemistry of HNSO<sub>2</sub> in cryogenic matrices: spectroscopic identification of the intermediates and mechanism. Changyun Chen, Lina Wang, Xiaofang Zhao, Zhuang Wu, Bastian Bernhardt, André K. Eckhardt, Peter R. Schreiner, and Xiaoqing Zeng *Phys. Chem. Chem. Phys.* **2020**, *22*, 7975–7983. (DOI: 10.1039/D0CP00962H)

Capture and Reactivity of an Elusive Carbon–Sulfur Centered Biradical. Dennis Gerbig, Bastian Bernhardt, Raffael C. Wende, and Peter R. Schreiner *J. Phys. Chem. A* **2020**, *124*, 2014–2018. (DOI: 10.1021/acs.jpca.9b11795)

Underline denotes shared first authors.



### 3. Acknowledgment – Danksagung

Diese Arbeit wäre ohne die Hilfe zahlreicher Personen nicht zustande gekommen. Gerade in Pandemiezeiten (Computer- und Coronavirus) war und ist diese Unterstützung nicht nur aus wissenschaftlicher Hinsicht von unschätzbarem Wert. Herzlich bedanken möchte ich mich bei:

**Prof. Dr. Peter. R. Schreiner, PhD** für die Aufnahme in seine Arbeitsgruppe, gute Ratschläge, die Freiheit in meiner Forschung und sein Vertrauen und das Fördern meiner Fähigkeiten.

**Prof. Dr. Bernd Smarsly** für die Übernahme des Zweitgutachtens dieser Arbeit.

**Prof. Dr. Wesley D. Allen** und seinen Mitarbeiter/innen für ihre Gastfreundschaft während meines Auslandsaufenthalts an der University of Georgia und die erfolgreiche Zusammenarbeit am Dihydroxycarben-Paper.

**Henrik Quanz** für die sehr gute Betreuung meiner Master-Thesis und seine ständige Unterstützung in computerchemischen Fragestellungen.

**Markus Schauer** für die gute Zusammenarbeit im Aminomercaptocarben-Projekt.

**Marcel Ruth** für seinen unermüdlichen Einsatz im Rahmen seiner Vertiefungs- und Spezialisierungsmodule und die erfolgreiche und gute Zusammenarbeit beim Schreiben zweier Publikationen.

**Friedemann Dressler, Frederik R. Erb, Finn M. Wilming** und **Gina M. Würfl** für die erfolgreiche und zuverlässige Durchführung einiger Synthesen von Matrixvorläuferverbindungen.

Meinen Kollegen aus Labor B201 **Finn M. Wilming, Lars Rummel** und **Henrik F. König** für die hervorragende Arbeitsatmosphäre und zahlreiche Gespräche über Wissenschaft und mehr. Jeder von ihnen hätte 25.000 Punkte mehr als verdient.

**Dr. André K. Eckhardt** für zahlreiche gute Ratschläge und seine externe Unterstützung in einigen Projekten.

**Dr. Dennis Gerbig** für seine Unterstützung in wissenschaftlichen Fragestellungen und die kompetente Einführung in die Kunst der Matrixisolation während meines Studiums.

**Dr. Artur Mardiyukov** für fachliche Unterstützung sowie einige abendliche Poker- und Schachpartien.

**Dr. Hans Peter Reisenauer** für seine hilfreichen Ratschläge bezüglich IR-Spektroskopie und die gute Zusammenarbeit im Aminohydroxycarben-Projekt.

**Ephrath Solel, PhD** für die Durchführung einiger computerchemischer Rechnungen im Aminomercaptocarben-Projekt.

**Benjamin Zonker, Jama Ariai** und **Dr. Sascha H. Combe** für die gute Arbeitsatmosphäre im Liebig-Office.

**Prof. Dr. Xiaoqing Zeng** und seinen Mitarbeiter/innen für die gute Zusammenarbeit in einem erfolgreichen Kooperationsprojekt.

**Dr. Marina Šekutor, Dr. Marija Alešković, und Dr. Nikola Basarić** für ihre Gastfreundschaft während meines Forschungsaufenthalts am Institut Ruđer Bošković in Zagreb.

**Dr. Fumito Saito** für synthetische Ratschläge.

**Cláudio M. Nunes, PhD** für einige fruchtbare Diskussionen über tunneleffektgesteuerte Reaktionen.

**Jan M. Schümann** und **Felix Keul** für Abwechslung im Doktorandenalltag.

**Dr. Michael M. Linden** für seine exzellente Betreuung meiner Bachelor-Thesis zu Beginn meiner Zeit in der PRS Group.

**Dr. J. Philipp Wagner** für seine Unterstützung während meiner Zeit in Athens, Georgia.

**Dr. Jonathan Becker** für die Analyse einiger Einkristalle.

**Dr. Heike Hausmann** für die Messung einiger NMR-Proben.

**Dr. Raffael C. Wende** für die Messung einiger massenspektrometrischer Proben.

**Edgar Reitz** für seine kompetente Unterstützung in technischen Fragestellungen und die Eindämmung des Computervirus.

Der gesamten **PRS Group** für die gute Arbeitsatmosphäre.

Den anderen Arbeitsgruppen des **Instituts für Organische Chemie** für das Bereitstellen einiger Materialien, insbesondere LED Lampen, und das stets freundliche Arbeitsumfeld.

**Michaela Richter** und **Dr. Jörg Neudert** für ihre Unterstützung in administrativen Angelegenheiten.

Meinen Kommilitonen und insbesondere **Ruben Maile, Finn M. Wilming, David S. Kröck, Jaqueline Beppler** und **Tabea Köhler** für die schöne und angenehme Zeit während meines Studiums.

Dem **Fonds der Chemischen Industrie** für die finanzielle Unterstützung in Form eines Kekulé Stipendiums während meiner Promotion.

Der **Sektion Gießen-Oberhessen des Deutschen Alpenvereins e.V.** und allen meinen Freunden für mein Leben abseits der Universität.

